

# **DESIGN, SYNTHESIS AND CHARACTERIZATION OF MODULAR PEPTIDE-BASED NANOMATERIALS**



A thesis submitted  
in partial fulfillment for the degree of  
*Master of Science*  
as a part of the  
*Integrated Ph.D. Programme*  
*(Materials Science)*  
by  
**M. PANDEESWAR**

**CHEMISTRY AND PHYSICS OF MATERIALS UNIT**  
**JAWAHARALAL NEHRU CENTRE FOR ADVANCED SCIENTIFIC RESEARCH**  
**(A DEEMED UNIVERSITY)**  
**JAKKUR, BANGLORE-560 064**  
**(March- 2011)**

*Dedicated to my parents*



CHEMISTRY AND PHYSICS OF MATERIALS UNIT,  
JNCASR, BANGALORE-560064.

---

## CERTIFICATE

I hereby certify that the work described in this thesis entitled “**Design, Synthesis and Characterization of modular peptide-based nanomaterials**” has been carried out by Mr. M. Pandeewar under my supervision at the Bioorganic Chemistry Lab, New Chemistry Unit, JNCASR, India and that it has not been submitted elsewhere for the award of any degree or diploma.

NCU  
JNCASR  
March-2011

**Dr. T. Govindaraju**  
(Research Supervisor)

## **DECLARATION**

I hereby declare that the matter embodied in this thesis “**Design, Synthesis and Characterization of modular peptide-based nanomaterials**” is the result of investigations carried out by me under the supervision of **Dr. T. Govindaraju** at the New chemistry Unit, Jawaharlal Nehru Centre for Advanced Scientific Research, Bangalore, India and that it has not been submitted elsewhere for the award of any degree or diploma.

In keeping with the general practice in reporting the scientific observations, due acknowledgement has been made whenever the work described is based on the findings of other investigators. Any omission that might have occurred due to oversight or error in judgement is regretted.

**CPMU**  
**JNCASR**  
**March 2011**

**M. PANDEESWAR**

## ACKNOWLEDGEMENT

*First and foremost I would like to thank Professor C. N. R. Rao, for his support and encouragement. His presence has given me immense inspiration to indulge in active research.*

*At the very outset, I would like to express my heartfelt gratitude to my supervisor, Dr. T. Govindaraju, Faculty Fellow, Bioorganic chemistry lab, New Chemistry Unit, JNCASR, who right from the beginning of my project, provided me all the facilities he could offer to carry on my project and monitored my work. I shall remain ever thankful to him for giving me enough freedom to work on my own area of interests.*

*I am extremely thankful to, Mr. M. B. Avinash, Mr. Debabrata Maity, Mr. Nagarjun and Mr. Shivaprasad Research fellows, Bioorganic chemistry lab, New Chemistry Unit, JNCASR, for their help in various capacities, co-operation and maintaining cheerful atmosphere in the lab.*

*My special thanks to Mr. M. B. Avinash for his constant support and fruitful discussion we had throughout my project work. The confidence he had in me, willingness to share new ideas, excitements helped me in a real sense to shape my thesis work.*

*I would like thank to my collaborators Dr. T. K. Maji, K. Jayaramulu for their help in X-ray analysis, Dr. H. S. Atreya and G. Jaipuria for their help in solid state NMR analysis.*

*I shall be ever thankful to Prof. G. U. Kulkarni, Prof. S. Balasubramanian, Prof. A. Sundaresan, Prof. S. M. Shivaprasad, Prof. Chandrabhas Narayana, Dr. T. K. Maji, Dr. Eswaramoorthy, Prof. K. S. Narayan, Prof. S. K. Pati, Prof. U. V. Waghmare, Dr. S. Narasimhan, Dr. N. S. Vidhyadhiraja, Prof. S. Ranganathan (Materials Engineering, IISc) and Dr. Ranjan Datta for their valuable courses.*

*I would like to thank the past and present Int. Ph. D. conveners, Prof. S. Balasubramanian and Dr. T. K. Maji for given opportunity to do this project.*

*I would like to thank all Integrated Ph.D-2008 friends for extending their help and cooperation for the successful completion of my project work. Finally, I have to mention the contribution by my parents, in my endeavor to take up the project work with in flinching fidelity.*

*M. Pandeewar*

# **PREFACE**

The thesis entitled “**Design, Synthesis and Characterization of modular peptide-based nanomaterials**” is divided into 4 chapters as follows

## **Chapter 1: Introduction:**

Brief overview of the chemical structure and physicochemical properties of amino acids and peptides. And also it describes briefly on recent advances in the bioactive peptide-based functional nanomaterials.

## **Chapter 2: Developing New Protecting Group Strategy for Solution and Solid Phase Peptide Synthesis**

Describes the developing new protecting group strategy to amino functionality of amino acid, which can easily and quickly deprotected by appropriate deprotecting agents without effecting any other protecting groups. And characterization of resulting compound through various spectroscopic techniques.

## **Chapter 3: Spontaneous self-assembly of designed cyclic dipeptide (Phg-Phg) into two dimensional nano and mesosheets**

Describes the design and synthesis of cyclic dipeptide (Phg-Phg) which can self-assemble into 2D nano and mesosheets spanning several micrometers in lateral dimensions. And characterization using different microscopy techniques.

## **Chapter 4: Design, Synthesis, photophysical and self-assembly properties of dipeptide appended naphthalenediimide**

Describes the design, synthesize and study the supramolecular assembly of a series of N, N-bis-(dipeptide) appended naphthalenetetracarboxylicaciddiimide (NDI) chromophores. The aromatic functionalities of amino acids side chain was systematically varied to understand the effect of this simple structural variations on the self-assembly.

## CONTENTS

<b>List of Figures</b> .....	3
<b>List of Tables</b> .....	6
<b>List of Schemes</b> .....	7
<b>Abbreviations</b> .....	8
<b>Chapter 1 Introduction</b>	
1. 1 Amino acids: Chemical structure .....	11
1. 2 Physicochemical properties of amino acids .....	15
1. 3 Peptide bonds .....	17
1. 4 General spectroscopic characterization techniques .....	18
1. 5 Self-assembly .....	21
1. 6 Non-covalent interactions .....	22
1. 7 Bioactive peptide-based functional nanomaterials .....	23
1. 8 Present work .....	25
1. 9 References .....	26
<b>Chapter 2 Developing New Protecting Group Strategy for Solution and Solid Phase Peptide Synthesis</b>	
2. 1 Introduction .....	31
2. 2 Objective of the present work .....	37
2. 3 Design strategy .....	38
2. 4 Results and discussions .....	40
2. 5 Conclusion .....	42
2. 6 Experimental section .....	43
2. 7 References .....	45

**Chapter 3 Spontaneous self-assembly of designed cyclic dipeptide (Phg-Phg) into two dimensional nano and mesosheets**

3. 1 Introduction.....	52
3. 2 Objective of the present work.....	55
3. 3 Design Strategy .....	55
3. 4 Synthesis of cyclic dipeptide .....	57
3. 5 Results and Discussion .....	58
3. 6 Proposed mechanism.....	66
3. 7 Conclusion .....	67
3. 8 Experimental section .....	68
3. 9 Appendix.....	69
3. 10 References.....	72

**Chapter 4 Design, Synthesis, photophysical and self-assembly properties of dipeptide appended naphthlenediimide**

4. 1 Introduction.....	76
4. 2 Objective of the present work.....	78
4. 3 Design Strategy .....	78
4. 4 Results and discussion.....	79
4. 7 Proposed mechanism.....	93
4. 8 Conclusion .....	94
4. 9 Experimental.....	95
4. 10 Appendix.....	97
4. 11 References.....	107



## List of Figures

Figure 1. 1 Existence of amino acid in different forms depends on the pH of the solution in which the amino acid dissolved. ....	16
Figure 1. 2 Condensation of $m$ number of $\alpha$ -amino acids to form a peptide. ....	17
Figure 1. 3 Self-assembled bioactive nanostructures. ....	23
Figure 2. 1 Our strategy for screening new protecting group for amine functionality of amino acid based on phthaloyl protecting group. $R_1, R_2, R_3$ and $R_4$ are electron withdrawing groups. $X_1, X_2, X_3$ are electronegative atoms. $R$ = substituent. $R'$ = carboxylic acid protecting group. ....	39
Figure 2. 2 a) UV-vis spectra of compound <b>16</b> ( $\lambda_{max} = 389$ nm), b) Photoluminescence emission spectra of compound <b>16</b> (emission maximum at $E_{max} = 491$ nm) .....	41
Figure 3. 1 Molecular structure of cyclic ( <i>D, L</i> ) dipeptide. ....	56
Figure 3. 2 Cyclic dipeptide forming molecular-layers through intermolecular (N–H--O) hydrogen bonding. ....	56
Figure 3. 3 (a) FESEM micrograph of 2D mesosheets formed from the solution of <b>1</b> in MeOH (inset shows the high resolution image of an isolated mesosheet). (b) FESEM micrographs of cyclic dipeptide <b>1</b> (in MeOH) showing rhomboid mesosheets formed by the self-organisation of nanosheets. (d) and (e) FESEM micrograph, nanosheets formed from the solution of <b>1</b> in $CHCl_3$ -TFA. ....	59
Figure 3. 4 (a) HRTEM micrograph of 2D mesosheet of <b>1</b> , the electron diffraction (ED, inset) shows the non-crystalline nature of the mesosheet. (c) AFM image of 2D mesosheets (rhomboid), inset show the height profile ( $\sim 200$ nm). ....	61

Figure 3. 5 Thermogravimetric analysis (TGA) of 2D mesosheets of cyclo ( <i>D</i> -Phg- <i>L</i> -Phg) <b>1</b> . .....	62
Figure 3. 6 Crystals of <b>1</b> (a) diamondoid shape crystals formed from MeOH, (b) rhomboid crystals formed from 2-methoxyethanol. ....	63
Figure 3. 7 (a) Optical profiler (Wyko NT9100, Veeco, USA) image of a single-crystalline rhomboid 2D sheet of cyclo ( <i>D</i> -Phg- <i>L</i> -Phg) <b>1</b> (crystallized from 2-methoxyethanol). The shape of this crystal is similar to that of rhomboid 2D mesosheets formed by self- assembly based aggregation. (b-d) Optical profiler analysis: single-crystalline rhomboid 2D sheet is larger in dimension compare to non-crystalline 2D mesosheets obtained by self-assembly based aggregation (lateral dimension > 600 $\mu\text{m}$ ). ....	64
Figure 3. 8 (a) Ortep-diagram and molecular interactions of cyclo ( <i>D</i> -Phg- <i>L</i> -Phg) <b>1</b> to form molecular-layers. (b and c) Packing of molecular-layers along c-axis to form single- crystalline 2D sheet. ....	66
Figure 3. 9 Proposed schematic model for the formation of the two dimensional nano and mesosheet structures by the cyclo( <i>D</i> -Phg- <i>L</i> -Phg) <b>1</b> and FESEM image of <b>1</b> . (i) formation of molecular layer, (ii) self-assembly of molecular layers into nanosheet and (iii) two dimensional arrangement of nanosheets to form mesosheet. ....	67
Figure 4. 1.....	78
Figure 4. 2 Schematic representation of self-assembly of randomly oriented N,N-bis- (dipeptide) appended NDI molecules into a ordered stacks under appropriate solvent system through H-bonding and $\pi$ - $\pi$ interactions.....	79
Figure 4. 3 UV-vis absorption (red curve) and Photoluminescence (black curve) studies at 5x 10 <sup>-5</sup> M (a) absorption and emission ( $\lambda_{\text{ex}} = 380 \text{ nm}$ ) of NDI <b>4</b> in CHCl <sub>3</sub> , (b) absorption	

and emission ( $\lambda_{ex} = 380$  nm) of NDI **4** in DMSO, (c absorption and emission ( $\lambda_{ex} = 380$  nm) of NDI **5** in  $CHCl_3$  (d) absorption and emission ( $\lambda_{ex} = 380$  nm) of NDI **5** in DMSO, (e) absorption and emission ( $\lambda_{ex} = 380$  nm) of NDI **6** in  $CHCl_3$ , (f) absorption and emission ( $\lambda_{ex} = 380$  nm) of NDI **6** in DMSO..... 82

Figure 4. 4 Photophysical studies of NDI **4** ( $5 \times 10^{-5}$  M) in  $CHCl_3$  (black curve) and in MCH(methylcyclohexane)/ $CHCl_3$ (95:5)(red curve). (a) UV-vis spectra, (b) Photoluminescence emission spectra(PL) ( $\lambda_{exi}$  at 380 nm), (c) and (d) SEM micrograph of NDI **4** nanospheres obtained from the MCH/ $CHCl_3$  (95:5) solvent system on glass substrate..... 84

Figure 4. 5 Photophysical studies of NDI **4** ( $5 \times 10^{-5}$  M) in  $CHCl_3$  (black curve) and in MeOH/ $CHCl_3$  (95:5) (red curve). (a) UV-vis absorption spectra, (b) photoluminescence emission spectra ( $\lambda_{exi}$  at 380 nm)..... 85

Figure 4. 6 (a) and (b) SEM micrograph open mouth nanovesicles obtained from the solution of NDI **4** [MeOH/ $CHCl_3$  (95:5)] on glass substrate..... 86

Figure 4.7 Photophysical studies of NDI **4** ( $5 \times 10^{-5}$  M) in DMSO (black curve) and in  $H_2O$ /DMSO (95:5) (red curve). (a) UV-vis absorption spectra, (b) photoluminescence emission spectra ( $\lambda_{exi}$  at 380 nm), (c) and (d) SEM micrograph of NDI **4** nanotapes obtained from  $H_2O$ /DMSO (95:5) solvent system on glass substrate..... 87

Figure 4. 8 Photophysical studies of NDI **5** ( $5 \times 10^{-5}$  M), UV-vis absorption spectra (a and c), Photoluminescence emission spectra ( $\lambda_{exi}$  at 380 nm) (b and d)..... 88

Figure 4. 9 Photophysical studies of NDI **5** ( $5 \times 10^{-5}$  M) in  $CHCl_3$  (black curve) and in MeOH/ $CHCl_3$  (95:5) (red curve). (a) UV-vis absorption spectra, (b) photoluminescence emission spectra ( $\lambda_{exi}$  at 380 nm)..... 89

Figure 4. 10 Microscopic studies of NDI <b>5</b> . (a) and (b) SEM micrograph of open mouth nanovesicles obtained from the solution of NDI <b>5</b> in MeOH/CHCl <sub>3</sub> (95:5) solvent system on glass substrate. ....	90
Figure 4. 11 Photophysical studies of NDI <b>6</b> (5x10 <sup>-5</sup> M) in CHCl <sub>3</sub> (black curve) and in MCH/CHCl <sub>3</sub> (95:5) (red curve ). (a) UV-vis absorption spectra, (b) photoluminescence emission spectra ( $\lambda_{\text{exi}}$ at 380 nm), (c) and (d) SEM micrograph of NDI <b>6</b> nanocubes obtained from the MCH/CHCl <sub>3</sub> (95:5) solution on glass substrate. ....	91
Figure 4. 12 Photophysical studies of NDI <b>6</b> (5x10 <sup>-5</sup> M), (a) and (c) UV-vis absorption spectra, (b) and (d) Photoluminescence emission spectra ( $\lambda_{\text{exi}}$ at 380 nm), (e)FESEM micrograph of NDI <b>6</b> nanocubes obtained from the H <sub>2</sub> O/DMSO (95:5) solvent system.	92
Figure 4. 13 Proposed schematic model to explain the self-assembly process of N, N-bis-(dipeptide) appended NDI systems <b>4</b> , <b>5</b> and <b>6</b> into zero-, one-, two- and three-dimensional nanostructures (nanosphere, nanotape, open mouth nanovesicle and nanocube) .....	94

## List of Tables

Table 1. 1 The naturally occurring Amino acids and their UV-vis ( $\lambda_{\text{max}}$ ) values.....	12
Table 1. 2 IR features for various conformations of peptides .....	19
Table 1. 3 CD features for $\alpha$ -helix, $\beta$ -sheet and random coil conformation .....	21
Table 1. 4 Summary of non-covalent interactions. ....	22
Table 1. 5 Typical amyloid fibril formation by remarkably short aromatic peptide fragments .....	25
Table 2. 1 $\alpha$ -Amino-protecting groups removed by acid .....	33
Table 2. 2 $\alpha$ -Amino-protecting groups removed by base.....	34

Table 2. 3 $\alpha$ -Carboxylic acid-protecting groups removed by acid .....	36
Table 2. 4 $\alpha$ -Carboxylic acid-protecting groups removed by base .....	37
Table 3. 1 Summary of the molecular structures and morphologies of the self-assembled nanostructures formed by aromatic homo dipeptides .....	54

### List of Schemes

Scheme 2. 1 Peptide synthesis strategy.P1, P2, P3= protecting groups.....	31
Scheme 2. 2 Protection of amino group functionality of glycine ethyl ester with various phthaloyl derivatives ( <b>1-8</b> ). <i>Reagents and conditions:</i> i) Microwave irradiation, Dimethylformamide, 8 min. or Et <sub>3</sub> N, Dichloromethane, reflux, 24 h. or Neat reaction, 200°C.....	39
Scheme 2. 3 Deprotection studies of $\alpha$ -amino-protected glycine ethyl ester with hydrazine.	40
Scheme 3. 1 Synthesis of cyclic dipeptide ( <i>D</i> -Phg- <i>L</i> -Phg) <b>1</b> . Reagents and conditions: i) EDC, HOBt, DIPEA, CH <sub>2</sub> Cl <sub>2</sub> , RT. ii) 15% piperidine in CH <sub>2</sub> Cl <sub>2</sub> . EDC = 1-Ethyl-3-(3-dimethylaminopropyl)carbodiimide, HOBt = 1-hydroxybenzotriazole, DIPEA = Diisopropylethylamine.....	57
Scheme 4. 1 Synthesis of dipeptide appended NDIs. Reagents and conditions: (i) C <sub>6</sub> H <sub>15</sub> N, DMF, reflux,12 h. (ii) EDC.HCl, HOBT and DIPEA, DMF, rt, 12 h. ....	80

## Abbreviations

Aq	Aqueous
Calcd	Calculated
CD	Circular Dichroism
Ch	Cyclohexyl
CSR	Chemical shift reagent
DCC	Dicyclohexylcarbodiimide
DCM	Dichloromethane
DIPEA/DIEA	Diisopropylethylamine
DMF	N, N-dimethylformamide
DMSO	N, N-Dimethyl sulfoxide
EtOAc	Ethyl acetate
Fmoc	9-Fluorenylmethoxycarbonyl
HOBt	1-Hydroxybenzotriazole
Hz	Hertz
IR	Infra red
MOLDI-TOF	Matrix Assisted Laser Desorption Ionisation-Time of Flight
MF	Molecular formula
mg	milligram
MHz	Megahertz
Min	minutes
μl	Microliter
μM	Micromolar
mmol	millimoles
MS	Mass spectrometry

MW	Molecular weight/Microwave
nm	Nanometer
NMR	Nuclear Magnetic Resonance
ppm	Parts per million
SPPS	Solid Phase Peptide Synthesis
TEA/Et <sub>3</sub> N	Triethylamine
TFA	Trifluoroacetic acid
TLC	Thin layer chromatography
UV-vis	Ultraviolet-Visible

**Chapter 1**

**INTRODUCTION**



## Chapter 1

### **INTRODUCTION**

#### **1. 1 Amino acids: Chemical structure**

The term ‘*amino acid*’ is generally understood to refer to the *aminoalkanoic acids*. They are compounds containing an amino group(  $-\text{NH}_2$ ) and a carboxylic acid group ( $-\text{COOH}$ ) with general formula  $\text{H}_3\text{N}^+(\text{CR}_1\text{R}_2)_n\text{COO}^-$  [ $n = 1$  for the series of  $\alpha$ - amino acids,  $n = 2$  for  $\beta$ -amino acids series and  $n = 3$  for  $\gamma$ - amino acids series, etc.]. More than 700 amino acids have been discovered in nature and most of them are  $\alpha$ -amino acids. Bacteria, fungi algae and plants are source for all these amino acids, which exist either in the free form or bound up into larger molecules (as constituents of peptides, proteins, other types of amide, alkylated and esterified structures). Among 700 amino acids twenty amino acids (actually, nineteen  $\alpha$ -amino acids and one  $\alpha$ -imino acid) that are utilised in living cells for protein synthesis under the control of genes are in a special category since they are fundamental to all life forms as building blocks of peptides and proteins. The structures of the 20 most common naturally occurring amino acids are shown in Table.1.1. All the amino acids except proline contain a primary amino group. Proline contains a secondary amino group incorporated in to a five-membered ring. The  $\alpha$ -amino acids differ only in the substituent ( $\text{R}_1$  in general formula,  $\text{R}_2=\text{H}$ ) attached to the  $\alpha$ -carbon. The wide variation in these substituents is what gives peptide and proteins their great structural diversity and is responsible for their great functional multiplicity. Eight kinds of side chains ( $\text{R}_1$ = aliphatic chain, hydroxyl containing, sulphur containing, acidic, amides, basic, benzene containing and heterocyclic) are present in the most common natural amino acids, in that ten are essential amino acids (denoted by red asterisks (\*) in Table 1.1.

**Table 1. 1** The naturally occurring Amino acids and their UV-vis ( $\lambda_{\max}$ ) values.

	Name	Abbreviations		MW	Structure	UV Abs Log $\epsilon$ ( $\lambda_{\max}$ ) pH ~ 7.0
		Three Letter Code	One Letter Code			
Aliphatic side chain amino acids	Glycine	Gly	G	75.07	$^+\text{H}_3\text{N}-\underset{\text{H}}{\overset{\text{H}}{\text{C}}}-\overset{\text{O}}{\parallel}{\text{C}}-\text{O}^-$	
	Alanine	Ala	A	89.09	$^+\text{H}_3\text{N}-\underset{\text{CH}_3}{\overset{\text{O}}{\parallel}{\text{C}}}-\text{O}^-$	
	Valine*	Val	V	117.15	$^+\text{H}_3\text{N}-\underset{\text{CHCH}_3}{\overset{\text{O}}{\parallel}{\text{C}}}-\text{O}^-$	
	Leucine*	Leu	L	131.17	$^+\text{H}_3\text{N}-\underset{\text{CH}_2}{\overset{\text{O}}{\parallel}{\text{C}}}-\text{O}^-$	
					$\text{CHCH}_3$	
					$\text{CH}_3$	
Hydroxy-containing amino acids	Serine	Ser	S	105.09	$^+\text{H}_3\text{N}-\underset{\text{CH}_2}{\overset{\text{O}}{\parallel}{\text{C}}}-\text{O}^-$	
	Threonine*	Thr	T	119.12	$^+\text{H}_3\text{N}-\underset{\text{CHOH}}{\overset{\text{O}}{\parallel}{\text{C}}}-\text{O}^-$	
				$\text{CH}_3$		

**Table 1.1**

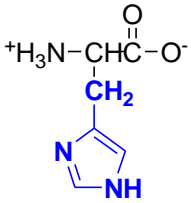
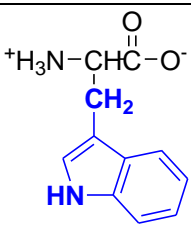
(Continued)

	Name	Abbreviations		MW	Structure	UV Abs Logε (λ <sub>max</sub> ) pH ~ 7.0
		Three Letter Code	One Letter Code			
Sulfer- containing amino acids	Cysteine	Cys	C	121.15	$  \begin{array}{c}  \text{O} \\  \parallel \\  ^+\text{H}_3\text{N}-\text{CHC}-\text{O}^- \\    \\  \text{CH}_2 \\    \\  \text{SH}  \end{array}  $	2.46  (250 nm)
	Methionine*	Met	M	149.21	$  \begin{array}{c}  \text{O} \\  \parallel \\  ^+\text{H}_3\text{N}-\text{CHC}-\text{O}^- \\    \\  \text{CH}_2 \\    \\  \text{CH}_2 \\    \\  \text{S} \\    \\  \text{CH}_3  \end{array}  $	
Acidic amino acids	Aspartate (Aspartic acid)	Asp	D	133.10	$  \begin{array}{c}  \text{O} \\  \parallel \\  ^+\text{H}_3\text{N}-\text{CHC}-\text{O}^- \\    \\  \text{CH}_2 \\    \\  \text{C}=\text{O} \\    \\  \text{O}^-  \end{array}  $	
	Glutamate (Glutamic acid)	Glu	E	147.13	$  \begin{array}{c}  \text{O} \\  \parallel \\  ^+\text{H}_3\text{N}-\text{CHC}-\text{O}^- \\    \\  \text{CH}_2 \\    \\  \text{CH}_2 \\    \\  \text{C}=\text{O} \\    \\  \text{O}^-  \end{array}  $	
Amides of acidic amino acids	Asparagine	Asn	N	132.12	$  \begin{array}{c}  \text{O} \\  \parallel \\  ^+\text{H}_3\text{N}-\text{CHC}-\text{O}^- \\    \\  \text{CH}_2 \\    \\  \text{C}=\text{O} \\    \\  \text{NH}_2  \end{array}  $	
	Glutamine	Gln	Q	146.15	$  \begin{array}{c}  \text{O} \\  \parallel \\  ^+\text{H}_3\text{N}-\text{CHC}-\text{O}^- \\    \\  \text{CH}_2 \\    \\  \text{CH}_2 \\    \\  \text{C}=\text{O} \\    \\  \text{NH}_2  \end{array}  $	

	Name	Abbreviations		MW	Structure	UV Abs Log $\epsilon$ ( $\lambda_{max}$ ) pH ~ 7.0
		Three Letter Code	One Letter Code			
Basic amino acids	Lysine*	Lys	K	146.19	$  \begin{array}{c}  \text{O} \\  \parallel \\  ^+\text{H}_3\text{N}-\text{CH}-\text{C}-\text{O}^- \\    \\  \text{CH}_2 \\    \\  \text{CH}_2 \\    \\  \text{CH}_2 \\    \\  \text{CH}_2 \\    \\  ^+\text{NH}_3  \end{array}  $	
	Arginine*	Arg	R	174.20	$  \begin{array}{c}  \text{O} \\  \parallel \\  ^+\text{H}_3\text{N}-\text{CH}-\text{C}-\text{O}^- \\    \\  \text{CH}_2 \\    \\  \text{CH}_2 \\    \\  \text{CH}_2 \\    \\  \text{NH} \\    \\  \text{C}=\text{N}^+\text{H}_2 \\    \\  \text{NH}_2  \end{array}  $	
Benzene-containing amino acids	Phenylalanine*	Phe	F	165.19	$  \begin{array}{c}  \text{O} \\  \parallel \\  ^+\text{H}_3\text{N}-\text{CH}-\text{C}-\text{O}^- \\    \\  \text{CH}_2 \\    \\  \text{C}_6\text{H}_5  \end{array}  $	3.97 (206 nm) 2.30 (257 nm)
	Tyrosine	Try	Y	181.19	$  \begin{array}{c}  \text{O} \\  \parallel \\  ^+\text{H}_3\text{N}-\text{CH}-\text{C}-\text{O}^- \\    \\  \text{CH}_2 \\    \\  \text{C}_6\text{H}_4 \\    \\  \text{OH}  \end{array}  $	3.90 (222 nm) 3.15 (274 nm)
Heterocyclic amino acids	Proline	Pro	P	115.13	$  \begin{array}{c}  \text{O} \\  \parallel \\  \text{C}-\text{O}^- \\    \\  \text{H}_2^+\text{N}  \end{array}  $	

**Table 1.1**

(Continued)

	Name	Abbreviations		MW	Structure	UV Abs Log $\epsilon$ ( $\lambda_{\max}$ ) pH ~ 7.0
		Three Letter Code	One Letter Code			
Heterocyclic amino acids	Histidine*	His	H	155.16		3.77 (211 nm)
	Tryptophan*	Trp	W	204.23		4.67 (219 nm) 3.75 (280 nm)

\*essential amino acids

Humans can produce 10 of the 20 amino acids. The others must be supplied through food supplements. Failure to obtain enough of even one of the ten essential amino acids, those that we cannot make, results in degradation of the body's proteins, muscle and so forth to obtain the one amino acid that is needed. Unlike fat and starch, the human body does not store excess amino acids for later use; the amino acids must be supplement through food every day. The  $\alpha$ -carbon of all the naturally occurring amino acids (except glycine) is chiral. Therefore 19 of the 20 amino acids can exist as enantiomers and most amino acids found in nature have the *L*- configuration.

## 1. 2 Physicochemical properties of amino acids

The physicochemical properties of amino acids depend on a) the presence of functional groups (e.g. amino, carboxy, thiol, phenolic hydroxy, guanidino and imidazole) that can be

titrated in the pH range 0–14, b) the presence or absence of hydrophobic groups (e.g. alkyl, aryl and indole) and c) the presence or absence of neutral hydrophilic groups (e.g. aliphatic hydroxy and side-chain amide groups). The properties of peptides also depend on the same factors, but it must be remembered that in a linear peptide containing  $n$  amino-acid residues all amine and carboxyl acid groups (except one N-terminal  $\alpha$ -amino group and one C-terminal  $\alpha$ -carboxy group) are incorporated into neutral peptide via amide bonds. In a cyclic peptide there are no free  $\alpha$ -amino or  $\alpha$ -carboxy groups. Moreover, some peptides contain groups such as carbohydrate, phosphate ester, lipids and porphyrins that further modify this physical properties.

Generally amino acids are crystalline solids with high melting points (200-300°C) and soluble in water. The extent of solubility in water depends on the nature of side chain ( $R_1$ ). At physiological pH (pH = 7.3) an amino acid exist as a dipolar ion called a zwitterion. A zwitterion is a compound that has a negative charge on one atom and a positive charge on a nonadjacent atom. Therefore an amino acid can exist in an acidic form or a basic form depending on the pH of the solution in which the amino acid dissolved as shown in Figure 1.1.

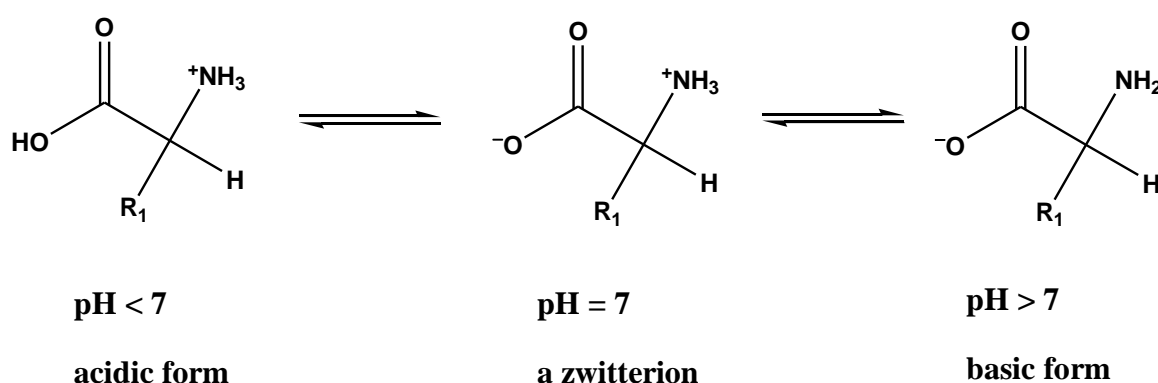


**Figure 1. 1** Existence of amino acid in different forms depends on the pH of the solution in which the amino acid dissolved.

The carboxyl groups of the amino acids have  $pK_a$  values of approximately 2 and the protonated amino groups have  $pK_a$  values near 9. Therefore, both groups will be in their acidic forms in a strong acidic solution ( $pH < 7$ ). At  $pH = 7$ , the  $pH$  of the solution is greater than the  $pK_a$  of the carboxyl group but less than the  $pK_a$  of protonated amino group. The carboxyl group therefore will be in its basic form and the amino group will be in its acidic form. Where as in basic solution ( $pH > 7$ ) both carboxyl and amino groups will be in their basic form as shown in Figure 1.1. Therefore in acidic solution an amino acid exists as a positive ion and migrates towards the cathode in an electric field, while in alkaline solution it exists as a negative ion and migrates towards anode. At a certain hydrogen ion concentration ( $pH$ ), the dipolar ion exists as a neutral ion and does not migrate to either electrode. This  $pH$  is known as the isoelectric point of the amino acid.

### 1. 3 Peptide bonds

Peptide bond is a covalent bond formed between carboxylic acid of one amino acid molecule and amino group on other amino acid; therefore it is an amide bond which holds amino acid residues together in a peptide or a protein. Conventional writing of peptide and proteins are start with the free amino group (the N-terminal amino acid) on the left and ends with the free carboxyl group (the C- terminal amino acid) on the right. Figure 1.2 showing the condensation of  $m$  number of  $\alpha$ -amino acids to give one oligopeptide containing  $m$  number of  $\alpha$ -amino acid residues and  $(m-1)$  number of water molecules.

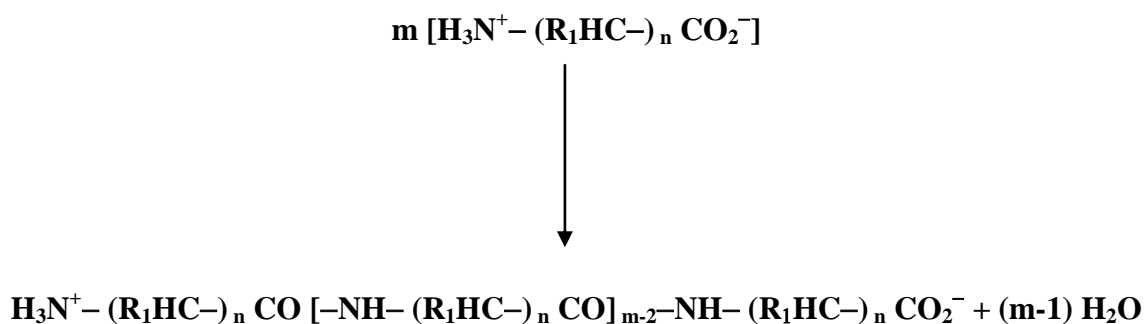


**Figure 1. 2** Condensation of  $m$  number of  $\alpha$ -amino acids to form a peptide.

The numbering of amino acids in a polypeptide starts with the N-terminal end and adjective names (ending in “yl”) are used for all the amino acids except the C-terminal amino acid. A peptide bond has partial double-bond character because of electron delocalisation over carbonyl oxygen and lone pair on amide nitrogen. Steric hindrance causes the *trans* configuration to be more stable than the *cis* configuration, i.e. the  $\alpha$ -carbons of adjacent amino acids are *trans* to each other. Free rotation about the peptide bond is not possible because of its partial double-bond character. Strategy of peptide bond synthesis and various protecting groups are discussed in Chapter 2 (Section 2.1).

#### **1. 4 General spectroscopic characterization techniques**

Interpretation of spectrometric features of amino acids and peptides provides specific information about the behaviour of amino acids and peptides in solution. These methods reveal the ways in which groupings within a peptide in solution relate to each other and these details are of major importance in determining the physical and physiological properties of amino acids and peptides.

##### **1.4.1 Infrared (IR) spectrometry**

The feature of IR spectra for solutions that is useful in the peptide area concerns the hydrogen bonding property of the amide group. The characteristic carbonyl stretching frequencies of the peptide bond depend on the conformation; therefore IR spectra give important information on conformation. IR spectra can also be interpreted to detect conformational changes that occur when solution parameters are altered; such as solution changes (changes of solvent polarity, ionic strength, etc.) can be deliberately designed either to disrupt or to augment hydrogen bonding interactions and these changes lead to differing stretching frequencies of the amide group as shown in Table 1.2.



**Table 1. 2** IR features for various conformations of peptides

	$\nu$ (cm <sup>-1</sup> )
N—H stretching frequency of the —CO—NH— grouping	$\nu = 3360\text{--}3260$
<i>trans</i> -amides	$\nu = 1250, 1550$
<i>cis</i> -amides	$\nu = 1350, 1500$
hydrogen-bonded amide bond of the $\alpha$ -helix conformation	$\nu = 620, 1650$
$\beta$ -sheet conformation	$\nu = 700, 1630$ (strong) and 1690 (weak)
peptide bond in random (disordered) conformations	$\nu = 650, 1660$

#### 1.4.2 Ultraviolet (UV) spectrometry, Circular dichroism (CD) and fluorescence spectrometry

These techniques are intimately related since their spectral features originate in the same physical event namely the absorption of light within locations (chromophores) of the amino acid or peptide from the ultraviolet wavelength region ( $\lambda = 200\text{--}400$  nm) and from longer (visible) wavelengths for coloured compounds.

##### 1.4.2.1 Ultraviolet (UV) spectrometry

The chromophores that respond to electronic excitation which are common to amino acids and peptides are the amino, carboxy and amide groups. All these functional groups show almost no absorption, i.e. they are nearly transparent, showing only small extinction coefficients within the UV range (200–400 nm),—NH<sub>2</sub> (as in ammonia, NH<sub>3</sub>,  $\lambda_{\max} = 194$  nm). UV  $\lambda_{\max}$  absorption of 20 most common amino acids are shown in Table 1.1.

### 1.4.2.2 Circular dichroism (CD)

CD spectrometer is an instrument that measures the intensity of absorption of left circularly polarised light relative to that of right-circularly polarised light over a continuous range of wavelengths. CD spectra carry much more information than UV absorption spectra. The intensity of the CD absorption is dependent upon the spatial relationship between the chromophore and groupings at the chiral centre and hence there is no chromophore intensity of absorption relationship such as that which exists for UV absorption spectra (i.e. the Bouguer–Beer–Lambert law does not apply to CD spectra). The sign of the CD feature can be positive or negative, unlike the isotropic absorption (i.e. the UV absorption spectrum), which has no sign.

The CD spectrum can be interpreted in terms of absolute configuration. The sign of a particular CD feature corresponds to a particular absolute configuration of the solute, for the chiral centre nearest the chromophore responsible for that CD feature. Information on conformation (based on the sign and specific details of an overall CD spectrum for a compound of known absolute configuration) can be obtained for amino acids and peptides. Polypeptides in a random conformation show strong CD features only at short wavelengths, but characteristically enhanced CD features are observed at longer wavelengths if a molecule adopts a regular conformation and it contains a chromophore that is repeated regularly with spatial uniformity throughout the molecule as in the case of ordered peptides ( $\alpha$ -helix and the  $\beta$ -sheet structures). CD characteristics for  $\alpha$ -helix,  $\beta$ -sheet and random coil are shown in Table 1.3.

**Table 1. 3** CD features for  $\alpha$ -helix,  $\beta$ -sheet and random coil conformation

	<b>Positive CD maximum</b>	<b>Zero CD</b>	<b>Negative CD maximum</b>
<b><math>\alpha</math>-Helix</b>	Very strong at 191 nm	202, 250 nm	Strong at 208, 222 nm
<b><math>\beta</math>-Sheet</b>	Strong at 195 nm	207, 250 nm	Medium intensity at 217 nm
<b>Random coil</b>	Weak at 218 nm	211, 234, 250 nm	Strong at 197 nm Very weak at 240 nm

### 1. 5 Self-assembly

The spontaneous and reversible association of molecular species to form larger, more complex supramolecular entities according to the intrinsic information contained in the components.

- There is no significant difference in size and no species is acting as a host for another.
- Self-assembling systems selectively produce the most thermodynamically stable products and therefore both the enthalpic and entropic contributions towards the final species must be considered.

**Intramolecular self-assembly** molecules are often complex polymers with the ability to assemble from the random coil conformation into a well-defined stable structure. An example of Intramolecular self-assembly is protein folding.

**Intermolecular self-assembly** is the ability of molecules to form supramolecular assemblies. A simple example is the formation of a micelle by surfactant molecules in solution.

## 1.6 Non-covalent interactions

Supramolecular chemistry exists because of non-covalent interactions. Nature also uses such supramolecular (non-covalent) interactions extensively in bringing proteins together to form enzyme super clusters, or sometimes to form structurally less defined fibrous aggregates. Supramolecular chemistry tries to mimic nature approach by utilizing interactions that are considerably weaker than covalent interactions. Non-covalent interactions can be a repulsive or attractive intermolecular forces having interaction energy ranging from 4-400  $\text{KJmol}^{-1}$ . Various non-covalent interactions and their strength are summarized in Table 1.4. From the Table 1.4 the order of supramolecular interaction strengths are ion-ion > ion-dipole > dipole-dipole > hydrogen bonding > cation- $\pi$  >  $\pi$ - $\pi$  interactions.

**Table 1.4** Summary of non-covalent interactions.<sup>2</sup>

Interaction	Energy( $\text{KJmol}^{-1}$ )	Example
Ion-ion	50-400	tetrabutylammonium chloride
Ion-dipole	50-200	sodium(15)crown-5
Dipole-dipole	4-40	acetone
Hydrogen bonding	4-120	HF complexes
Cation- $\pi$	5-80	$\text{K}^+$ in benzene
$\pi$ - $\pi$	4-20	benzene and graphite
van der Waals	<5	between two straight alkyl chains
hydrophobic	related to solvent-solvent interaction	cyclodextrin inclusion compound

## 1. 7 Bioactive peptide-based functional nanomaterials

Self-assembly of biomolecular building blocks plays an important role in the discovery of new biomaterials and scaffolds with a wide range of applications in nanotechnology and biomedical (Figure 1.3). Especially, coating nanostructures with peptides gives them with unique opportunities to explore the vast biological events that peptides mediate.<sup>32-38</sup>

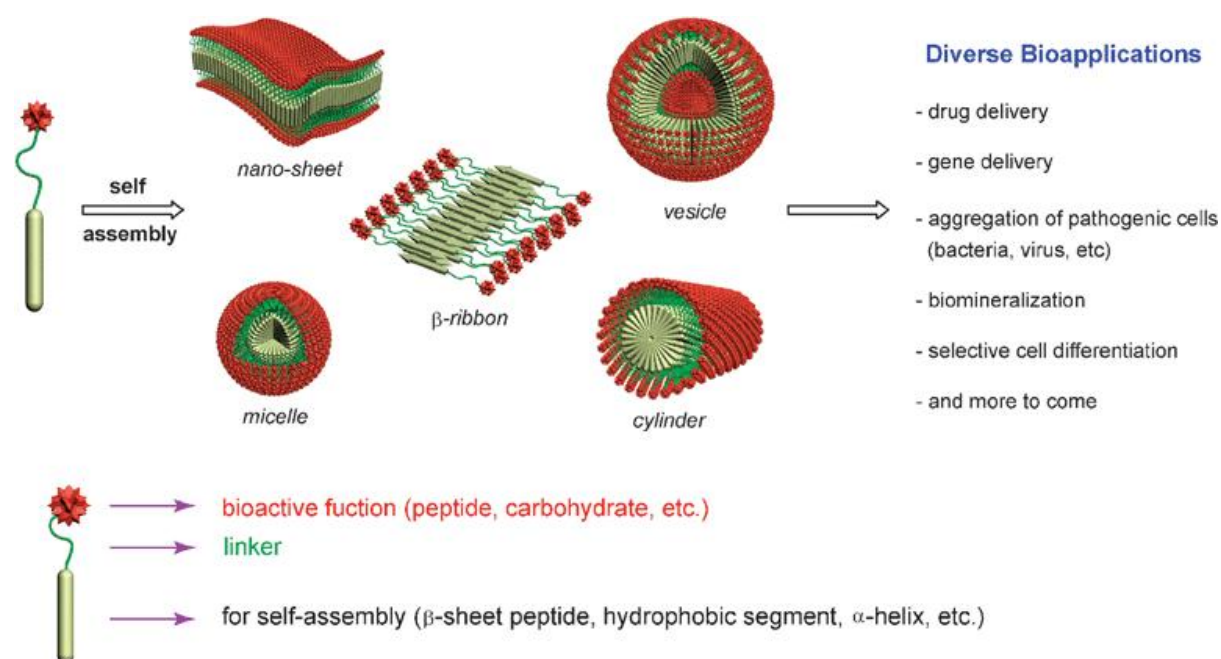


**Figure 1. 3** Self-assembled bioactive nanostructures.<sup>51</sup>

Peptide-based self-assembling systems are investigated for the construction of supramolecular structures which have potential applications as biocompatible multivalent scaffolds. The peptides usually assemble through  $\alpha$ -helical,  $\beta$ -sheet, and hydrophobic interactions.<sup>39-42</sup> Examples of peptide-based self-assembly systems include micelles from peptide amphiphiles,<sup>43</sup> coiled-coils from  $\alpha$ -helical peptide bundles,<sup>44</sup> nanotubes from cyclic peptides,<sup>45</sup> nanotubes and nanocages from dipeptides,<sup>46</sup> open mouth nanovesicles from diblock peptides of polylysine or polyarginine and polyleucine,<sup>47</sup> thermoresponsive elastin-like aggregates,<sup>48</sup> closed-micelles from peptide-PEG block copolymers,<sup>49</sup> and nanofibers

from  $\beta$ -sheet peptides.<sup>50</sup> The peptide nanostructures have mostly been used for applications in drug delivery, gene delivery and antimicrobial agent development. Among the peptide nanostructures, the  $\beta$ -sheet peptide nanostructures are likely to be especially suitable for applications where fibrous structures are advantageous in crosslinking cells and *in vivo* delivery experiments.

In nature formation of amyloid fibrils is a key example of polypeptide self-assembly into ordered nanoscale fibrillar structures. The accumulation of amyloid fibrils is a common characteristic of several unrelated diseases including Alzheimer's disease, prion disorders<sup>3-10</sup> (bovine spongiform encephalopathy and Creutzfeldt–Jakob disease), type II diabetes, and many other neurodegenerative disorders. Currently about 20 different known syndromes are associated with the formation of amyloid deposits. All these diseases are characterized by the transformation of soluble polypeptides or proteins into aggregated fibrillar deposits in different organs and tissues. The pathological significance of amyloid fibril formation is not completely understood in all cases. Some of the observations on amyloid formation suggests that a specific pattern of molecular interactions rather than nonspecific hydrophobic interactions should play a role in the formation of such an ordered amyloid structure.<sup>11</sup> Moreover, the synthesis of large peptides especially aggregative peptides is expensive and difficult. An important direction in studying amyloid formation has emerged from the use of remarkably short peptide fragments. Much of the pioneering work on the use of peptide models for the study of amyloid fibril formation was carried out by Westermark and co-workers<sup>12-14</sup> This group had already demonstrated (1990) that a short decapeptide fragment of the islet amyloid polypeptide (IAPP) a polypeptide associated with type II diabetes<sup>12,15</sup> can form amyloid fibrils similar to those formed by the full-length 37 amino acid polypeptide.<sup>12</sup> Table 1.5 list of short amyloidogenic peptides in the literature.<sup>16</sup>

**Table 1. 5** Typical amyloid fibril formation by remarkably short aromatic peptide fragments \*

Name of parent peptide	Pathological or physiological condition	Short active sequence	Reference
Islet amyloid polypeptide	Type II diabetes	1. <u>F</u> GAIL	17
		2. TNVGSNT <u>Y</u> <sup>b</sup>	18
		3. QRLAN <u>F</u> LVH <sup>b</sup>	19
β-Amyloid peptide	Alzheimer's disease	1. KLV <u>FF</u> (inhibitor)	20
		2. LV <u>FF</u> A (inhibitor)	21
		3. LP <u>FF</u> D (inhibitor)	22
		4. KLV <u>FF</u> AE <sup>b</sup>	23
Lactadherin	Aortic medial amyloid	NEGSVQ <u>F</u> V <sup>b</sup>	24
Gelsolin	Finnish hereditary amyloidosis	S <u>F</u> NNGDCC <u>F</u> ILD <sup>b</sup>	25
Serum amyloid A	Chronic inflammation amyloidosis	S <u>FF</u> S <u>F</u> LGEA <u>F</u> D <sup>b</sup>	26
PrP	Creutzfeldt-Jakob disease (CJD)	PHGGG <u>W</u> GQ	27 , 28
Sup35p	Yeast prion protein	PQGGY <u>Q</u> QYN <sup>c</sup>	29 , 30
		GNNQ <u>Q</u> NY	31

<sup>a</sup> Aromatic residues are underlined.

<sup>b</sup> The minimal active fragment may be shorter.

<sup>c</sup> Consensus sequence of six tandem repeats. In one of the repeats, Y is replaced by F.

\*Gazit E, *FASEB J* **2002**, 16, 77–83

## 1. 8 Present work

This project work was mainly focused on synthesis of a short acyclic/cyclic/hybrid peptide which can self-assemble through non-covalent interactions to form well defined nanostructures with nanoscale order and their potential applications. The studies involve the characterization of resulting self-assembled nanostructures using various spectroscopic and microscopic techniques. These peptide based nanomaterials find applications in organic electronics as well as biomaterials.

## 1. 9 References

- 1 Barret,G. C.; Elmore,D. T. (2004) Amino Acids and Peptides, Cambridge University Press
- 2 Williams,D. H.; Westwell,M.S,*Chem.Soc.Rev.*,**1998**, 27,57
- 3 Harper, J. D.; Lansbury, P.T. Jr. *Annu. Rev. Biochem*, **1997**, 66, 385.
- 4 Sunde, M.; Blake, C. C. F. *Q. Rev. Biophys.*, **1998**, 31, 1.
- 5 Dobson, C. M. *Trends Biochem. Sci.*, **1999**, 24, 329.
- 6 Sipe, J. D.; Cohen, A. S. *J. Struct. Biol.*, **2000**, 130, 88.
- 7 Moriyama, H.; Roberts, B. T. *J. Struct. Biol.*, **2000**, 130, 310.
- 8 Gazit, E. *Angew. Chem. Int. Edit.*, **2002**, 41, 257.
- 9 Gazit, E. *Curr. Med. Chem.*, **2002**, 9, 1667.
- 10 Gazit E, *FASEB J* **2002**, 16, 77–83
- 11 Westermark P, Engstrom U, Johnson KH, Westermark GT & Betsholtz C, *Proc. Natl. Acad Sci. USA* **1990**, 87, 5036–5040.
- 12 Westermark GT, Engstrom U & Westermark P, *Biochem Biophys Res Commun* **1992**, 182, 27–33.
- 13 Ha ggqvist B, Na slund J, Sletten K, Westermark GT, Mucchiano G, Tjernberg LO, Nordstedt C, Engstrom U & Westermark P *Medin, Proc. Natl. Acad. Sci. USA* **1999**, 96, 8669–8674.
- 14 Jaikaran ET & Clark A , *Biochim Biophys Acta* **2001**, 1537, 179–203
- 15 Westermark GT, Engstro¨m U & Westermark P, *Biochem Biophys Res Commun* **1992**, 182, 27–33.
- 16 Tenidis, K., Waldner, M., Bernhagen, J., Fischle, W., Bergmann. M., Weber, M., Merkle, M. L., Voelter, W., Brunner, H., and Kapurniotu, A., *J. Mol. Biol* **2000**, 295, 1055–1071
- 17 Nilsson, M. R., and Raleigh, D. P., *J. Mol. Biol* **1999**, 294, 1375–1385
- 18 Jaikaran, E. T. A. S., Higham, C. E., Serpell, L. C., Zurdo, J., Gross, M., Clark, A., Fraser, P. E. , *J. Mol. Biol* **2001**, 308, 515–525
- 19 Tjernberg, L. O., Na¨slund, J., Lindqvist, F., Iohansson, J., Karlstro¨m, A. R., Thyberg, J., Terenius, L., and Nordstedt, C., *J. Biol. Chem* **1996**, 271, 8545–8548



- 20 Findeis, M. A., Musso, G. M., Arico-Muendel, C. C., Benjamin, H. W., Hundal, A. M., Lee, J. J., Chin, J., Kelley, M., Wakefield, J., Hayward, N. J., Molineaux, S. M. , *Biochemistry* **1999**, *38*, 6791–6800
- 21 Soto, C., Sigurdsson, E. M., Morelli, L., Kumar, R. A., Castano, E. M., and Frangione, B. , *Nature Med* **1998**, *4*, 822–826
- 22 Balbach, J. J., Ishii, Y., Antzutkin, O. N., Leapman, R. D., Rizzo, N. W., Dyda, F., Reed, J., Tycko, R., *Biochemistry* **2000**, *39*, 13748–13759
- 23 Haˆggqvist, B., Naˆslund, J., Sletten, K., Westermark, G. T., Mucchiano, G., Tjernberg, L. O., Nordstedt, C., Engstroˆm, U., Westermark, P. *Proc. Natl. Acad. Sci. USA* **1999**, *96*, 8674–8669
- 24 Mucchiano, G., Cornwell, G. G., III., Westermark, P. *Am. J. Pathol* **1992**, *140*, 811–877
- 25 Maury, C. P., and Nurmiaho-Lassila, E. L., *Biochem. Biophys. Res. Commun* **1992**, *183*, 227–231
- 26 Westermark, G. T., Engstroˆm, U., Westermark, P., *Biochem. Biophys. Res. Commun* **1992**, *182*, 27–33
- 27 Prusiner, S. B., DeArmond, S. J., *Int. J. Exp. Clin. Invest* **1995**, *2*, 39–65
- 28 Priola, S. A., Chesebro, B., *J. Biol. Chem* **1998**, *273*, 11980–11985
- 29 Patino, M., Liu, J. J., Glover, J. R., Lindquist, S., *Science* **1996**, *273*, 622–626
- 30 Tuite, M. F., *Cell* **2000**, *100*, 289–292
- 31 Zhang. S., *Nat. Biotechnol.*, **2003**, *21*, 1171.
- 32 Langer. R., Tirrell D. A. , *Nature*, **2004**, *428*, 487.
- 33 Silva G. A., Czeisler C., Niece K. L., Beniash E., Harrington D. A., Kessler J. A., Stupp S. I., *Science*, **2004**, *303*, 1352.
- 34 Ghadiri M. R., Granja J. R., Milligan R. A., McRee D. E., Khazano-vich N., *Nature*, **1993**, *366*, 324.
- 35 Holowka E. P., Sun V. Z., Kamei D. T., Deming T. J., *Nat. Mater.*, **2007**, *6*, 52.
- 36 Y.-b. Lim, S. Park, E. Lee, H. Jeong, J.-H. Ryu, M. S. Lee, M. Lee, *Biomacromolecules*, **2007**, *8*, 1404.
- 37 Y.-R. Yoon, Y.-b. Lim, E. Lee , M. Lee, *Chem. Commun.*, **2008**, 1892

- 38 S. X. Ye, J. W. Strzalka, B. M. Discher, D. Noy, S. Y. Zheng, P. L. Dutton and J. K. Blasie, *Langmuir*, **2004**, *20*, 5897–5904.
- 39 S. G. Zhang, *Nat. Biotechnol.*, **2003**, *21*, 1171–1178.
- 40 S. Fernandez-Lopez, H. S. Kim, E. C. Choi, M. Delgado, J. R. Granja, A. Khasanov, K. Kraehenbuehl, G. Long, D. A. Weinberger, K. M. Wilcoxon and M. R. Ghadiri, *Nature*, **2001**, *412*, 452–455.
- 41 J. D. Hartgerink, E. Beniash and S. I. Stupp, *Science*, **2001**, *294*, 1684–1688.
- 42 (a) G. A. Silva, C. Czeisler, K. L. Niece, E. Beniash, D. A. Harrington, J. A. Kessler and S. I. Stupp, *Science*, **2004**, *303*, 1352–1355; (b) K. Rajangam, H. A. Behanna, M. J. Hui, X. Han, J. F. Hulvat, J. W. Lomasney and S. I. Stupp, *Nano Lett.*, **2006**, *6*, 2086–2090.
- 43 (a) M. M. Stevens, N. T. Flynn, C. Wang, D. A. Tirrell and R. Langer, *Adv. Mater.*, **2004**, *16*, 915–918; (b) M. J. Pandya, G. M. Spooner, M. Sunde, J. R. Thorpe, A. Rodger and D. N. Woolfson, *Biochemistry*, **2000**, *39*, 8728–8734; (c) E. B. Hadley and S. H. Gellman, *J. Am. Chem. Soc.*, **2006**, *128*, 16444–16445; (d) L. J. Leman, D. A. Weinberger, Z.-Z. Huang, K. M. Wilcoxon and M. R. Ghadiri, *J. Am. Chem. Soc.*, **2007**, *129*, 2959–2966.
- 44 (a) M. R. Ghadiri, J. R. Granja, R. A. Milligan, D. E. Mcrecree and N. Hazanovich, *Nature*, **1993**, *366*, 324–327; (b) J. H. van Maarseveen, W. S. Horne and M. R. Ghadiri, *Org. Lett.*, **2005**, *7*, 4503–4506.
- 45 (a) M. Reches and E. Gazit, *Science*, **2003**, *300*, 625–627; (b) S. Ghosh, M. Reches, E. Gazit and S. Verma, *Angew. Chem., Int. Ed.*, **2007**, *46*, 2002–2004.
- 46 (a) E. P. Holowka, V. Z. Sun, D. T. Kamei and T. J. Deming, *Nat. Mater.*, **2007**, *6*, 52–57; (b) E. P. Holowka, D. J. Pochan and T. J. Deming, *J. Am. Chem. Soc.*, **2005**, *127*, 12423–12428.
- 47 (a) D. W. Urry, C.-H. Luan, T. M. Parker, D. C. Gowda, K. U. Prasad, M. C. Reid and A. Safavy, *J. Am. Chem. Soc.*, **1991**, *113*, 4346–4348; (b) D. E. Meyer and A. Chilkoti, *Biomacromolecules*, **2004**, *5*, 846–851; (c) A. Valiaev, D. W. Lim, T. G. Oas, A. Chilkoti and S. Zauscher, *J. Am. Chem. Soc.*, **2007**, *129*, 6491–6497.

- 48 Y. Lee, S. Fukushima, Y. Bae, S. Hiki, T. Ishii and K. Kataoka, *J. Am. Chem. Soc.*, **2007**, *129*, 5362–5363.
- 49 (a) G. T. Dolphin, P. Dumy and J. Garcia, *Angew. Chem., Int. Ed.*, **2006**, *45*, 2699–2702; (b) C. W. G. Fishwick, A. J. Beevers, L. M. Carrick, C. D. Whitehouse, A. Aggeli and N. Boden, *Nano Lett.*, **2003**, *3*, 1475–1479; (c) D. Eckhardt, M. Groenewolt, E. Krause and H. G. Boerner, *Chem. Commun.*, **2005**, 2814–2816; (d) W. H. Binder and O. W. Smrzka, *Angew. Chem., Int. Ed.*, **2006**, *45*, 7324–7328; (e) H. Shao, J. W. Lockman and J. R. Parquette, *J. Am. Chem. Soc.*, **2007**, *129*, 1884–1885; (f) K. Janek, J. Behlke, J. Zipper, H. Fabian, Y. Georgalis, M. Beyermann, M. Bienert and E. Krause, *Biochemistry*, **1999**, *38*, 8246–8252; (g) H. Dong, S. E. Paramonov, L. Aulisa, E. L. Bakota and J. D. Hartgerink, *J. Am. Chem. Soc.*, **2007**, *129*, 12468–12472.
- 50 Y. Lim, K. S. Moon and M. Lee, *Chem. Soc. Rev.*, **2009**, *38*, 925–934

Chapter 2

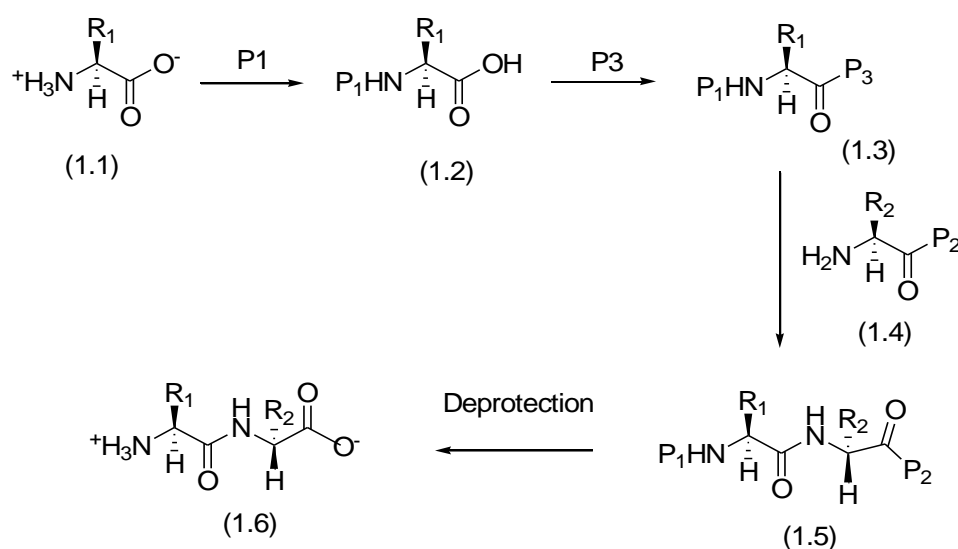
**Developing New Protecting Group Strategy for Solution and Solid  
Phase Peptide Synthesis**

## Chapter 2

### Developing New Protecting Group Strategy for Solution and Solid Phase Peptide Synthesis

#### 2. 1 Introduction

**2.1. 1 Basic principles of peptide synthesis and strategy:** The synthesis of a dipeptide  $^+\text{H}_3\text{NCHR}_1\text{CONHCHR}_2\text{COO}^-$  from the constituent amino acids involves forming the peptide bond so that the amino acid sequence is correct and racemization at the chiral  $\alpha$ -carbon atoms is avoided. The latter point does not arise, of course, with glycine. In order to produce the



**Scheme 2. 1** Peptide synthesis strategy. P1, P2, P3= protecting groups

correct sequence and to prevent the formation of a mixture of higher peptides, the amino group of the intended N-terminal residue and carboxyl group of the intended C-terminal residue are normally protected.

The synthesis of a dipeptide in general involves four steps (Scheme 2.1)-(a) protection of the amino group of the amino acid that is to be the N-terminal residue (1.1→1.2), (b) protection of the carboxyl group of the amino acid that is to be the C-terminal residue in the dipeptide (1.4), (c) activation of the carboxyl group of the N-terminal amino acid (1.2→1.3) and formation of the peptide bond to give a protected dipeptide (1.3+1.4→1.5) and (d) removal of protecting groups (1.5→1.6). If the amino acids contain functional groups such as —NH<sub>2</sub>, —COOH, —OH, and —SH, it may be desirable or even essential to protect these before step (c) or even before step (a) or step (b). If the dipeptide is to be further extended to a tripeptide, then step (d) would be modified to deprotect the  $\alpha$ -amino group selectively. Steps (a), (c) and (d) would then be carried out to couple the new *N*-terminal amino acid. The need for selective deprotection of the  $\alpha$ -amino group can be easily understood in the case in which Lys is the *N*-terminal residue. Lys has two amino groups and so different or *orthogonal*<sup>1</sup> protecting groups must be used so that one can be removed without affecting the other.

### **2.1. 2 Protection of $\alpha$ -amino group**

The  $\alpha$ -amino-protecting group should confer solubility in the most common solvents and prevent or minimize epimerization during the coupling, and its removal should be fast, efficient, and free of side reactions and should render easily eliminated byproducts. Other desired characteristics of  $\alpha$ -amino-protected amino acids are that they are crystalline solids, thereby facilitating manipulation, and stable enough.

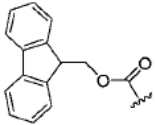
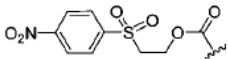
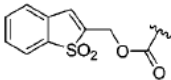
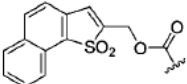
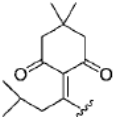
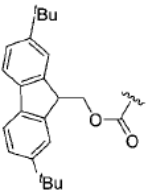
Almost all protecting groups currently used can be removed by mild methods such as hydrogenolysis and exposure to anhydrous acids or bases at room temperature. These three methods of deprotection afford the opportunity for orthogonal protection provided that particular protecting groups survive at least one type of deprotective treatment. Some of  $\alpha$ -aminoacids protecting groups and deprotection conditions have been reported (Table 2.1)

**Table 2.  $1\alpha$ -Amino-protecting groups removed by acid<sup>a</sup>**

Name and Structure	Removal conditions	Stability to the removal of	Ref.
<p><i>tert</i>-Butyloxycarbonyl (<i>Boc</i>)</p>	1) 25-50% TFA-DCM 2) 4 M HCl in dioxane 3) 2 M MeSO <sub>3</sub> H in dioxane 4) 1 M TMS-Cl, 1 M phenol-DCM	Fmoc, Z, <sup>a</sup> Trt, Alloc, <i>p</i> NZ	1, 2, 3, 4, 5, 6
<p>Tryl (<i>Trt</i>)</p>	1) 1% TFA-DCM 2) 0.1 M HOBT-TFE 3) 0.2% TFA, 1% H <sub>2</sub> O-DCM 4) 3% TCA-DCM	Fmoc, Alloc	7, 8, 9, 10, 11, 12, 13, 14
<p>3,5-Dimethoxyphenylisopropoxycarbonyl (<i>Ddz</i>)</p>	1-5% TFA-DCM	Fmoc, Alloc	15, 16, 17
<p>2-(4-Biphenyl)isopropoxycarbonyl (<i>Bpoc</i>)</p>	0.2-0.5%-TFA	Fmoc, Alloc	18, 19, 20, 21, 22, 23
<p>2-Nitrophenylsulfenyl (<i>Nps</i>)</p>	1) Diluted solutions of HCl-CHCl <sub>3</sub> -AcOH 2) 2-Mercaptopyridine-AcOH-MeOH, DMF or DCM 3) Ni Raney column in DMF	Fmoc	24, 25, 26, 27

<sup>a</sup>Chem. Rev. 2009, 109, 2455-2504.

Table 2. 2  $\alpha$ -Amino-protecting groups removed by base<sup>a</sup>

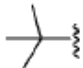
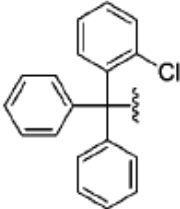
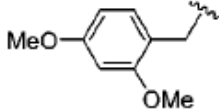
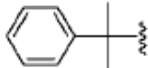
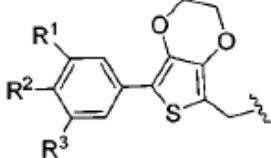
Name and Structure	Removal conditions	Stability to the removal of	Ref.
<p><b>9-Fluorenylmethoxycarbonyl (Fmoc)</b></p> 	<p><u>Solid phase:</u></p> <ol style="list-style-type: none"> <li>1) 20% piperidine-DMF</li> <li>2) 1-5% DBU-DMF</li> <li>3) morpholine-DMF (1:1)</li> <li>4) 2% HOBt, 2% hexamethyleneimine, 25% <i>N</i>-methylpyrrolidine in DMSO-NMP (1:1)</li> </ol> <p><u>Solution:</u></p> <ol style="list-style-type: none"> <li>1) NH<sub>3</sub> (10 h)</li> <li>2) morpholine or piperidine in organic solvents (within minutes)</li> <li>3) 10% DEA, DMA (2 h)</li> <li>4) polymeric secondary amines (i.e. piperidine, piperazines) in organic solvents</li> </ol>	Boc, Z, <sup>a</sup> Trt, Alloc, <i>p</i> NZ <sup>a</sup>	28, 29, 30, 32, 33, 34, 35, 36, 37, 38, 39, 40, 41, 42.
<p><b>2-(4-Nitrophenylsulfonyl)ethoxycarbonyl (Nsc)</b></p> 	<ol style="list-style-type: none"> <li>1) 20% of piperidine-DMF or DMF-dioxane (1:1)</li> <li>2) 1% DBU-DMF or DMF-dioxane (1:1)</li> </ol>	Boc, Trt, Alloc	43, 44, 45, 46, 47, 48
<p><b>(1,1-Dioxobenzob[<i>b</i>]thiophene-2-yl)methyloxycarbonyl (Bsmoc)</b></p> 	<ol style="list-style-type: none"> <li>1) 2-5% piperidine-DMF</li> <li>2) 2% TAEA-DCM</li> </ol>	Boc, Trt, Alloc	49, 50, 51, 53, 54
<p><b>(1,1-Dioxonaphtho[1,2-<i>b</i>]thiophene-2-yl)methyloxycarbonyl (<math>\alpha</math>-Nsmoc)</b></p> 	<ol style="list-style-type: none"> <li>1) 2-5% piperidine-DMF</li> <li>2) 2% TAEA-DCM</li> </ol>	Boc, Trt, Alloc	55
<p><b>1-(4,4-Dimethyl-2,6-dioxocyclohex-1-ylidene)-3-methylbutyl (ivDde)</b></p> 	2% N <sub>2</sub> H <sub>4</sub> ·H <sub>2</sub> O-DMF	Boc, Fmoc, Z, <sup>a</sup> Trt, Alloc	56
<p><b>2,7-Di-<i>tert</i>-butyl-Fmoc (Fmoc*)</b></p> 	20% piperidine-DMF (solid phase)	Boc, Trt, Alloc	58, 59, 60



### 2.1.3 Protection of $\alpha$ -carboxyl group

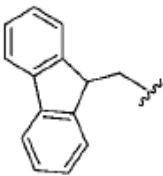
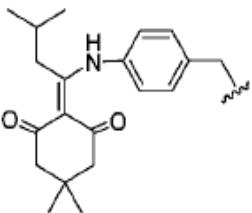
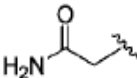
More generally, the *C*-terminal group is protected as an ester. Since esters of amino acids and peptides do not have a dipolar ion structure, they are soluble in aprotic solvents. There is also a striking difference in the  $pK_a$  values of amino acids and its esters. That the  $pK_a$  values of the esters are lower means that the  $NH_3^+$  group can lose its proton to a weaker base. These factors together mean that peptide-bond formation can be carried out in aprotic solvents with less risk of the reactive derivative of the *N*-protected *N*-terminal amino acid being racemised. It should also be noted that the lower  $pK_a$  of the amino group of an amino acid ester implies a weaker nucleophilic character. This is seldom a significant factor in peptide synthesis. Table 2.3 & 2.4 shows some of  $\alpha$ -carboxylic acid protecting groups reported in the literature.

Table 2. 3  $\alpha$ -Carboxylic acid-protecting groups removed by acid<sup>a</sup>

Name and Structure	Removal conditions	Stability to the removal of	Ref.
<p><i>tert</i>-Butyl (<i>t</i>Bu)</p> 	90% TFA-DCM (solid phase and solution) or 4 M HCl in dioxane (solution)	Fmoc, Z, <sup>a</sup> Trt Alloc, <i>p</i> NZ,	61, 62
<p>2-Chlorotrityl (2-Cl-Trt)</p> 	1% TFA-DCM	Fmoc, Alloc	63
<p>2,4-Dimethoxybenzyl (<i>Dmb</i>)</p> 	1% TFA-DCM	Fmoc, Alloc	64
<p>2-Phenylisopropyl (2-Ph<sup>i</sup>Pr)</p> 	4% TFA-DCM	Fmoc, Alloc	65
<p>5-Phenyl-3,4-ethylenedioxythienyl (<i>Phenyl-EDOTn</i>)</p>  <p>R<sup>1</sup>=R<sup>2</sup>=R<sup>3</sup>= OMe; R<sup>1</sup>=R<sup>2</sup>= OMe, R<sup>3</sup>= H; R<sup>1</sup>=R<sup>2</sup>= H, R<sup>3</sup>= OMe or R<sup>1</sup>=R<sup>2</sup>=R<sup>3</sup>= H.</p>	0.01%-0.5% TFA-DCM and scavengers	Fmoc	66

<sup>a</sup> Chem. Rev. 2009, 109, 2455-2504.

**Table 2. 4  $\alpha$ -Carboxylic acid-protecting groups removed by base<sup>a</sup>**

<b>Name and Structure</b>	<b>Removal conditions</b>	<b>Stability to the removal of</b>	<b>Ref.</b>
<p><b>9-Fluorenylmethyl (Fm)</b></p> 	15% DEA or 20% piperidine-DMF or DCM	Boc, Trt, Alloc	67, 68 69, 70
<p><b>4-(N-[1-(4,4-dimethyl-2,6-dioxocyclohexylidene)-3-methylbutyl]-amino)benzyl (Dmab)</b></p> 	2% hydrazine-H <sub>2</sub> O-DMF (1:1)	Boc, Fmoc, Trt,	71
<p><b>Methyl (Me) and Ethyl (Et)</b></p>	LiOH, NaOH or KOH	Boc, Z	72, 73
<p><b>Carbamoylmethyl (Cam)</b></p> 	NaOH or Na <sub>2</sub> CO <sub>3</sub> -DMF-H <sub>2</sub> O	Boc, Fmoc <sup>a</sup> Z <sup>b</sup>	74, 75

<sup>a</sup> Chem. Rev. 2009, 109, 2455-2504.

## 2. 2 Objective of the present work

The objective of this project is to develop new protecting group for amino functionality of amino acid, which can easily and quickly deprotected by appropriate deprotecting agents without effecting any other protecting groups. And also characterize the resulting compound through various spectroscopic studies.

### 2. 3 Design strategy

Conventionally benzoyloxycarbonyl (Z), tert-butoxycarbonyl (Boc) and Fluorenylmethoxycarbonyl (Fmoc) are used for protection of amino functionality. The main drawbacks of using these protecting groups is that they are expensive and requires harsh and tedious cleavage conditions which also leads to racemisation at  $\alpha$ -centres. It was found that phthalic anhydride offers excellent protection for the  $-\text{NH}_2$  functionality of amino acids but the deprotection step is particularly tedious requiring higher reaction time and nucleophilic deprotecting agent. An improved tetrachlorophthaloyl protecting group<sup>76</sup> has been developed but this again faces the problem of tedious deprotection and does not prove to be better than the normal phthaloyl protecting group in terms of deprotection time.

It occurs to us that addition of electron withdrawing groups to phthaloyl aromatic ring or electronegative atoms in the aromatic ring greatly enhances deprotection under milder condition and lower reaction time. We have decided to explore different electron withdrawing substituent's ( $\text{R}_1, \text{R}_2, \text{R}_3, \text{R}_4$ ) to the phthaloyl ring and electronegative atoms ( $\text{X}_1, \text{X}_2$  and  $\text{X}_3$ ) in the phthaloyl aromatic ring, as shown in Figure 2.1. For initial studies, we chose simple amino acid glycine ethyl ester and eight phthaloyl derivatives with different substituent groups in phthaloyl aromatic ring as shown in Figure 2.1.

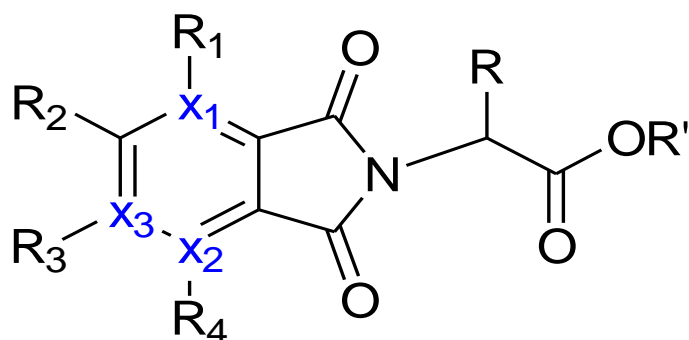
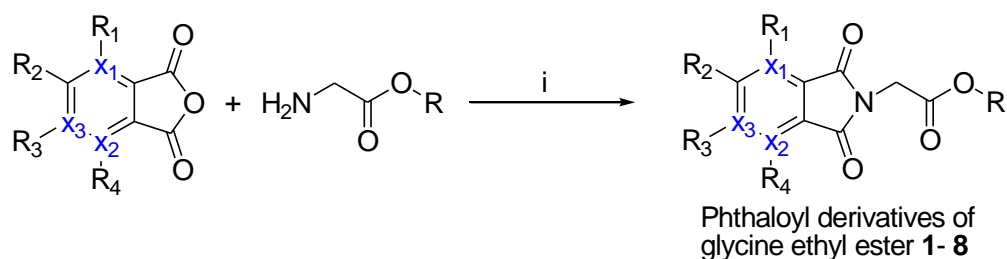


**Figure 2. 1** Our strategy for screening new protecting group for amine functionality of amino acid based on phthaloyl protecting group.  $R_1$ ,  $R_2$ ,  $R_3$  and  $R_4$  are electron withdrawing groups.  $X_1$ ,  $X_2$ ,  $X_3$  are electronegative atoms.  $R$  = substituent.  $R'$  = carboxylic acid protecting group.

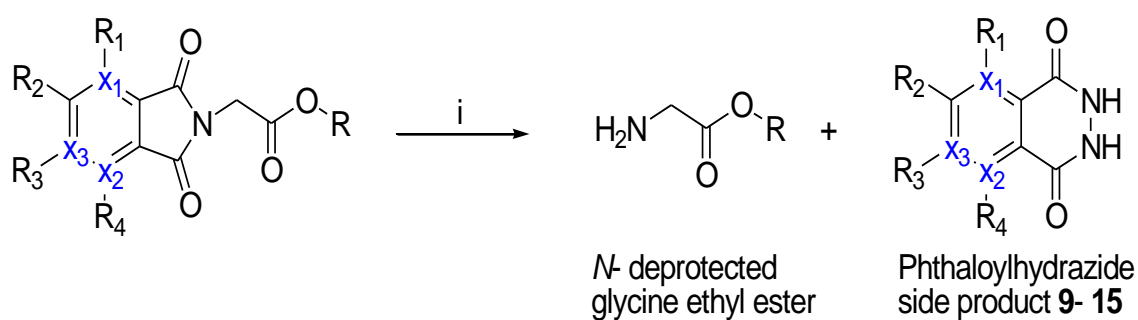


1.  $R_1 = R_3 = H$ ,  $X_1 = X_2 = N$ ,  $X_3 = C$ ,  $R = C_2H_5$
2.  $R_1 = R_2 = R_3 = R_4 = Br$ ,  $X_1 = X_2 = X_3 = C$ ,  $R = C_2H_5$
3.  $R_1 = R_4 = H$ ,  $R_2 = R_3 = Cl$ ,  $X_1 = X_2 = X_3 = C$ ,  $R = C_2H_5$
4.  $R_1 = R_2 = R_3 = R_4 = Br$ ,  $X_1 = X_2 = X_3 = C$ ,  $R = OH$ .
5.  $R_1 = R_2 = R_3 = R_4 = F$ ,  $X_1 = X_2 = X_3 = C$ ,  $R = C_2H_5$ .
6.  $R_1 = R_2 = R_3 = R_4 = Cl$ ,  $X_1 = X_2 = X_3 = C$ ,  $R = C_2H_5$ .
7.  $R_1 = R_2 = R_3 = R_4 = H$ ,  $X_1 = X_2 = X_3 = C$ ,  $R = C_2H_5$
8.  $R_1 = R_2 = R_4 = H$ ,  $X_1 = X_2 = C$ ,  $X_3 = N$ ,  $R = C_2H_5$

**Scheme 2. 2** Protection of amino group functionality of glycine ethyl ester with various phthaloyl derivatives (**1-8**). *Reagents and conditions:* i) Microwave irradiation, Dimethylformamide, 8 min. or  $Et_3N$ , Dichloromethane, reflux, 24 h. or Neat reaction,  $200^\circ C$ .

## 2. 4 Results and discussions

**2.4. 1** Protection of  $N_\alpha$ -amino-functionality of amino acid was tried with three different reaction conditions (microwave irradiation, reflux condition and neat reaction). Each process has its own advantages and disadvantages. Among these three methods we have found that microwave irradiation (MW) is better one because of the reduced reaction time. Microwave reaction was carried out safely using conventional glassware in domestic microwave ovens with reaction time of few minutes compared to 22-24 h using other conventional methods. In



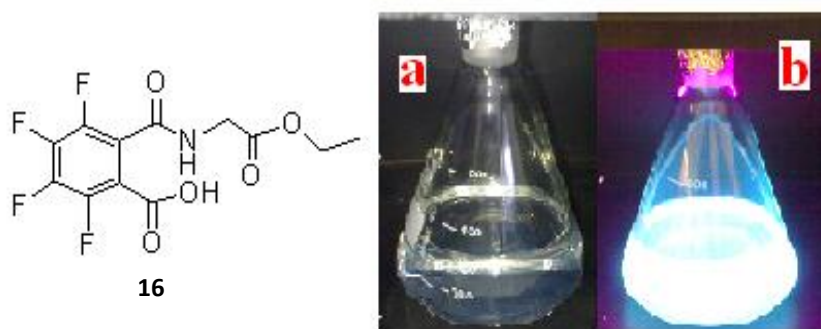
- 9.**  $R_1 = R_3 = H$ ,  $X_1 = X_2 = N$ ,  $X_3 = C$ ,  $R = C_2H_5$   
**10.**  $R_1 = R_2 = R_3 = R_4 = Br$ ,  $X_1 = X_2 = X_3 = C$ ,  $R = C_2H_5$   
**11.**  $R_1 = R_4 = H$ ,  $R_2 = R_3 = Cl$ ,  $X_1 = X_2 = X_3 = C$ ,  $R = C_2H_5$   
**12.**  $R_1 = R_2 = R_3 = R_4 = F$ ,  $X_1 = X_2 = X_3 = C$ ,  $R = C_2H_5$ .  
**13.**  $R_1 = R_2 = R_3 = R_4 = Cl$ ,  $X_1 = X_2 = X_3 = C$ ,  $R = C_2H_5$ .  
**14.**  $R_1 = R_2 = R_3 = R_4 = H$ ,  $X_1 = X_2 = X_3 = C$ ,  $R = C_2H_5$   
**15.**  $R_1 = R_2 = R_4 = H$ ,  $X_1 = X_2 = C$ ,  $X_3 = N$ ,  $R = C_2H_5$

**Scheme 2. 3** Deprotection studies of  $\alpha$ -amino-protected glycine ethyl ester with hydrazine.

*Reagents and conditions:* i)  $NH_2NH_2 \cdot H_2O$ , Dimethylformamide (DMF), room temperature.

Peptide synthesis, microwave irradiation has been used to complete long peptide sequences with high product yield and low degrees of racemization.

Microwave irradiation during the coupling of amino acids to a growing polypeptide chain is not only catalyzed through the increase in temperature, but also due to the alternating electromagnetic radiation to which the polar backbone of the polypeptide continuously aligns to. Due to this phenomenon, the microwave energy can prevent aggregation and thus



Photograph of conical flask containing compound **16** in  $\text{CHCl}_3$  under a) white light and b) violet region of visible light (around 400 nm).

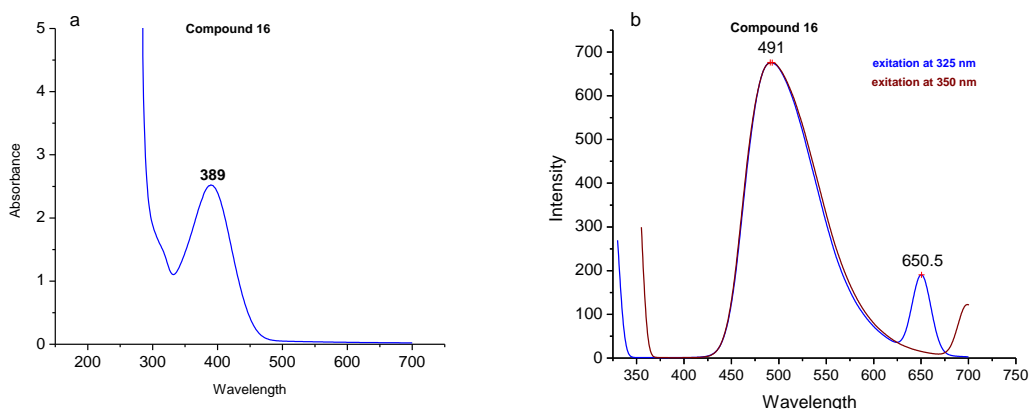


**Figure 2. 2** a) UV-vis spectra of compound **16** ( $\lambda_{\text{max}} = 389$  nm), b) Photoluminescence emission spectra of compound **16** (emission maximum at  $E_{\text{max}} = 491$  nm)

Increases yields of the final peptide product. Except compound **3** (reflux), **4** (Neat), all other Compounds (**1**, **2**, **4**, **5**, and **6**) in Scheme 2.3 were prepared by MW process and characterized by NMR spectroscopy. In case of compound **5**, on thin layer chromatography (TLC, 5% MeOH in Chloroform) four spots was observed, among them three are florescent spots ( $R_f = 0.15, 0.63, 0.72$ ), one is the expected product which is nonflurescent spot ( $R_f$

=0.86). Lower  $R_f$  value compound was characterized by  $^1\text{H}$  NMR as just a ring opened structure (compound **16**) of compound **5**, as shown in the Figure 2.2

UV-vis, photoluminescence spectroscopic studies of compound **16** was studied. In UV-VIS spectra, maximum absorbance was seen at 389 nm and Photoluminescence emission maximum at 491 nm was observed as shown in Figure 2.2

#### **2.4. 2 Deprotection studies**

Phthaloyl derivatives **1-8** were subjected to deprotection studies in 15%  $\text{NH}_2\text{NH}_2\cdot\text{H}_2\text{O}$  in DMF as shown in Scheme 2.2. Deprotection reactions were monitored by thin layer chromatography (TLC). Different phthaloyl derivatives undergo deprotection at different time periods anywhere from 5 min. to 6 h. We found the order of deprotection reaction time as compound **8** (5 min) > **1** (10 min) > **3** (30 min) > **7** (1 h) > **4**(3 ½ h) ~ **5**(3 ½ h.) > **6**. (6 h.). The observed reaction rates were very much expected based on electron withdrawing effects.

#### **2. 5 Conclusion**

We have developed new improved protecting group for amino-functionality of amino acids based on phthaloyl derivatives (compound **1**, **3** and **8**). The main advantages of using these newly developed phthaloyl protecting groups is that i) easy protection (MW or neat reaction) and deprotection (with hydrazine), ii) reduced deprotection time, which is preferred in peptide synthesis, iii) orthogonal to other protecting groups present in the amino acid and iii) cheaper process compared to standard protecting groups available. Further we use these protecting groups for solution and solid phase peptide synthesis (work is in progress in the lab). During this project we also found that compounds derived from tetrafluorophthaloyl glycine ethyl ester (in general any amino acid) are fluorescent. Currently we are working on developing fluorescent probes based on tetrafluorophthaloyl-amino acid core structure



## 2. 6 Experimental section

### 2.6. 1 General procedure Synthesis of $\alpha$ -amino-protected glycine ethyl ester

**I. Under microwave irradiation:** A mixture of phthalicanhydride derivative (500 mg, 1 mmol) and the glycine ethyl ester hydrochloride (1 mmol) was thoroughly grounded and transferred to a 250 mL beaker. DMF (1.8 mL) was added, the beaker was covered with the watch glass, placed in the microwave oven, and subjected to irradiation at 100P (cooking mode) at 30 s intervals for 6 to 8 min. Reaction progress was followed by TLC. Then the beaker was removed from the oven and allowed to cool to room temperature. The reaction mixture was dried in rotovapor and washed with water, the organic layer was separated out and purified by column chromatography.

**Characterization data:** Compound **1**. Yield 50 %, Compound **2**. Yield 82.81 %

Compound **5**.  $^1\text{H NMR}$  ( $\text{CHCl}_3$ -*d*, 400 MHz)  $\delta_{\text{H}}$  1.27-1.31 (3H, s), 4.22-4.27 (2H,m), 4.41 (2H, s). Compound **16**:  $^1\text{H NMR}$  ( $\text{CHCl}_3$ -*d*, 400 MHz)  $\delta_{\text{H}}$  1.09-1.12 (3H, s), 3.98 (2H, s), 4.04-4.09 (2H, m). Compound **6**. Yield. 67.5%.

**II. Under Reflux conditions:** Dichlorophthalic anhydride (500 mg, 2 mmol) was added to a solution of Glycine ethyl ester hydrochloride (300 mg, 2 mmol) and  $\text{Et}_3\text{N}$  (400 mg, 4 mmol) in  $\text{CH}_2\text{Cl}_2$  (100 ml). The resultant solution was heated to reflux and stirred for 22 h. After cooling to room temperature the mixture was concentrated under reduced pressure, washed with 0.01 M HCl and water. The solid was dissolved in EtOH and the solution was concentrated to dryness. Yield. 69.6%.

**III. Neat reaction:** A mixture of phthalicanhydride (500 mg, 3.9 mmol) and Glycine ethyl ester hydrochloride (500 mg, 3.9 mmol) was taken in to a Pyrex test tube, and placed in oil bath (at  $180^\circ\text{C}$ - $185^\circ\text{C}$ ) for 15 min. during the first 10 min the mixture was stirred occasionally. The phthalicanhydride which sublimes and deposits on the walls of the test tube

was scratched down into the reaction mixture by means of a glass rod. The test tube carefully removed from oil bath and allowed to cool until the reaction mixture solidified. Solid was purified by recrystallization in 10%EtOH and CHCl<sub>3</sub>. Yield. 70%.

**2.6. 2 General procedure for deprotection of N<sub>α</sub>-Phthaloyl protected glycine ethyl ester** (compounds 9- 15): Phthaloyl glycine ethyl ester (5 mg, 0.02 mmol) was added to a solution of 15% NH<sub>2</sub>NH<sub>2</sub>.H<sub>2</sub>O (200 μL) in sample vial. Reaction mixture was allowed to stir continuously and reaction progress was followed by TLC for every 5 min intervals of time. It was observed that deprotection of different phthaloyl derivatives occurred from 5 min to 6 h. as discussed in the results and discussion section.

## 2. 7 References

- 1) Carpino, L. A. *J. Am. Chem. Soc.* **1957**, 79, 4427.
- 2) Anderson, G. W.; Alberston, N. F. *J. Am. Chem. Soc.* **1957**, 79, 6180.
- 3) Merrifield, R. B. *J. Am. Chem. Soc.* **1963**, 85, 2149.
- 4) Merrifield, R. B. *Adv. Enzymol.* **1969**, 32, 221.
- 5) Kaiser, E.; Picart, F.; Kubiak, T.; Tam, J. P.; Merrifield, R. B. *J. Org. Chem.* **1993**, 58, 5167.
- 6) Stewart, J. M.; Young, J. D. *Solid Phase Peptide Synthesis*, 2nd ed.; Pierce Chemical Company: Rockford, IL, 1984.
- 7) Barlos, K.; Mamos, P.; Papaioannou, D.; Patrianakou, S.; Sanida, C.; Schaefer, W. *Liebigs Ann. Chem.* **1987**, 12, 1025.
- 8) Bodanszky, M.; Bednarek, M. A.; Bodanszky, A. *Int. J. Pept. Prot. Res.* **1982**, 20, 387.
- 9) Alsina, J.; Giralt, E.; Albericio, F. *Tetrahedron Lett.* **1996**, 37, 4195.
- 10) de la Torre, B. G.; Marcos, M. A.; Eritja, R.; Albericio, F. *Lett. Peptide Sci.* **2001**, 8, 331.
- 11) Floersheimer, A.; Riniker, B. *Peptides 1990: Proceedings of the 21<sup>st</sup> European Peptide Symposium*; Giralt, E., Andreu, D., Eds.; ESCOM Sci. Publ.: Leiden, The Netherlands, 1991; p 131.
- 12) 2,5-Diketopiperazines can be formed after the removal of the R-amino group from the second C-terminal amino acid due to nucleophilic attack of the free amine to the carboxylate group of the C-terminal amino acid.
- 13) Gairi', M.; Lloyd-Williams, P.; Albericio, F.; Giralt, E. *Tetrahedron Lett.* **1990**, 31, 7363.
- 14) Barlos, K.; Papaioannou, D.; Patrianakou, S.; Tseggenidis, T. *Liebigs Ann. Chem.* **1986**, 11, 1950.
- 15) Birr, C.; Lochinger, W.; Stahnke, G.; Lang, P. *Liebigs Ann. Chem.* **1972**, 763, 162.

- 16) Birr, C. *In Innovation and Perspectives in Solid Phase Synthesis*; Epton, R., Ed.; SPCC (UK) Ltd.: Birmingham, U.K., 1990; pp 155-181.
- 17) Jensen, K. J.; Alsina, J.; Songster, M. F.; Va'gner, J.; Albericio, F.; Barany, G. *J. Am. Chem. Soc.* **1998**, *120*, 5441.
- 18) Wang, S. S.; Yang, C. C.; Kulesha, I. D.; Sonenberg, M.; Merrifield, R. B. *Int. J. Pept. Prot. Res.* **1974**, *6*, 103.
- 19) Mojsov, S; Merrifield, R. B. *Biochemistry* **1981**, *20*, 2950.
- 20) Albericio, F. *Biopolymers* **2000**, *55*, 123.
- 21) Carey, R. I.; Bordas, L. W.; Slaughter, R. A.; Meadows, B. C.; Wadsworth, J. L.; Huang, H.; Smith, J. J.; Furusjo, E. *J. Pept. Res.* **1997**, *49*, 570.
- 22) Attard, T. J.; Reynolds, E. C.; Perich, J. W. *Org. Biomol. Chem.* **2007**, *5*, 664–670.
- 23) Zaramella, S.; Yeheskiely, E.; Stroemberg, R. *J. Am. Chem. Soc.* **2004**, *126*, 14029.
- 24) Zervas, L.; Borovas, D.; Gazis, E. *J. Am. Chem. Soc.* **1963**, *85*, 3660.
- 25) Najjar, V. A.; Merrifield, R. B. *Biochemistry* **1966**, *5*, 3765.
- 26) Tun-Kyi, A. *Helv. Chim. Acta* **1978**, *61*, 1086.
- 27) Meienhofer, J. *Nature* **1965**, *205*, 73.
- 28) Carpino, L. A.; Han, G. Y. *J. Am. Chem. Soc.* **1970**, *92*, 5748.
- 29) Carpino, L. A.; Han, G. Y. *J. Org. Chem.* **1972**, *37*, 3404.
- 30) Rabanal, F.; Haro, I.; Reig, F.; Garcí'a-Anto'n, J. M. *An. Quim.* **1990**, *86*, 84.
- 31) Butwell, F. G. W.; Haws, E. J.; Epton, R. *Makromol. Chem., Macromol. Symp.* **1988**, *19*, 69.

- 32) Carpino, L. A.; Mansour, E. M. E.; Cheng, C. H.; Williams, J. R.; MacDonald, R.; Knapczyk, J.; Carman, M.; Lopusinski, A. *J. Org. Chem.* **1983**, *48*, 661.
- 33) Carpino, L. A.; Mansour, E. M. E.; Knapczyk, J. *J. Org. Chem.* **1983**, *48*, 666.
- 34) Atherton, E.; Fox, H.; Harkiss, D.; Logan, C. J.; Sheppard, R. C.; Williams, B. J. *J. Chem. Soc., Chem. Commun.* **1978**, *13*, 537.
- 35) Chang, C.-D.; Meienhofer, J. *Int. J. Pept. Prot. Res.* **1978**, *11*, 246.
- 36) Wade, J. D.; Bedford, J.; Sheppard, R. C.; Tregear, G. W. *Pept. Res.* **1991**, *4*, 194.
- 37) Meldal, M.; Bielfeldt, T.; Peters, S.; Jensen, K. J.; Paulsen, H.; Bock, K. *Int. J. Pept. Prot. Res.* **1994**, *43*, 529.
- 38) Liebe, B.; Kunz, H. *Angew. Chem. Int. Ed. in Eng.* **1997**, *36*, 618.
- 39) Li, X.; Kawakami, T.; Aimoto, S. *Tetrahedron Lett.* **1998**, *39*, 8669.
- 40) Martinez, J.; Bodanszky, M. *Int. J. Peptide Protein Res.* **1978**, *12*, 277.
- 41) Doelling, R.; Beyermann, M.; Haenel, J.; Kernchen, F.; Krause, E.; Franke, P.; Brudel, M.; Bienert, M. *J. Chem. Soc., Chem. Commun.* **1994**, 853.
- 42) Han, Y.-K.; Johnston, D. A.; Khatri, H. N. *PCT Int. Appl. WO 2006069727 A2*, 2006; *Chem. Abstr.* **2006**, *145*, 103960.
- 43) Samukov, V. V.; Sabirov, A.; Pozdnyakov, P. I. *Tetrahedron Lett.* **1994**, *35*, 7821.
- 44) Sabirov, A. N.; Kim, Y.-D.; Kim, H.-J.; Samukov, V. V. *Protein Peptide Lett.* **1997**, *4*, 307.
- 45) Ramage, R.; Jiang, L.; Kim, Y.-D.; Shaw, K.; Park, J.-L.; Kim, H.-J. *J. Pept. Sci.* **1999**, *5*, 195.
- 46) Carreño, C.; Mendez, M. E.; Kim, Y.-D.; Kim, H.-J.; Kates, S. A.; Andreu, D.; Albericio, F. *J. Pept. Res.* **2000**, *56*, 63.
- 47) Maier, T. C.; Podlech, J. *Adv. Synth. Cat.* **2004**, *346*, 727.

- 48) Lauer, J. L.; Fields, C. G.; Fields, G. B. *Lett. Pept. Sci.* **1995**, *1*, 197.
- 49) Carpino, L. A.; Philbin, M.; Ismail, M.; Truran, G. A.; Mansour, E. M. E.; Iguchi, S.; Ionescu, D.; El-Faham, A.; Riemer, C.; Warrass, R.; Weiss, M. S. *J. Am. Chem. Soc.* **1997**, *119*, 9915.
- 50) Carpino, L. A.; Philbin, M. *J. Org. Chem.* **1999**, *64*, 4315.
- 51) Carpino, L. A.; Mansour, E. M. E. *J. Org. Chem.* **1999**, *64*, 8399.
- 52) Carpino, L. A.; Ismail, M.; Truran, G. A.; Mansour, E. M. E.; Iguchi, S.; Ionescu, D.; El-Faham, A.; Riemer, C.; Warrass, R. *J. Org. Chem.* **1999**, *64*, 4324.
- 53) Carpino, L. A.; Ghassemi, S.; Ionescu, D.; Ismail, M.; Sadat-AAlaee, D.; Truran, G. A.; Mansour, E. M. E.; Siwruk, G. A.; Eynon, J. S.; Morgan, B. *Org. Process Res. DeV.* **2003**, *7*, 28.
- 54) Carpino, L. A.; Abdel-Maksoud, A. A.; Ionescu, D.; Mansour, E. M. E.; Zewail, M. A. *J. Org. Chem.* **2007**, *72*, 1729.
- 55) Hillman, J. D.; Orugunty, R. S.; Smith, J. L. U.S. Pat. Appl. 2007037963 A1, 2007; *Chem. Abstr.* **2007**, *146*, 252110.
- 56) Stigers, K. D.; Koutroulis, M. R.; Chung, D. M.; Nowick, J. S. *J. Org. Chem.* **2000**, *65*, 3858.
- 57) Chinchilla, R.; Dodsworth, D. J.; Najera, C.; Soriano, J. M. *Bioorg. Med. Chem. Lett.* **2002**, *12*, 1817.
- 58) Woods, R. J.; Brower, J. O.; Castellanos, E.; Hashemzadeh, M.; Khakshoor, O.; Russu, W. A.; Nowick, J. S. *J. Am. Chem. Soc.* **2007**, *129*, 2548.
- 59) Hasegawa, K.; Sha, Y. L.; Bang, J. K.; Kawakami, T.; Akaji, K.; Aimoto, S. *Lett. Pept. Sci.* **2002**, *8*, 277.
- 60) Wessig, P.; Czapla, S.; Moellnitz, K.; Schwarz, J. *Synlett* **2006**, *14*, 2235.
- 61) Cros, E.; Planas, M.; Barany, G.; Bardaji, E. *Eur. J. Org. Chem.* **2004**, *17*, 3633.

- 62) Hojo, K.; Maeda, M.; Kawasaki, K. *J. Pept. Sci.* **2001**, 7, 615.
- 63) Hojo, K.; Maeda, M.; Kawasaki, K. *Tetrahedron* **2004**, 60, 1875.
- 64) Hojo, K.; Maeda, M.; Smith, T. J.; Kita, E.; Yamaguchi, F.; Yamamoto, S.; Kawasaki, K. *Chem. Pharm. Bull.* **2004**, 52, 422.
- 65) Hojo, K.; Maeda, M.; Kawasaki, K. *Tetrahedron Lett.* **2004**, 45, 9293.
- 66) Lloyd-Williams, P.; Albericio, F.; Giralt, E. *Chemical Approaches to the Synthesis of Peptides and Proteins*; CRC Press: Boca Raton, FL, 1997.
- 67) Gatos, D.; Athanassopoulos, P.; Tzavara, C.; Barlos, K. *Peptides 1998: Proceedings of the 25th European Peptide Symposium*; Bajusz, S., Hudecz, F., Eds.; Akademiai Kiado: Budapest, Hungary, 1999; pp 146-147.
- 68) McMurray, J. S. *Tetrahedron Lett.* **1991**, 32, 7679.
- 69) Yue, C.; Terry, J.; Potier, P. *Tetrahedron Lett.* **1993**, 34, 323.
- 70) Isidro-Llobet, A.; Alvarez, M.; Albericio, F. *Tetrahedron Lett.* **2008**, 49, 3304.
- 71) Kessler, H.; Siegmeier, R. *Tetrahedron Lett.* **1983**, 24, 281.
- 72) Bednarek, M. A; Bodanszky, M. *Int. J. Pept. Prot. Res.* **1983**, 21, 196.
- 73) Valero, M.-L.; Giralt, E.; Andreu, D. *Peptides 1996: Proceedings of the 24th European Peptide Symposium*; Ramage, R., Epton, R., Eds.; Mayflower Scientific Ltd.: Kingswinford, U.K., 1998; pp 857-858.
- 74) Chan, W. C.; Bycroft, B. W.; Evans, D. J.; White, P. D. *J. Chem. Soc., Chem. Commun.* **1995**, 2209.
- 75) Bodanszky, M. *Int. J. Pept. Prot. Res.* **1984**, 23, 111.
- 76) Martinez, J.; Laur, J.; Castro, B. *Tetrahedron Lett.* **1983**, 24, 5219.

77) Martinez, J.; Laur, J.; Castro, B. *Tetrahedron* **1985**, *41*, 739.



Chapter 3

**Spontaneous self-assembly of designed cyclic dipeptide  
(Phg-Phg) into two dimensional nano and mesosheets\***

\* T. Govindaraju, M. Pandeeswar, K. Jayaramulu, G. Jaipuria and H. S. Atreya, *Supramol. Chem.*, (2010). In Press.

## Chapter 3

# **Spontaneous self-assembly of designed cyclic dipeptide (Phg-Phg) into two dimensional nano and mesosheets**

### **3. 1 Introduction**

The self-assembly of peptides, carbohydrates and phospholipids drawing much interest in the fields of biology and nanotechnology due to their wide range of applications. Especially, studies have been carried out to control self-assembly processes in order to design desirable structures at the nanometric scale with correct orientation and configuration. These nanomaterials find applications as biomaterials, biomolecular nanoelectromechanical systems (bioMEMS), biosensors and in tissue engineering. Amino acids combinations in short peptides, polypeptides and large proteins represent an exorbitant chemical diversity (Rajagopal and Schneider 2004,<sup>1</sup> Zhang 2003<sup>2</sup>) for the design of complex architecture at the nanometer to macroscopic scale among natural building blocks. The other applications of biomolecular self-assemblies includes the formation of nanoscale objects that could be used in future molecular electronics applications (Braun *et al* 1998,<sup>3</sup> Patolsky *et al* 2004,<sup>4</sup> Reches and Gazit 2003,<sup>5</sup> Song *et al* 2004,<sup>6</sup> Scheibel *et al* 2003<sup>7</sup>), as a tool in molecular lithography (Keren *et al* 2003,<sup>8</sup> Sleytr and Beveridge 1999<sup>9</sup>), fabrication of inorganic nano-ordered structures such as silicone devices, the formation of ordered macroscopic calcium and silica structures in biomineralization processes.

Due to the diverse structural and functional properties, biocompatibility and easy producability of peptides-based assemblies, various research groups have explored several approaches to design peptide-based nanostructures such as fibers, tapes, tubes and spheres (Madhavaiah and Verma 2004,<sup>10</sup> Matsumura *et al* 2004,<sup>11</sup> Zhao and Zhang 2004,<sup>12</sup> Wagner *et al* 2005,<sup>13</sup> Holmes *et al* 2000,<sup>14</sup> Aggeli *et al* 1997,<sup>15</sup> Matsuura *et al* 2005<sup>16</sup>). Ghadiri and co-

workers (Ghadiri *et al* 1993)<sup>17</sup> used cyclic peptides produced with an altering even number of *D*- and *L*-amino acids that interact with each other to form nanotubes array. Amphiphilic peptides are also being used to form nano-assemblies. One example is the use of self-complementary ionic peptides which adopt  $\beta$ -sheet conformation that self-assembled into nanofibers (Hartgerink *et al* 2002).<sup>18</sup> Another example is surfactant-like peptides which are characterized by well defined hydrophilic and hydrophobic residues self-assembled into nanotubes and nanovesicles (Vauthey *et al* 2002).<sup>19</sup> In addition, amphiphile peptides could be conjugated to cell adhesion motifs (Silva *et al* 2004)<sup>20</sup> and were shown to assemble into fibers or hydrogel (Yokoi *et al* 2005).<sup>21</sup> Table 3.1 showing Summary of some of the molecular structures and morphologies of the self-assembled nanostructures formed by aromatic homo-dipeptides.<sup>35</sup>

The simplest cyclic forms comprise of the cyclic dipeptides which are more stable structurally and chemically compared to their acyclic congeners and hence their nanostructures offer higher stability. Here we have under taken the design, synthesis and morphological characterization of self-assembled nanostructures of cyclic dipeptide with simple unnatural amino acid phenylglycine (Phg).

**Table 3. 1** Summary of the molecular structures and morphologies of the self-assembled nanostructures formed by aromatic homo dipeptides<sup>35</sup>

Homo-aromatic dipeptide	Molecular structure	Assemblies morphology
NH <sub>2</sub> -Phe-Phe-COOH		Nanotubes
NH <sub>2</sub> -Phg-Phg-COOH		Nanospheres
Ac-Phe-Phe-NH <sub>2</sub>		Nanotubes
NH <sub>2</sub> -Phe-Phe-NH <sub>2</sub>		Tubular structures
Boc-Phe-Phe-COOH		Tubular structures
Fmoc-Phe-Phe-COOH		Amyloid-like structures
Cbz-Phe-Phe-COOH		Amyloid-like structures
NH <sub>2</sub> -((D-1-Nal)-(D-1-Nal))-COOH		Tubular structures
NH <sub>2</sub> -(D-2-Nal)-(D-2-Nal)-COOH		Tubular structures
NH <sub>2</sub> -(p-fluoro-Phe)-(p-fluoro-Phe)-COOH		Tubular structures
NH <sub>2</sub> -(pentafluoro-Phe)-(pentafluoro-Phe)-COOH		Tubular structures
NH <sub>2</sub> -(p-iodo-Phe)-(p-iodo-Phe)-COOH		Fibrillar structures
NH <sub>2</sub> -(p-nitro-Phe)-(p-nitro-Phe)-COOH		Fibrillar structures and spheres
NH <sub>2</sub> -(4-phenyl-Phe)-(4-phenyl-Phe)-COOH		Squared plates

### 3. 2 Objective of the present work

#### **Spontaneous self-assembly of designed cyclic dipeptide (Phg-Phg) into two dimensional**

**nano and mesosheets:** The formation of 2D nano and mesosheets by cyclic dipeptide (Phg-Phg) spanning several micrometers in lateral dimensions. The structural morphologies of the 2D sheets have been extensively characterized using different microscopy techniques such as field emission scanning electron microscopy (FESEM), high resolution transmission electron microscopy (HRTEM), atomic force microscopy (AFM), NMR spectroscopy and single crystal X-Ray diffraction studies. Their hierarchy and morphology resemble that of natural materials with layered structure<sup>22, 23</sup> and are distinct from the earlier reports on cyclic- and acyclic peptide-based nanomaterials.

### 3. 3 Design Strategy

In recent years, a number of nanostructures formed by cyclic and acyclic peptides have been reported.<sup>24</sup> The simplest cyclic forms comprise of the cyclic dipeptides which are more stable structurally and chemically compared to their acyclic congeners and hence their nanostructures offer higher stability. Utility of cyclic dipeptides or their derivatives have been demonstrated with the formation of molecular-chains (tapes) in crystalline form and macro capsules in self-assembly based aggregated forms.<sup>25</sup> At the molecular level, cyclic dipeptide scaffolds can form hydrogen bonded one dimensional chain or layers.<sup>25</sup> Such structures are formed as a result of two pairs of (N-H--O) hydrogen bonds formed between two or four neighbouring molecules, respectively (Figure 3.1). However, the formation of higher order self-assembled structures is not commonly observed. This is owing to the fact that absence of a suitable  $\alpha$ -substituent (R, Scheme 2.1) to participate in intermolecular interactions prevents the formation of two-dimensionally extended structures by self-assembly.<sup>26, 27</sup> This can be accomplished by introducing additional orthogonal non-covalent interactions such as  $\pi$ - $\pi$  interactions involving aromatic groups at the  $\alpha$ -position.<sup>27</sup> We designed the cyclic dipeptide

molecules which self-organize via molecular-chains and layers into nano and mesosheets utilizing aromatic  $\pi$ - $\pi$  interactions Figure 3.2.

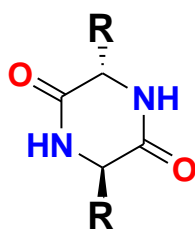


**Figure 3. 1** Molecular structure of cyclic (*D*, *L*) dipeptide.

We have designed cyclic dipeptide with aromatic side chain at  $\alpha$ -position (R in Figure 3.1), this aromatic group would introduce additional intermolecular orthogonal non-covalent  $\pi$ - $\pi$  interactions between cyclic dipeptide units. The simplest aromatic side chain such as phenylglycine has selected accordingly we have synthesized the cyclic dipeptide **1**, which is substituted with phenyl ring at  $\alpha$ -position (Scheme 3.1). The amide groups will introduce highly directional hydrogen bonding (layers, Figure 3.2) and phenyl aromatic  $\alpha$ -substituent will introduce  $\pi$ - $\pi$  interactions, as a result of these two orthogonal interactions the aromatic  $\alpha$ -substituent functionalized cyclic dipeptide **1** was expected to self-assemble into two-dimensional structures. Figure 3.2 showing proposed model of formation of molecular-layers through (N-H--O) hydrogen bonding between cyclic dipeptide **1**.

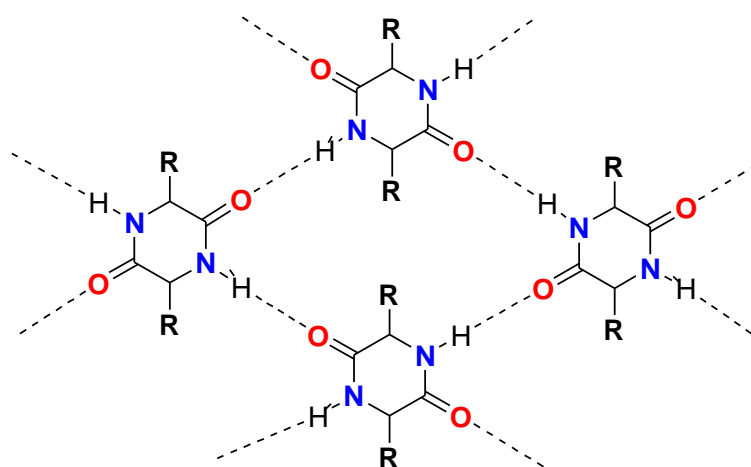


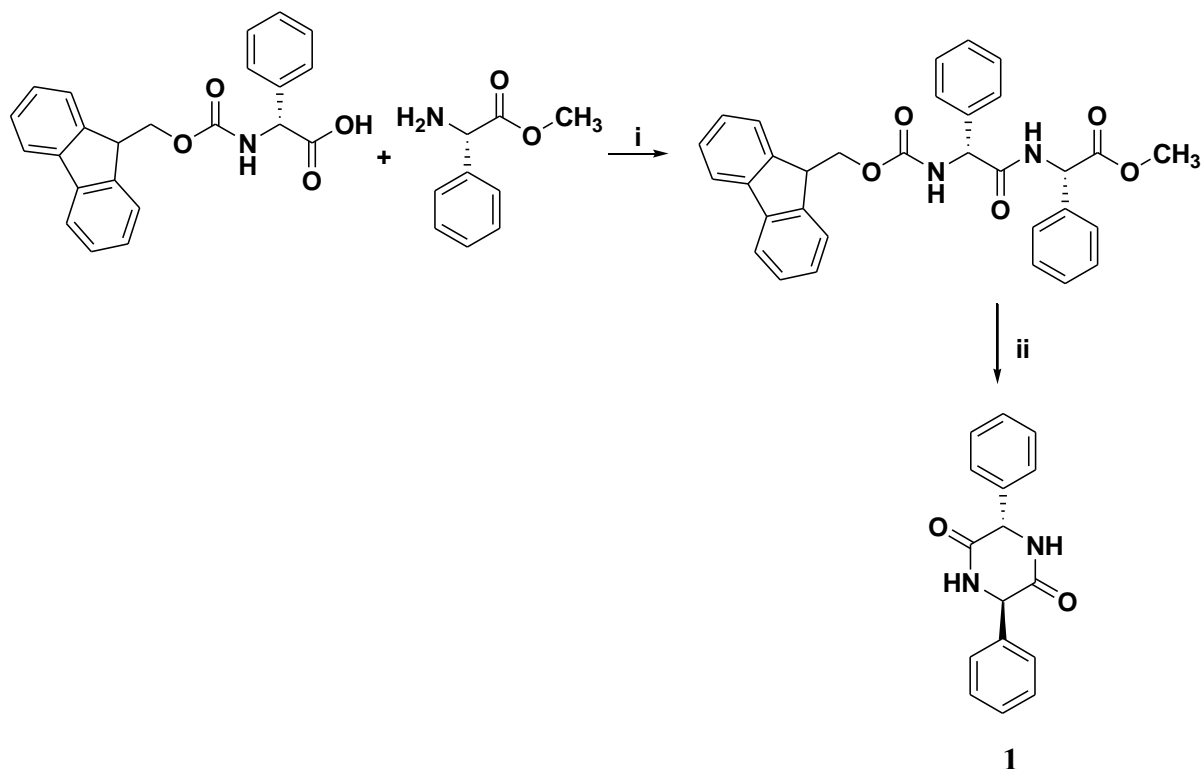
**Figure 3. 2** Cyclic dipeptide forming molecular-layers through intermolecular (N-H--O) hydrogen bonding.

### 3. 4 Synthesis of cyclic dipeptide

Cyclic dipeptide **1** has been synthesized according to the synthetic route shown in Scheme 3.1.

#### 3.4. 1 Synthesis of cyclo (*D*-Phg-*L*-Phg) **1**

Cyclic dipeptide of *D*-Phg-*L*-Phg (**1**) (Scheme 3.1) was prepared by coupling corresponding Fmoc-*D*-Phg-OH with H-*L*-Phg-OMe using peptide coupling reagents. The protected dipeptide (Fmoc-*D*-Phg-*L*-Phg-OMe) under Fmoc-deprotection conditions resulted in cyclo (*D*-Phg-*L*-Phg) **1** in quantitative yield.



**Scheme 3. 1** Synthesis of cyclic dipeptide (*D*-Phg-*L*-Phg) **1**. Reagents and conditions: i) EDC, HOBT, DIPEA, CH<sub>2</sub>Cl<sub>2</sub>, RT. ii) 15% piperidine in CH<sub>2</sub>Cl<sub>2</sub>. EDC = 1-Ethyl-3-(3-dimethylaminopropyl)carbodiimide, HOBT = 1-hydroxybenzotriazole, DIPEA = Diisopropylethylamine.

### 3. 5 Results and Discussion

Cyclic dipeptide **1** was characterized by nuclear magnetic resonance spectroscopy ( $^1\text{H}$  NMR,  $^{13}\text{C}$  NMR) and single-crystal X-ray diffraction. The self-assembly properties of **1** were investigated by field emission scanning electron microscope (FESEM) and atomic force microscopy (AFM).

#### 3.5. 1 Microscopic studies of cyclo(*D*-Phg-*L*-Phg) **1**

##### (a) FESEM

Field emission scanning electron microscopy: FESEM measurements were performed on FEI Nova nanoSEM-600 equipped with field emission gun operating at 30 kV. Samples were prepared by placing a aliquot of the cyclic dipeptide suspension or solution on to a fresh, clean silicon surface, dried in the air before using the sample for analysis.

FESEM micrograph of **1** (in MeOH suspension) show the 2D mesosheets with rhomboid morphology (Figure 3.3a) self-assembled with 2D nanosheets as shown in Figure 3.3b. Attempts to solubilise the self-assembled mesosheets of **1** in organic solvents was unsuccessful, as there exist strong intermolecular hydrogen bonding interactions Figure 3.2. To solubilise **1** we use strong acid Trifluoroaceticacid (TFA) organic solution, which break the hydrogen bonds between the cyclic dipeptide molecules **1**. The solution of **1** in  $\text{CHCl}_3$ -TFA upon solvent evaporation formed well separated 2D nanosheets (Figure 3.3c and 3.3d). Nanosheets were also obtained from the solution of **1** in  $\text{CH}_2\text{Cl}_2$ -TFA. This represents an indirect and alternative method for the exfoliation of nanosheets from 2D mesosheets. On the other hand its acyclic congener (*L*-Phg-*L*-Phg) has been shown to form closed-cage nanospheres<sup>28</sup> (Table 3.1).



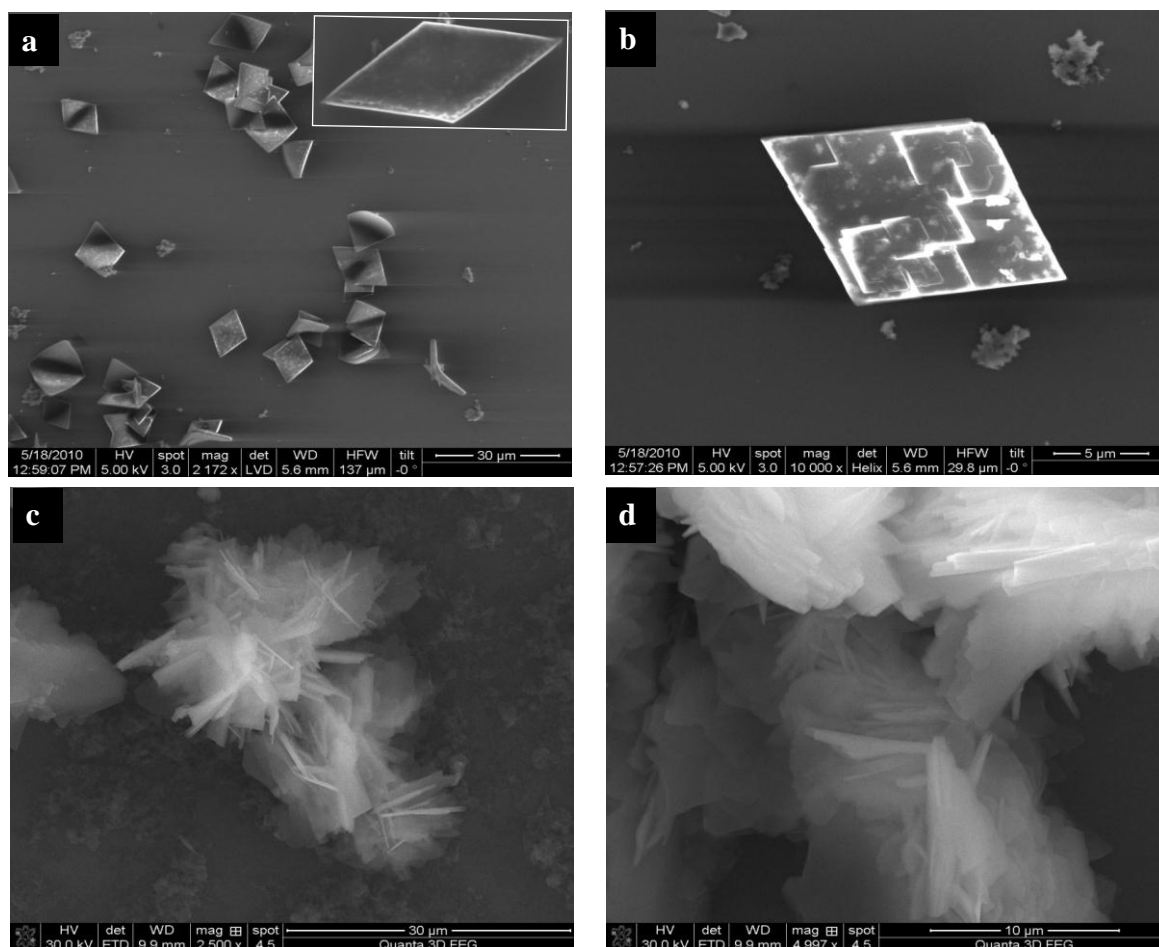


**Figure 3.3** (a) FESEM micrograph of 2D mesosheets formed from the solution of **1** in MeOH (inset shows the high resolution image of an isolated mesosheet). (b) FESEM micrographs of cyclic dipeptide **1** (in MeOH) showing rhomboid mesosheets formed by the self-organisation of nanosheets. (d) and (e) FESEM micrograph, nanosheets formed from the solution of **1** in  $\text{CHCl}_3$ -TFA.

### (b) HRTEM

High resolution transmission electron microscopy (HRTEM): Samples were prepared by placing a 10  $\mu\text{l}$  aliquot of the cyclic dipeptide suspension or solution on a 200 mesh holey carbon supported copper grid. After removing excess fluid, the sample was dried at room temperature to remove the solvent. HRTEM images were obtained with a JEOL JEM 3010 electron microscope operating at 300 kV.

The formation of self-assembled rhomboid 2D-mesosheets was further substantiated by HRTEM micrograph (Figure 3.4a).

### **(c) AFM**

Atomic Force Microscopy (AFM): AFM measurements were performed on a Veeco diInnova SPM operating in tapping mode regime. Micro-fabricated silicon cantilever tips doped with phosphorus and with a frequency of 250-300 kHz and a spring constant of  $40 \text{ Nm}^{-1}$  were used. The samples prepared by drop casting cyclic dipeptide suspension or solution on a fresh, ultra clean silicon substrate, dried in air followed by vacuum drying at room temperature.

AFM data also revealed the formation of 2D mesosheets with large lateral surface as shown in Figure 3.4b. The height profile indicates a topographical thickness of  $\sim 200 \text{ nm}$  with a well defined rhomboid shape (Figure 3.4b inset). On the other hand, the AFM height profile of 2D nanosheets (formed by the solution of **1** in  $\text{CHCl}_3$ -TFA) indicate a layer thickness of  $\sim 60 \text{ nm}$ , suggesting that the nanosheets initially form by self-assembly which then self-organize to produce 2D mesosheets with large lateral surface area and sub-micrometer multi-layer thickness. AFM micrograph (Figure 3.4b) also show the presence of structural hierarchy similar to that of natural materials with layered structure.

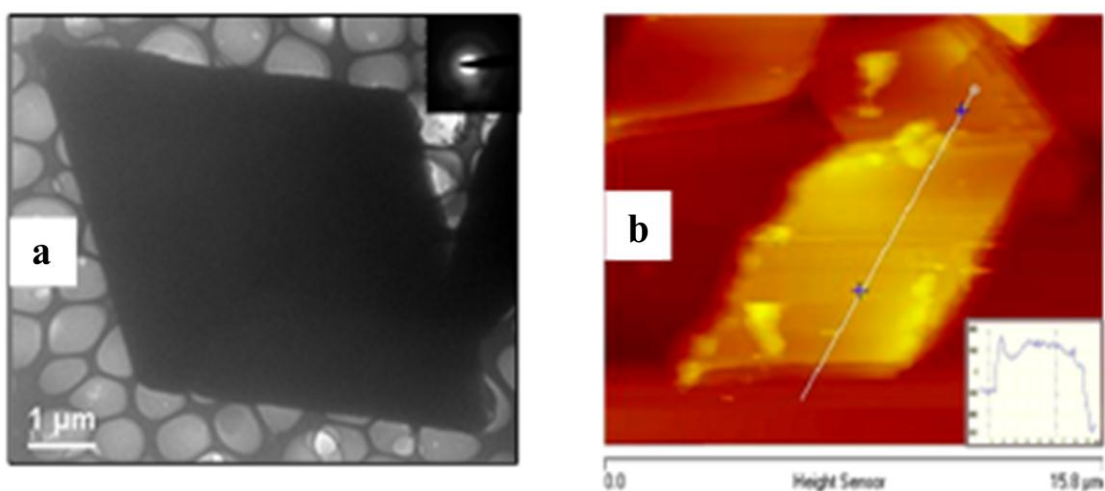


**Figure 3. 4** (a) HRTEM micrograph of 2D mesosheet of **1**, the electron diffraction (ED, inset) shows the non-crystalline nature of the mesosheet. (c) AFM image of 2D mesosheets (rhomboid), inset show the height profile (~ 200 nm).

#### **(d) Thermo gravimetric analysis**

Thermo gravimetric analysis (TGA) was carried out on a Mettler Toledo TG-850 instrument under flowing nitrogen atmosphere ( $40 \text{ mL min}^{-1}$ ) at a heating rate of  $10 \text{ }^\circ\text{C min}^{-1}$ , with total temperature range of  $30 - 700 \text{ }^\circ\text{C}$ .

To know the thermal stability cyclic dipeptide **1** was subjected to thermogravimetric analysis (TGA). The 2D mesosheets possessed high thermal stability as determined from thermogravimetric analysis (Figure 3.5). The cyclo (*D*-Phg-*L*-Phg) **1** (solid sample) showed two transitions which can be attributed to a hierarchical organization of the 2D sheets. Major transitions were observed at  $306$  and  $497 \text{ }^\circ\text{C}$  for **1**. High thermal decomposition temperatures clearly indicate the high stability associated with 2D mesosheets. This provides supporting evidence for the existence of morphological hierarchy involving the self-organized nanosheets to form stable mesosheets.

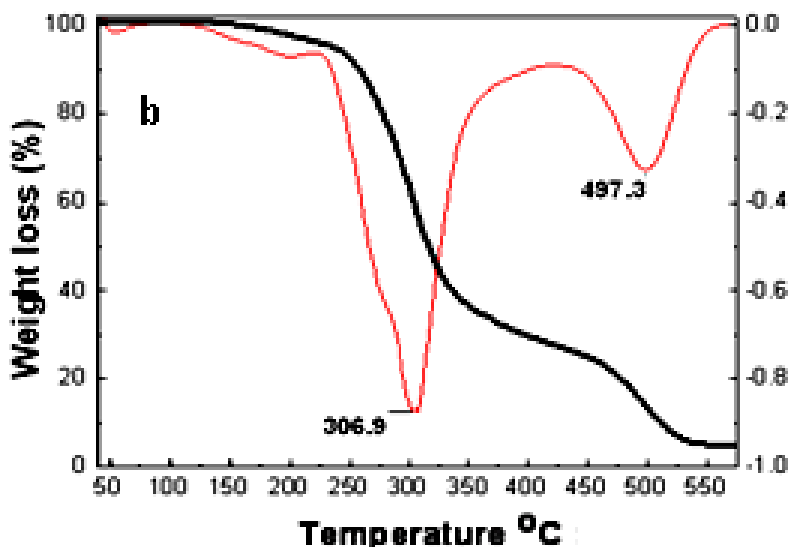


**Figure 3. 5** Thermogravimetric analysis (TGA) of 2D mesosheets of cyclo (*D*-Phg-*L*-Phg) **1**.

The weight losses are shown by the first derivative curve (red).

Where as in the case of cyclo(*L*-Phg-*L*-Phg), the major transitions were observed at 220 and 310 °C indicating relative low thermal stability of cyclo(*L*-Phg-*L*-Phg) compare to cyclo(*D*-Phg-*L*-Phg) **1**.<sup>36</sup> The observed difference in the thermal stability of

Cyclo (*L*-Phg-*L*-Phg) and cyclo (*D*-Phg-*L*-Phg) **1** are predictably due to the (N–H--O) and  $\pi$ - $\pi$  interactions driven 2D-extended molecular-chains and molecular-layers respectively.<sup>36</sup>

Though formation of self-assembled nanostructure of peptides have been explained using molecular packing determined from the crystallographic data, the actual shape of nano- or mesostructures differ considerably.<sup>29,30</sup> However, the formation of 2D sheets has not been achieved through self-assembly based aggregation and crystallization with identical shapes. We succeeded in crystallizing **1** into large 2D single-crystalline sheets (Figure 3.6b) using 2-methoxyethanol as a solvent. In contrast non-crystalline 2D mesosheets of **1** suspended in methanol converted to single crystals with diamondoid shape over a period of 8 weeks (Figure 3.6a). The crystal parameters obtained for diamondoid single crystals were similar to that of 2D single crystalline sheets. The shape of 2D single crystalline sheets resembled that

of 2D mesosheets obtained by self-assembly based aggregation as shown in Figure 3.3a. These 2D single-crystalline sheets were much larger in dimension compare to non-crystalline 2D mesosheets.

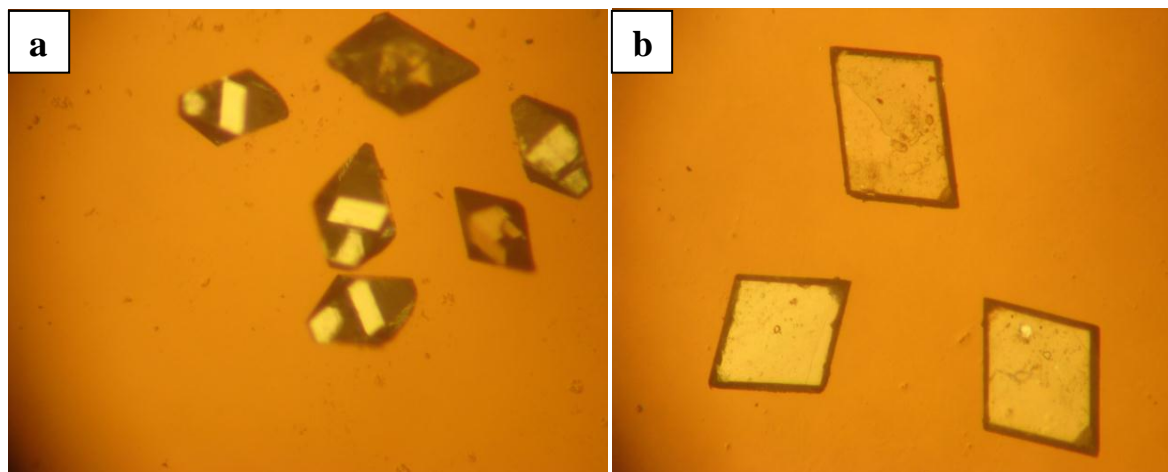


**Figure 3. 6** Crystals of **1** (a) diamondoid shape crystals formed from MeOH, (b) rhomboid crystals formed from 2-methoxyethanol.

#### **(e) Optical profiler analysis**

The dimensions of the single-crystalline 2D sheet of **1** were measured using a Wyko NT9100 (Veeco, USA) optical profiler. The VSI mode was employed with a field of view and objective lens magnifications of 1X and 5X respectively.

The lateral dimensions of rhomboid single-crystalline 2D sheets were found to be  $> 600$   $\mu\text{m}$  as determined from the optical profiler analysis as shown in Figure 3.7.

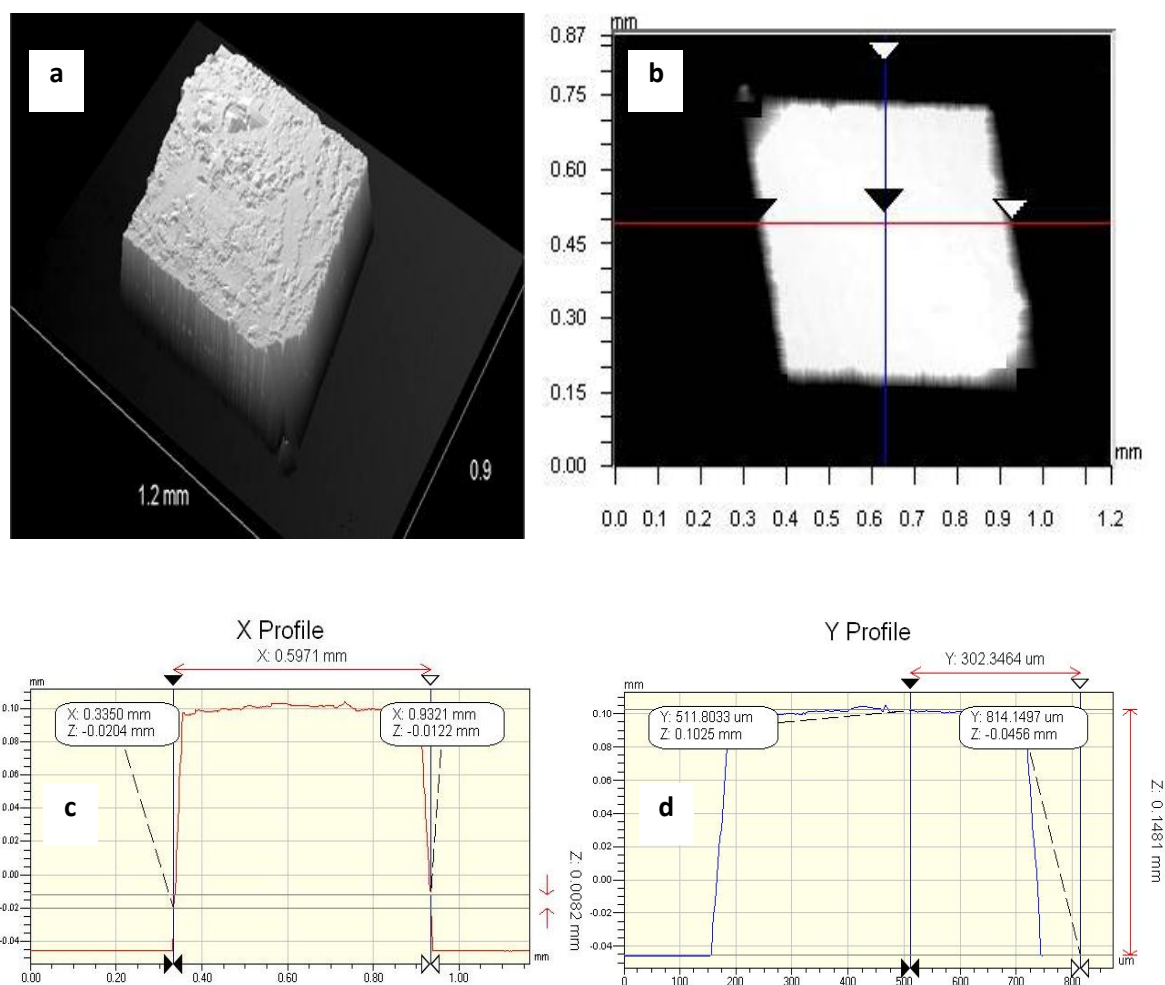


**Figure 3. 7** (a) Optical profiler (Wyko NT9100, Veeco, USA) image of a single-crystalline rhomboid 2D sheet of cyclo (*D*-Phg-*L*-Phg) **1** (crystallized from 2-methoxyethanol). The shape of this crystal is similar to that of rhomboid 2D mesosheets formed by self-assembly based aggregation. (b-d) Optical profiler analysis: single-crystalline rhomboid 2D sheet is larger in dimension compare to non-crystalline 2D mesosheets obtained by self-assembly based aggregation (lateral dimension > 600  $\mu\text{m}$ ).

### X-Ray single crystal measurement

Single crystal was mounted on a thin glass fiber with commercially available super glue. X-Ray single crystal structural data was collected on a Bruker Smart-CCD diffractometer equipped with a normal focus, 2.4 kW sealed tube X-ray source with graphite monochromated ( $\text{MoK}\alpha$  radiation,  $\lambda = 0.71073 \text{ \AA}$ ) operating at 50 kV and 30 mA. The data was collected at 100 K. The program SAINT was used for integration of diffraction profiles

and absorption correction was made with SADABS program. The structure was solved by SIR 92<sup>31</sup> and refined by full matrix least squares method using SHELXL97.<sup>32</sup> The non-hydrogen atoms were refined anisotropically. The hydrogen atoms were fixed by HFIX and placed in ideal positions. Potential solvent accessible area or void space was calculated using the PLATON 99<sup>33</sup> multipurpose crystallographic software. The crystallographic and structure refinement data was found to be as Formula C<sub>16</sub>H<sub>14</sub>N<sub>2</sub>O<sub>2</sub>, Mr = 266.29, Orthorhombic, Space group Pbc<sub>a</sub> (no. 61), a = 10.1275 Å, b = 8.2053(7) Å, c = 15.5781(12) Å, V = 1294.53 Å<sup>3</sup>, Z = 4, ρ<sub>calc</sub> = 1.366 g cm<sup>-3</sup>, μ (MoKα) = 0.092 mm<sup>-1</sup>, F(000) = 560, T = 293 K, λ ( MoKα) = 0.71073 Å, θ max = 22.2°, Total data = 6211, Unique data = 815, Rint = 0.084, Observed data [I > 2σ(I)] = 588, R = 0.0383, R<sub>w</sub> = 0.0983, GOF = 1.04. All calculations were carried out using SHELXL 97<sup>32</sup>, PLATON 99<sup>33</sup>, SHELXS 97<sup>34</sup> and WinGX system, Ver 1.70.01.21.

Cyclic dipeptide **1** crystallized in orthorhombic *Pbc<sub>a</sub>* space group and structure determination reveals that the dipeptide has two phenyl groups in reverse direction and the dihedral angle between the phenyl rings is around 95°. The cyclic ring has two O=C-N-H part in two side, i.e. each unit has two H-bonding donor and two acceptor sites (Figure 3.8b). Therefore each unit connects to the four different units by H7-N1...O1 H-(N1..O1; 2.947Å)<sup>33</sup> bonding interactions, resulting in a 2D corrugated sheet (molecular-layers, Figure 2.7 b) lying in the crystallographic *ab* plane (Figure 3.8b). The cyclic dipeptide **1** stacks along the *c*-axis to form 2D single-crystalline sheet (Figure 3.8d). All the bond distances and angles are in the range of reported values in the literature. The arrangement of hydrogen bonded molecular-layers of **1** in two-dimension as a result of aromatic aromatic π-π interactions is shown in Figure 3.8c. The single-crystalline 2D sheets do not possess layered structural hierarchy that was observed in non-crystalline 2D mesosheets obtained from self-assembly based aggregation as shown in Figure 3.3b.

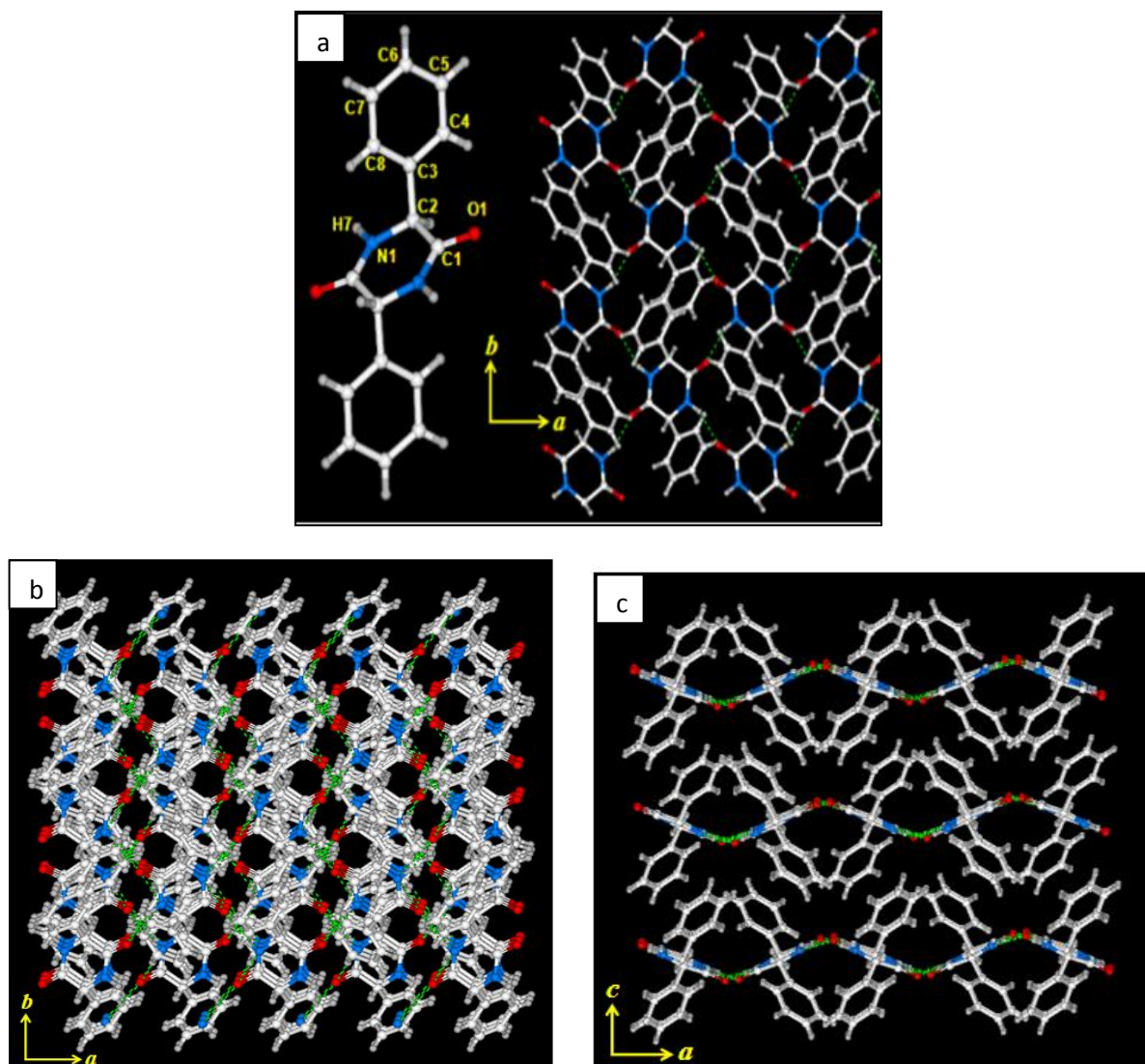


**Figure 3. 8** (a) Ortep-diagram and molecular interactions of cyclo (*D*-Phg-*L*-Phg) **1** to form molecular-layers. (b and c) Packing of molecular-layers along *c*-axis to form single-crystalline 2D sheet.

### 3. 6 Proposed mechanism

We proposed a schematic model to explain the two dimensional nanosheet formed by the self-assembly of cyclo (*D*-Phg-*L*-Phg) **1** as illustrated in Figure 3.9. The cyclic dipeptide possess two hydrogen bonding donors (amide protons) and two hydrogen bonding acceptors (carbonyl group). These four hydrogen bonding sites of molecule **1** form molecular-layers as shown in Figure 3.9i. The molecular layers further self-assemble into two-dimensional rhomboid nanosheets (Figure 3.9ii) with the help of orthogonal  $\pi$ - $\pi$  interactions (two phenyl



side chains on cyclic dipeptide). Two dimensional organizations of nanosheets results in the formation of 2D mesosheets (Figure 3.9iii).

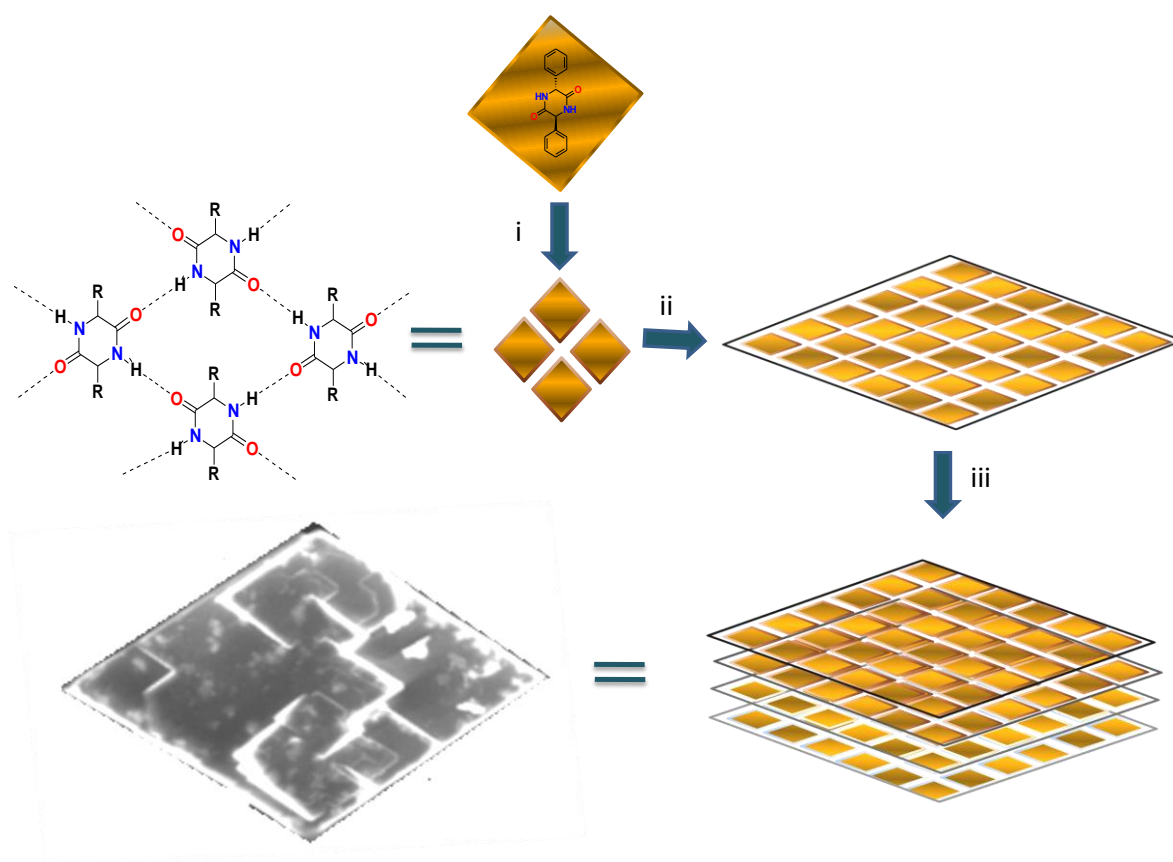


**Figure 3. 9** Proposed schematic model for the formation of the two dimensional nano and mesosheet structures by the cyclo(*D*-Phg-*L*-Phg) **1** and FESEM image of **1**. (i) formation of molecular layer, (ii) self-assembly of molecular layers into nanosheet and (iii) two dimensional arrangement of nanosheets to form mesosheet.

### 3. 7 Conclusion

In this project we have demonstrated that the simplest aromatic cyclic dipeptide of (Phg-Phg) form well defined 2D nano and mesosheets with large lateral dimensions. The self-assembly of cyclo (*D*-Phg-*L*-Phg) **1** begins by formation of 2D nanosheets, followed by self-organization of these nanosheets to form 2D mesosheets resembling the natural materials with layered structure. For the first time we also demonstrated the formation of non-crystalline and single- crystalline 2D sheets with large lateral dimension using cyclo (*D*-Phg-

*L*-Phg) **1**. The single crystal X-Ray data revealed the presence of molecular-layers which stacked along *c*-axis to form rhomboid 2D sheet. Highlight of this work is the large scale production of 2D sheets from the simplest aromatic cyclic dipeptides which in turn can be obtained by a simple and straight forward synthetic route. The formation of nanosheets by solution of cyclo (*D*-Phg-*L*-Phg) in acidified organic solvent-mixture such as CHCl<sub>3</sub>-TFA is an indication that mesosheets consist of layered assembly of nanosheets and represents an easy route for the exfoliation of mesosheets. X-Ray diffraction studies on **1** reveal that 2D sheets consist of a strong network of (N–H--O) hydrogen bonded molecular-layers of cyclo (*D*-Phg-*L*-Phg), supported by aromatic  $\pi$ - $\pi$  interactions. Taken together, the formation of such 2D sheets with large lateral surface area, their topographical hierarchy, high thermal stability, and in particular strong hydrogen bonds along with aromatic  $\pi$ - $\pi$  interactions opens up new avenues for the design of novel biomaterials. For instance, 2D nano and mesosheets of cyclo (Phg-Phg) can be viewed as potential candidates in applications such as biomineralization, 2D sheets derived composites and optoelectronic materials scaffolds.

### **3. 8 Experimental section**

#### **General Experimental Procedure**

All the solvents and reagents were obtained from Sigma-Aldrich and used as received unless otherwise mentioned. <sup>1</sup>H and <sup>13</sup>C NMR spectra were measured on a Bruker AV-400 spectrometer with chemical shifts reported as ppm.

#### **Synthesis of Fmoc protected *D*-phg-*L*-Phg-OMe**

Fmoc-*D*-Phg-*L*-Phg-OMe was prepared using peptide coupling protocols. Fmoc-*D*-Phg-OH (2 g, 5.16 mmol) was dissolved in dichloromethane, H-*L*-Phg-OMe (1.23 g, 5.67 mmol), 1-ethyl-3-(3-dimethylaminopropyl) carbodiimide (EDC·HCl, 1.19 g, 6.19 mmol), 1-hydroxybenzotriazole and (HOBT, 1.2 g, 6.19 mmol) were added. The solution was cooled to ice temperature. Diisopropylethylamine (DIPEA, 2.14 g, 16.51 mmol) was added and the

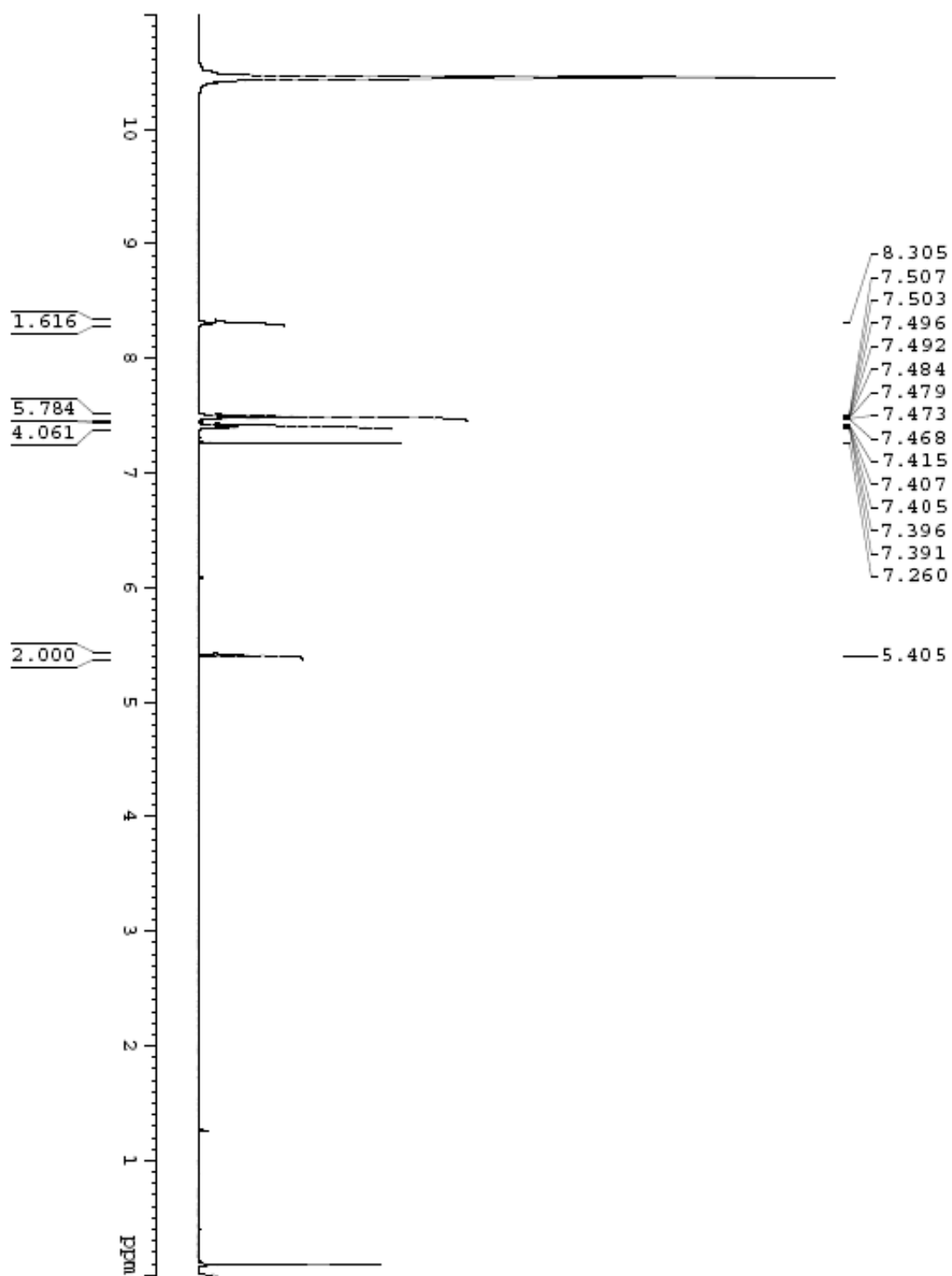
reaction mixture was stirred at ice temperature for 1 h and then at room temperature for 5 h. The reaction progress was monitored by thin layer chromatography (TLC). Reaction mixture was evaporated to dryness and extracted from dichloromethane, washed with water, dried over anhydrous sodium sulfate. The solvent was evaporated to obtain Fmoc-*D*-Phg-*L*-Phg-OMe in quantitative yield.

**Synthesis of (3R, 6S)-3, 6-diphenylpiperazine-2,5-dione (1):** The dipeptide Fmoc-*D*-Phg-*L*-Phg-OMe (1 g, 1.82 moles) was subjected to Fmoc-deprotection in 15% piperidine/dichloromethane, the deprotected dipeptide undergo cyclization to give cyclo (*D*-Phg-*L*-Phg) **1**. The *meso* cyclic dipeptide spontaneously self-assembled to form 2D mesosheets which was filtered, washed with dichloromethane, methanol and the white solid material was dried to obtain **1** in quantitative yield.  $^1\text{H NMR}$  ( $\text{CDCl}_3\text{-CF}_3\text{COOH}$ , 400 MHz)  $\delta_{\text{H}}$  5.40 (s, 2H, CH), 7.39-7.50 (m, 10H, Ar), 8.30 (s, 2H, NH);  $^{13}\text{C NMR}$  ( $\text{CDCl}_3\text{-CF}_3\text{COOH}$ , 400 MHz)  $\delta_{\text{C}}$  59.1, 127.1, 129.6, 130.0, 133.9, 169.7. MS: 267.0 [ $\text{M}+\text{H}^+$ ]; calcd for  $\text{C}_{16}\text{H}_{14}\text{N}_2\text{O}_2$ . MW. 266.29. Elemental analysis. Found: C, 72.08; H, 5.37; N, 10.58. Calcd: C, 72.12; H, 5.30; N, 10.52 for  $\text{C}_{16}\text{H}_{14}\text{N}_2\text{O}_2$ .

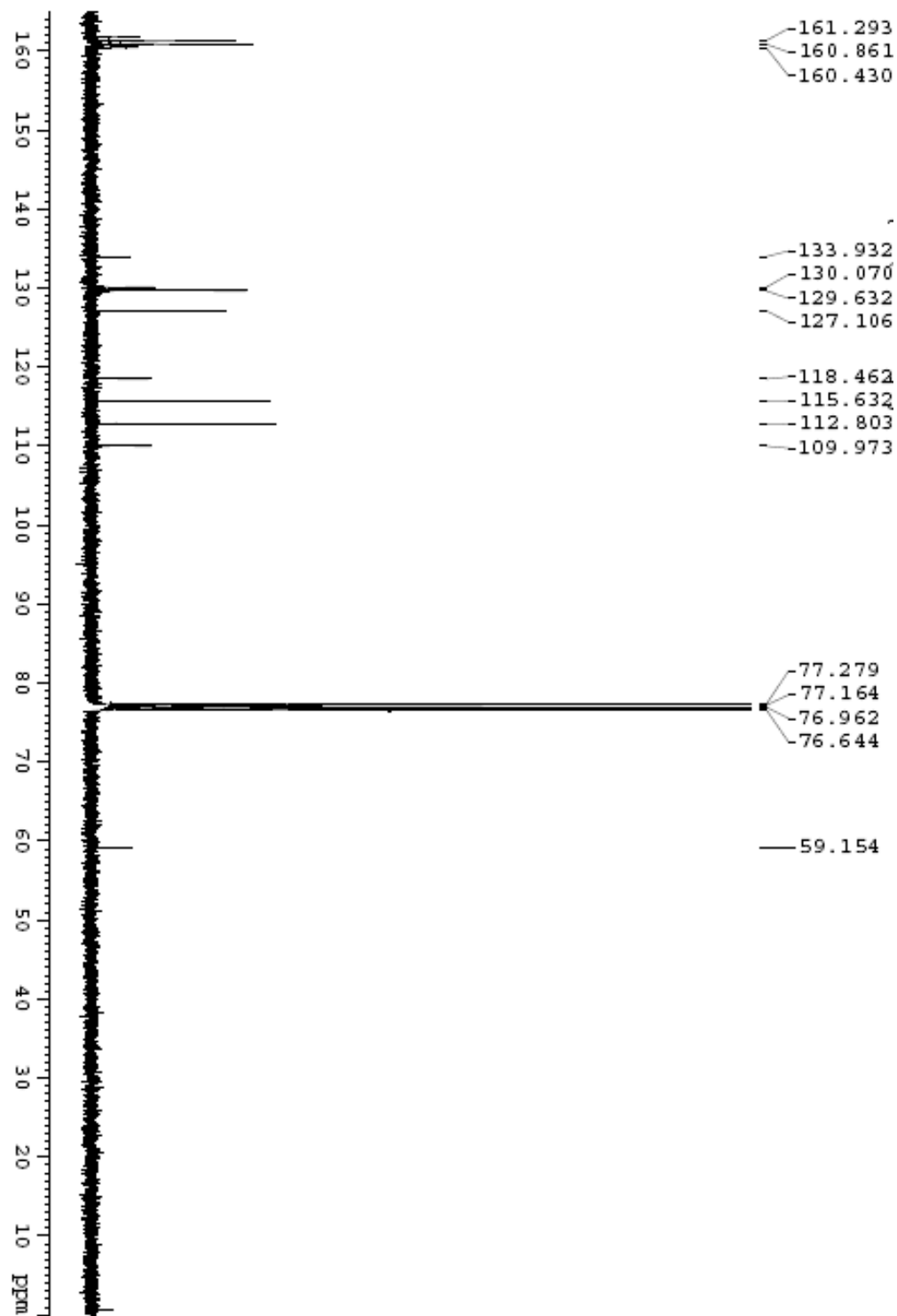
### 3. 9 Appendix

- $^1\text{H NMR}$
  
- $^{13}\text{C NMR}$

$^1\text{H}$  NMR ( $\text{CDCl}_3+\text{TFA}$ , 400 MHz) of **1**



$^{13}\text{C}$  NMR ( $\text{CDCl}_3+\text{TFA}$ , 400 MHz) of 1



### 3. 10 References

1. Rajagopal K and Schneider J P, *Curr. Opin. Struct. Biol.*, **2004**, *14*, 480–6
2. Zhang S, *Nat. Biotechnol.*, **2003**, *21*, 1171–8
3. Braun E, Eichen Y, Sivan U and Ben-Yoseph G, *Nature* **1998**, *391*, 775–8
4. Patolsky F, Weizmann Y and Willner I, *Nat. Mater* **2004**, *3*, 692–5
5. Rechtes M and Gazit E, *Science* **2003**, *300*, 625–7
6. Song Y J, Challa S R, Medforth C J, Qiu Y, Watt R K, Pena D, Miller J E, van Swol F and Shelnut J A, *Chem. Commun* **2004**, *9*, 1044–45
7. Scheibel T, Parthasarathy R, Sawicki G, Lin X M, Jaeger H and Lindquist S L, *Proc. Natl Acad. Sci. USA* **2003**, *100*, 4527–32
8. Keren K, Berman R S, Buchstab E, Sivan U and Braun E, *Science* **2003**, *302*, 1380–2
9. Sleytr U B and Beveridge T J, *Trends Microbiol* **1999**, *7*, 253–60
10. Madhavaiah C and Verma S, *Chem. Commun* **2004**, *6*, 638–9
11. Matsumura S, Uemura S and Mihara H, *Chem-Eur. J* **2004**, *10*, 2789–94
12. Zhao X and Zhang S, *Trends Biotechnol* **2004**, *22*, 470–6
13. Wagner D E, Phillips C L, Ali W M, Nybakken G E, Crawford E D, Schwab A D, Smith W F and Fairman R, *Proc. Natl Acad. Sci. USA* **2005**, *102*, 12656–61
14. Holmes T C, de Lacalle S, Su X, Liu G S, Rich A and Zhang S, *Proc. Natl Acad. Sci. USA* **2000**, *97*, 6728–33
15. Aggeli A, Bell M, Boden N, Keen J N, Knowles P F, McLeish T C, Pitkeathly M and Radford S E, *Nature* **1997**, *386*, 259–62
16. Matsumura S, Uemura S and Mihara H, *Chem-Eur. J* **2004**, *10*, 2789–94
17. Ghadiri M R, Granja J R, Milligan R A, McRee D E and Khazanovich N, *Nature* **1993**, *366*, 324–7
18. Hartgerink J D, Beniash E and Stupp S I, *Proc. Natl Acad. Sci. USA* **2002**, *99*, 5133–38
19. Vauthey S, Santoso S, Gong H, Watson N and Zhang S, *Proc. Natl Acad. Sci. USA* **2002**, *99*, 5355–60

20. Silva G A, Czeisler C, Beniash E, Harrington D A, Kessler J A and Stupp S I, *Science* **2004**, *303*, 1352–5
21. Yokoi H, Kinoshita T and Zhang S, *Proc. Natl Acad. Sci. USA* **2005**, *102*, 8414–19
22. Dankers, P.Y.W.; Meijer, E.W. *Bull. Chem. Soc. Jpn.* **2007**, *80*, 2047-2073
23. Yang, X.; Dou, X.; Rouhanipour, A.; Zhi, L.; Räder, H.J.; Müllen, K. *J. Am. Chem. Soc.* **2008**, *130*, 4216-4217
24. Ghadiri, M.R.; Granja, J.R.; Milligan, R.A.; McRee, D. E.; Khazanovich, N. *Nature* **1993**, *366*, 324-327; (b) Bong, D.T.; Clark, T.D.; Granja, J.R.; Ghadiri, M.R. *Angew. Chem. Int. Ed.* **2001**, *40*, 988 -1011; (c) Hartgerink, J.D.; Beniash, E.; Stupp, S.I. *Science* **2001**, *294*, 1684-1688; (d) Gelain, F.; Horii, A.; Zhang, S. *Macromol. Biosci.* **2007**, *7*, 544-551; (e) Reches, M.; Gazit, E. *Science* **2003**, *300*, 625-627; (f) Reches, M.; Gazit, E. *Nano Lett.* **2004**, *4*, 581-585
25. Corey, R.B. *J. Am. Chem. Soc.* **1938**, *60*, 1598-1604; (b) MacDonald, J.C.; Whitesides, G.M. *Chem. Rev.* **1994**, *94*, 2383-2420; (c) Bergeron, R.J.; *J. Am. Chem. Soc.* **1994**, *116*, 8479-8484; (d) Palmore, G.T.R.; Luo, T-J.M.; McBride-Wieser, M.T.; Picciotto, E.A.; Reynoso-Paz, C.M. *Chem. Mater.* **1999**, *11*, 3315-3328; (e) Benedetti, E.; Corradini, P.; Pedone, C. *J. Phy. Chem.* **1969**, *73*, 2891-2895
26. Schwiebert, K.E.; Chin, D.N.; MacDonald, J.C.; Whitesides, G.M. *J. Am. Chem. Soc.* **1996**, *118*, 4018-4029.
27. Palacin, S.; Chin, D.N.; Simanek, E.E.; MacDonald, J.C.; Whitesides, G.M.; McBride, M.T.; Palmore, G.T.R. *J. Am. Chem. Soc.* **1997**, *119*, 11807-11816
28. Reches, M.; Gazit, E. *Nano Lett.* **2004**, *4*, 581-585
29. (a) Kar, S.; Drew, M.G.B.; Pramanika, A. *ARKIVOC* **2009**, (xii), 43-59; (b) Leclair, S.; Baillargeon, P.; Skouta, R.; Gauthier, D.; Zhao, Y.; Dory, Y.L. *Angew. Chem. Int. Ed.* **2004**, *116*, 353-357; (c) Gupta, M.; Bagaria, A.; Mishra, A.; Mathur, P.I.; Basu, A.; Ramakumar, S.; Chauhan, V. S. *Adv. Mater.* **2007**, *19*, 858–861; (d) Zhu, P. ; Yan, X. ; Su, Y. ; Yang, Y. ; Li, J. *Chem. Eur. J.* **2010**, *16*, 3176-3183 ; (e) Görbitz, C.H. *Chem. Eur. J.* **2001**, *7*, 5153-5159.

30. (a) Görbitz, C.H.; Nilsen, M.; Szeto, K.; Tangen, L.W. *Chem. Commun.* **2005**, 4288-4290;  
(b) Görbitz, C.H. *Chem. Eur. J.* **2007**, *13*, 1022-1031; (c) Luo, T-J.M.; Palmore, G.T.R. *J. Phys. Org. Chem.* **2000**, *13*, 870-879
31. (1) Altomare, A.; Cascarano, G.; Giacovazzo, C.; Gualaradi, A. *J. Appl. crystallogr.* **1993**, *26*, 343.
32. Sheldrick, G.M. SHELXL 97, Program for the Solution of crystal structure, University of Göttingen, Germany, **1997**.
33. Spek, A.L. *J. Appl. Crystallogr.* **2003**, *36*, 7.
34. Sheldrick, G.M. SHELXS 97, Program for the solution of crystal structure, University of Göttingen, Germany, **1997**.
35. M. Reches and E. Gazit, *Phys. Biol* **2006**, *3*, 10-19
36. T. Govindaraju, M. Pandeeswar, K. Jayaramulu, G. Jaipuria and H. S. Atreya, *Supramol. Chem* **2010**. In Press



Chapter 4

**Design, Synthesis, photophysical and self-assembly  
properties of dipeptide appended naphthenediimide**

## **Design, Synthesis, photophysical and self-assembly properties of dipeptide appended naphthalenediimide**

### **4. 1 Introduction**

Fabrication of new nanomaterials using natural building blocks such as amino acids, peptides and proteins is a fascinating area of research in recent years. Peptides based materials have been showed to be a great promise in the "bottom up" approach due to their diverse chemical and physical properties. They can be synthesized in large amounts and can be modified/decorated with functional elements which can be used in diverse applications.<sup>18</sup> The simplest peptide assemblies are of dipeptide assemblies, which are the excellent building blocks for the formation of more complex nanostructures. Gazit and co-workers have been demonstrated the ability to use aromatic dipeptide as building blocks to form ordered nanoscale structures. Self-assembled nanostructures of dipeptide building blocks may find variety of applications such as in controlled drug delivery systems, in the field of tissue engineering, energy-related applications, biomineralisation, molecular electronics and biomaterial science.

We recently reported simple route for fabricating bioinspired tryptophan-appended naphthalenediimide into well-defined architectures by using molecular interactions.<sup>19</sup> Among organic electronic materials, 1, 4, 5, 8-naphthalenediimides (NDIs) are attractive due to their n-type semiconducting property and air stability. These are compact electron deficient class of aromatic compounds having tendency to form n-type semiconductor materials.<sup>1</sup> NDI derivatives have got wide range of applications in biological, biomedical as well as in supramolecular chemistry. Its derivatives have been used as intercalators of DNA, chemotherapy, conducting materials, optical brighteners, electrophotography, fluorescent labelling systems, metalomacrocycles, models for the photosynthetic reaction centre (due to

ease of synthesis and electron accepting properties), sensors (seven different positional isomers of dihydroxynaphthalene<sup>2</sup> and DNA sensing<sup>3</sup>) and anticancer agents.<sup>4-7</sup> Because of their desired electronic, spectroscopic and enhanced solubility properties NDIs can act as ideal components for the creation of supramolecular functional materials (donor-acceptor complexes, barrels, catenanes and rotaxanes).<sup>8-9</sup> The absorption and emission bands of NDIs are variable upon functionalization through the diimide nitrogens or via core substitution. Photophysical properties of N, N-dialkyl- substituted NDIs have been studied. The absorption and emission spectra of these compounds are mirror images to each other and readily aggregate in acetonitrile and in aqueous medium.<sup>10</sup> In aromatic solvents (toluene) excimer-like emissions were observed due to ground-state aggregation. In the case of core substituted NDIs photophysical properties are different than unsubstituted ones,<sup>11</sup> and are highly colourful and conducting functional materials.<sup>12</sup>

1,4,5,8-Naphthalenediimides are neutral, planar, chemically robust, redox-active compounds usually with high melting points.<sup>12</sup> Its derivatives can exhibit relatively high electron affinities, high electron mobility, and excellent chemical, thermal, and photochemical stabilities. Because of its electron transfer behaviour and the ability to tune molecular electronic properties through either variation of substituents on the imide nitrogen atoms or core substitution, they have been used as building blocks for electronic and optoelectronic devices such as electron-transfer processes,<sup>17</sup> photodetectors,<sup>16</sup> organic light-emitting diodes,<sup>13</sup> optical switches,<sup>15</sup> dye lasers,<sup>14</sup> and also as electron acceptors for studying photo induced energy.

In this chapter the synthesis and characterization of aromatic conjugated NDIs are presented. This study demonstrates the use of small peptide sequences with  $\pi$  system directly embedded in the backbone to promote assembly of NDI into well ordered nano architectures

with strong  $\pi$ - $\pi$  intermolecular electronic communication in the mixture of polar/non polar solvents.

## 4. 2 Objective of the present work

The objective of this project is to synthesize and study the supramolecular assembly of a series of N, N-dipeptide appended naphthalenetetracarboxylic diimide (NDI) chromophores. The aromatic functionalities of amino acids side chain was systematically varied to understand the effect of this simple structural variations on the self-assembly. The properties of resulting self-assembled nanomaterials and their architectures were studied using various spectroscopic and microscopic techniques.

## 4. 3 Design Strategy

For the fabrication of self-assembled nanostructure with well defined order an appropriate balance of solvophobic, hydrogen bonding,  $\pi$ - $\pi$  stacking and steric interactions is required. Hence we have designed the N,N-bis-(dipeptide) appended NDI molecules as shown in Scheme 4.1. A small peptide sequences with  $\pi$ -conjugated NDI directly embedded in the backbone promote molecular self-assembly into various nanostructures with strong  $\pi$ - $\pi$  intermolecular interactions and hydrogen bonding. The planar NDI and aromatic side chain on dipeptides ( $R_1$  and  $R_2$  in Figure 4.1) will induce  $\pi$ - $\pi$  stacking and amide groups will induce highly directional hydrogen bonding between the molecules.

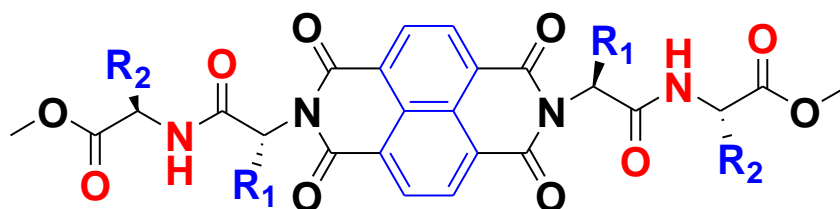
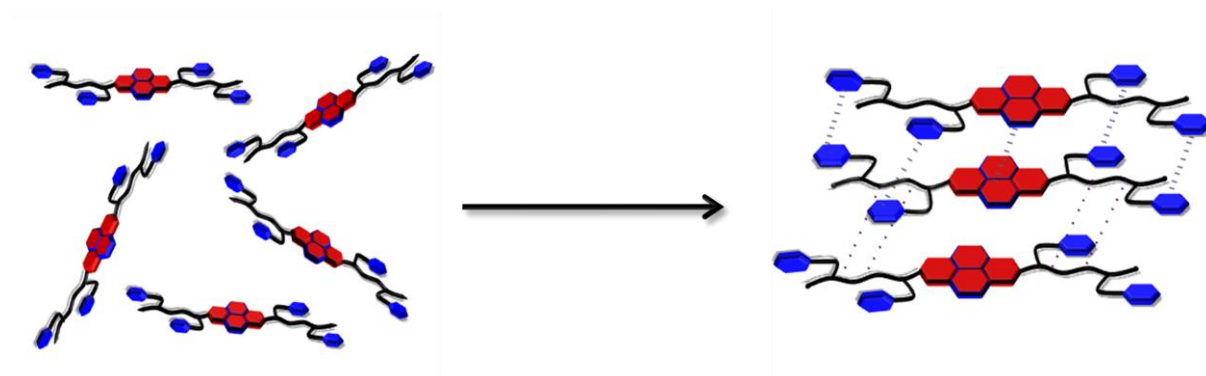


Figure 4. 1

As a result of these combined non-covalent interactions and appropriate solvent conditions the N, N-bis-(dipeptide) appended NDI molecule expected to self-assemble into nanostructures with well defined architectures.

We have synthesized the NDIs **4**, **5** and **6** by appending aromatic dipeptides (Phe-Phe, Phe-Trp and Trp-Trp) to NDA (1,4,5,8-Naphthalenetetracarboxylic dianhydride) as shown in Figure 4.1. Aromatic dipeptide modified NDIs **4**, **5** and **6** are expected to self-assemble into well ordered architectures through intermolecular hydrogen bonding and aromatic  $\pi$ - $\pi$  stacking in an appropriate environment. Figure 4.2 shows the schematic representation of self-assembly of NDIs **4**, **5** and **6** from randomly oriented molecules to ordered assemblies with the help of proposed amide hydrogen bonding and  $\pi$ - $\pi$  interactions between the amide groups and planar  $\pi$  conjugated NDI and aromatic side chains on dipeptide moieties respectively.



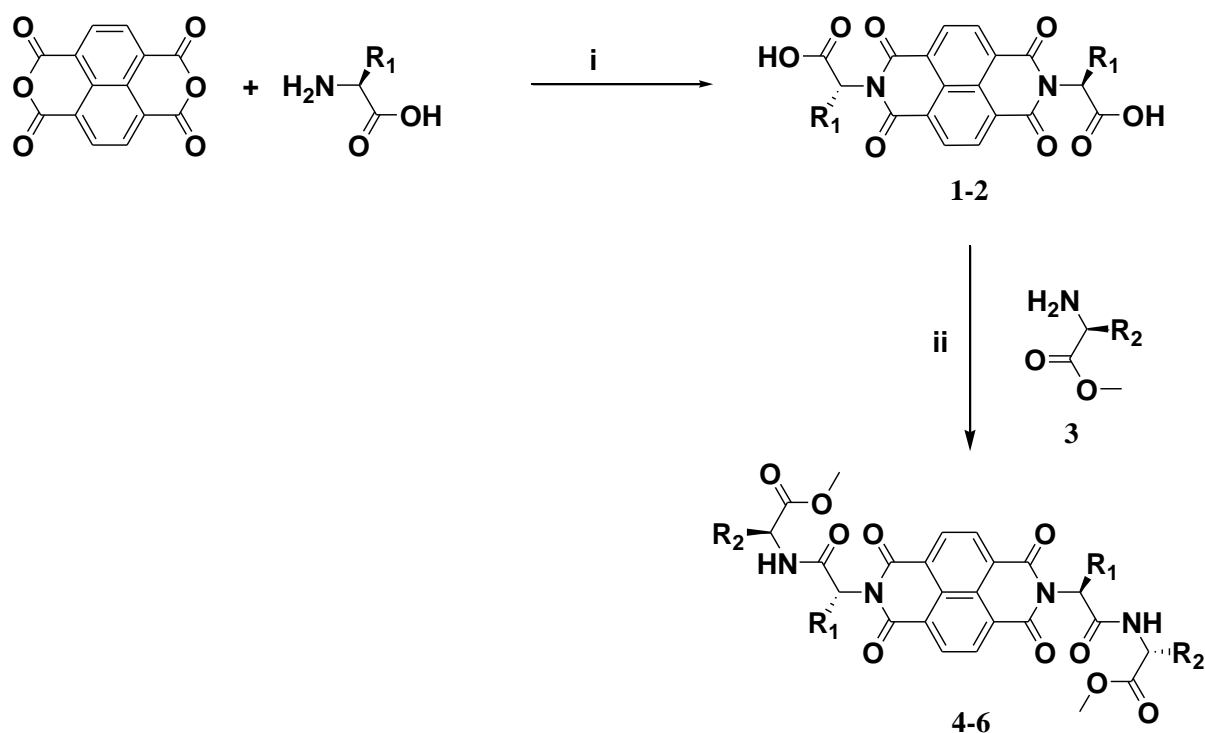
**Figure 4. 2** Schematic representation of self-assembly of randomly oriented N,N-bis-(dipeptide) appended NDI molecules into a ordered stacks under appropriate solvent system through H-bonding and  $\pi$ - $\pi$  interactions.

## 4. 4 Results and discussion

### 4.4. 1 Synthesis of peptide appended NDIs

N, N bis-(dipeptide) appended 1, 4, 5, 8-Naphthalenediimides (**4**, **5** and **6**) was synthesised according to Scheme 4.1.

N, N-bis-(di-peptide) appended NDIs (**4**, **5** and **6**) were synthesized and characterised by Matrix-assisted laser desorption ionization (MALDI), Nuclear magnetic resonance spectroscopy ( $^1\text{H}$  NMR,  $^{13}\text{C}$  NMR). Self-assembly properties have been studied in different solvent systems. The resulting self-assembled structures were characterized using various spectroscopic and microscopy techniques.



1.  $\text{R}_1 = \text{C}_7\text{H}_7$
2.  $\text{R}_1 = \text{C}_9\text{H}_8\text{N}$
4.  $\text{R}_1 = \text{R}_2 = \text{C}_7\text{H}_7$
5.  $\text{R}_1 = \text{C}_7\text{H}_7$ ,  $\text{R}_2 = \text{C}_9\text{H}_8\text{N}$
6.  $\text{R}_1 = \text{R}_2 = \text{C}_9\text{H}_8\text{N}$

**Scheme 4. 1** Synthesis of N, N-bis-(di-peptide) appended NDIs. Reagents and conditions: (i)  $\text{C}_6\text{H}_{15}\text{N}$ , DMF, reflux, 12 h. (ii) EDC.HCl, HOBT and DIPEA, DMF, rt, 12 h.

#### 4.4. 2 Self-Assembly Studies

We have investigated the self-assembly of NDIs **4**, **5** and **6**, in various polar and mixture of polar and non polar solvents such as chloroform, DMSO (dimethyl sulfoxide), CHCl<sub>3</sub>/MeOH(methanol), CHCl<sub>3</sub>/MCH(methylcyclohexane) and DMSO/H<sub>2</sub>O respectively. We have used UV-vis absorption spectroscopy, photoluminescence spectroscopy and scanning electron microscopy (SEM) to investigate their electronic and self-assembly properties of NDIs to form nanostructures with well defined architectures.

#### 4.4. 3 Absorption and Emission Studies

Electronic absorption spectra were recorded on a Perkin Elmer Lambda 900 UV-VIS-NIR Spectrometer and emission spectra were recorded on Perkin Elmer LS55 Luminescence Spectrometer. UV-vis absorption and emission spectra were recorded in 10 mm path length cuvette. Fluorescence spectra of solutions were recorded with 380 nm excitation wavelength.

The UV-vis absorption and emission spectra of molecularly dissolved NDI **4** in chloroform (CHCl<sub>3</sub> known to be a good solvent for  $\pi$  systems) and DMSO (hydrogen bond accepting solvent) were showed the typical spectral features of N, N di-substituted NDI molecule as reported in the literature<sup>20</sup> (Figure 4.2b). The absorption spectra of **4** in chloroform ( $5 \times 10^{-5}$ M) showed a broad band with shoulder at 340 nm, two maxima at 361 nm and 381 nm (Figure 4.3a red curve) which are the characteristic of z-polarized  $\pi$ - $\pi^*$  transitions in NDI chromophore.<sup>20</sup> In DMSO also NDI **4** ( $5 \times 10^{-5}$ M) showed almost similar spectral features with  $\lambda_{\text{max}}$  at 340 nm, 361 nm and 381 nm (Figure 4.3b). The emission spectra is mirror image to absorption spectra in chloroform for NDI **4** ( $5 \times 10^{-5}$ M) showed broad band with two maxima at 408 nm and 432 nm (Figure 4.2a black curve). Where as in DMSO the intensity of emission spectra was slightly decreased (Figure 4.2b, black curve). Since the absorption and emission spectra in chloroform and DMSO are almost identical (except with some minor changes) it can be considered that NDI **4** did not form self-

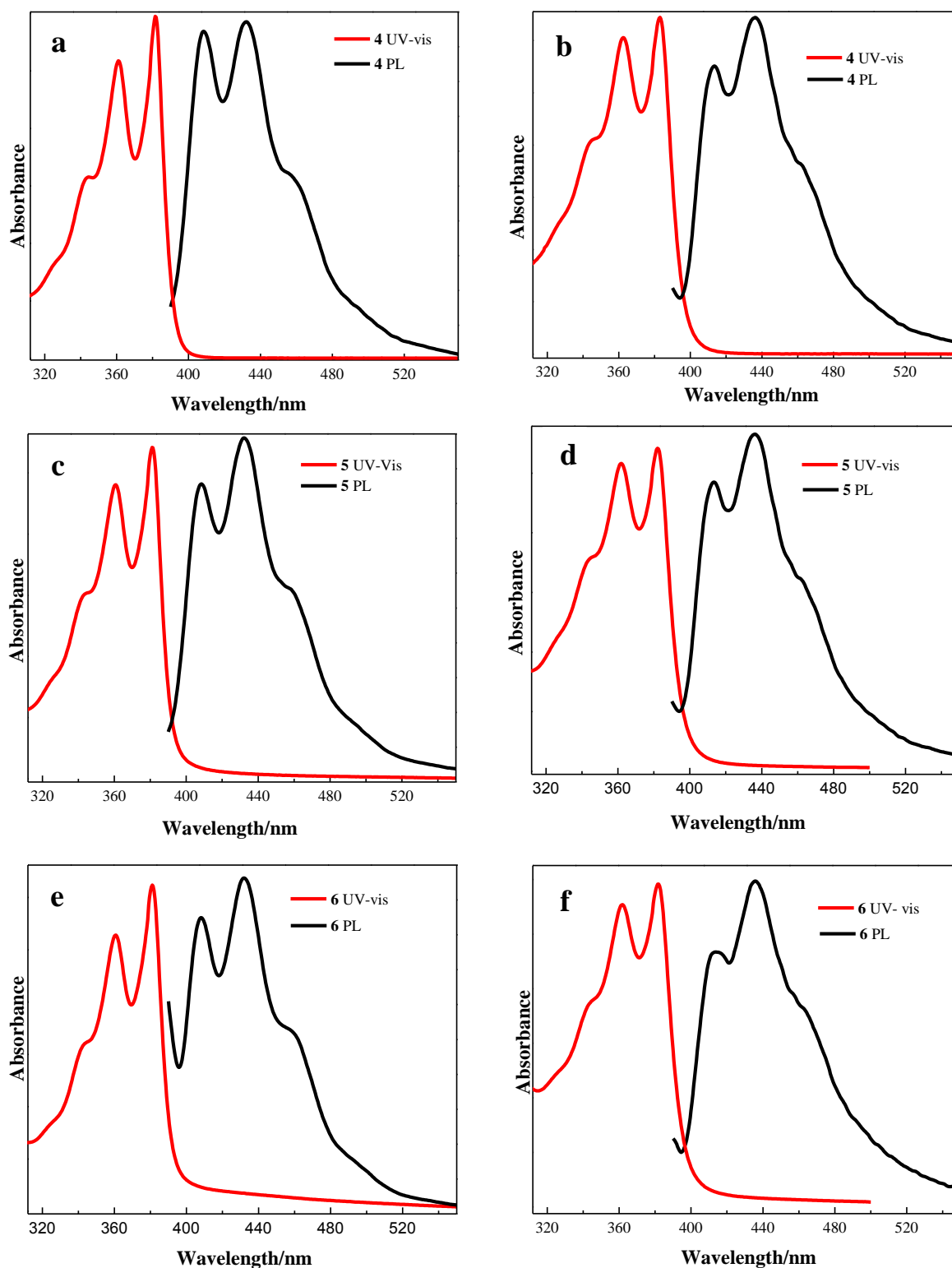


**Figure 4.3** UV-vis absorption (red curve) and Photoluminescence (black curve) studies at  $5 \times 10^{-5} \text{M}$  (a) absorption and emission ( $\lambda_{\text{ex}} = 380 \text{ nm}$ ) of NDI **4** in  $\text{CHCl}_3$ , (b) absorption and emission ( $\lambda_{\text{ex}} = 380 \text{ nm}$ ) of NDI **4** in DMSO, (c) absorption and emission ( $\lambda_{\text{ex}} = 380 \text{ nm}$ ) of NDI **5** in  $\text{CHCl}_3$  (d) absorption and emission ( $\lambda_{\text{ex}} = 380 \text{ nm}$ ) of NDI **5** in DMSO, (e) absorption and emission ( $\lambda_{\text{ex}} = 380 \text{ nm}$ ) of NDI **6** in  $\text{CHCl}_3$ , (f) absorption and emission ( $\lambda_{\text{ex}} = 380 \text{ nm}$ ) of NDI **6** in DMSO.



assembled aggregates in these solvents. Similar spectral features were observed in the case of NDIs **5** and **6** as shown in Figure 4.2 (c, d) and (e, f) respectively.

In order to gain further insight into the aggregation behaviour of NDIs **4**, **5** and **6**, detailed absorption and emission spectral studies were carried out in presence mixture of solvent systems such as MCH/CHCl<sub>3</sub>, MeOH/CHCl<sub>3</sub> and H<sub>2</sub>O/DMSO. Here MCH is known to facilitate the  $\pi$ - $\pi$  stacking and hydrogen bonding between the molecules, MeOH will break the hydrogen bonding but it can enhance the  $\pi$ - $\pi$  staking between the molecules. While H<sub>2</sub>O is a highly polar solvent and due to solvophobic effects organic molecules expected to form self-assembled aggregates in this solvent.

#### **4.5. 1 NDI 4 [N, N-bis-(Phe-Phe-OMe) appended NDI]**

##### **4.5.3. 1 MCH/CHCl<sub>3</sub> solvent system**

UV-vis absorption and emission studies of NDI **4** in MCH/CHCl<sub>3</sub> solvent system at  $5 \times 10^{-5}$  M concentration are shown Figure 4.4. In CHCl<sub>3</sub> NDI **4** showed an broad absorption band with two maxima at 361 nm and 381 nm. Which is characteristic of molecularly dissolved (un-assembled molecules) NDIs. However, in MCH/CHCl<sub>3</sub> (95:5) observed a slight (3 nm) blue shift (hypsochromic shift) in absorption maxima (Figure 4.4 a), suggesting the self-assembly of NDIs. More interestingly emission studies upon addition of MCH to CHCl<sub>3</sub> (95:5) showed an eximer like emission at 482 nm which is not observed in CHCl<sub>3</sub> solution (Figure 4.4b). Figure 4.4 show UV-vis absorption and emission spectra and their corresponding scanning electron microscopic (SEM) images of NDI **4** in MCH/CHCl<sub>3</sub> (95:5) solvent system.

##### **4.5.3. 2 Morphological studies**

Morphological studies of NDI **4** indicated the formation of spherical aggregates from MCH/CHCl<sub>3</sub> (95:5) solvent system as shown in the SEM micrograph (Figure 4.4b and c). The non-covalent interactions such as hydrogen bonding, solvophobic forces and aromatic

$\pi$ - $\pi$  stacking decides the molecular organization and hence their morphology. The intermolecular

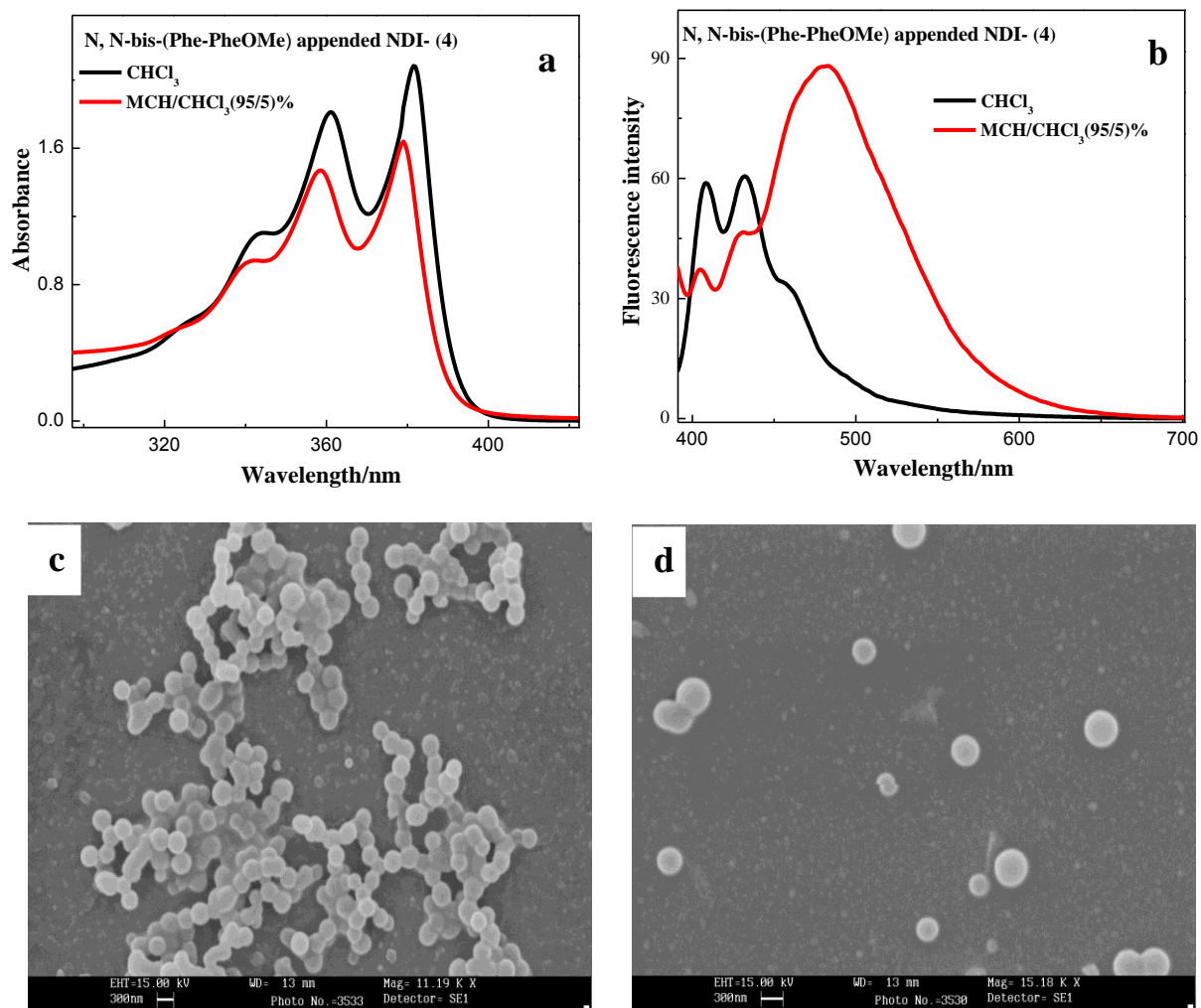


**Figure 4. 4** Photophysical studies of NDI **4** ( $5 \times 10^{-5}$  M) in CHCl<sub>3</sub> (black curve) and in MCH(methylcyclohexane)/CHCl<sub>3</sub>(95:5)(red curve). (a) UV-vis spectra, (b) Photoluminescence emission spectra(PL) ( $\lambda_{\text{exi}}$  at 380 nm), (c) and (d) SEM micrograph of NDI **4** nanospheres obtained from the MCH/CHCl<sub>3</sub> (95:5) solvent system on glass substrate.

hydrogen bonding between amide groups of NDI **4** and cooperative aromatic  $\pi$ - $\pi$  interaction leads to formation of nanospheres in MCH/CHCl<sub>3</sub> (95:5) solution.

From these results, it is clear that the NDI **4** undergo molecular self-assembly in MCH/CHCl<sub>3</sub> (95:5,  $5 \times 10^{-5}$  M) solvent system. At high volume percent of MCH (95%) in

$\text{CHCl}_3$ (5%) NDI **4** exist as self-assembled spherical aggregate which corresponds to slight blue shift in absorption maximum and excimer formation due to ground state aggregation. Whereas in  $\text{CHCl}_3$  NDI **4** exist as a molecularly dissolved form (un-aggregate form) and hence suggest that MCH induces self-assembly between NDI **4** molecules through  $\pi$ - $\pi$  and amide hydrogen bonding.

#### 4.5.3. 3 MeOH/ $\text{CHCl}_3$ solvent system.

With the addition of 95% MeOH to  $\text{CHCl}_3$  solution of NDI **4** decrease in absorbance and fluorescence intensity was observed as shown in Figure 4.5 (a and b). It is a clear indication of transformation of NDI **4** from molecularly dissolved state (in  $\text{CHCl}_3$ ) to aggregate state (in 95% MCH) through noncovalent  $\pi$ - $\pi$  interactions.

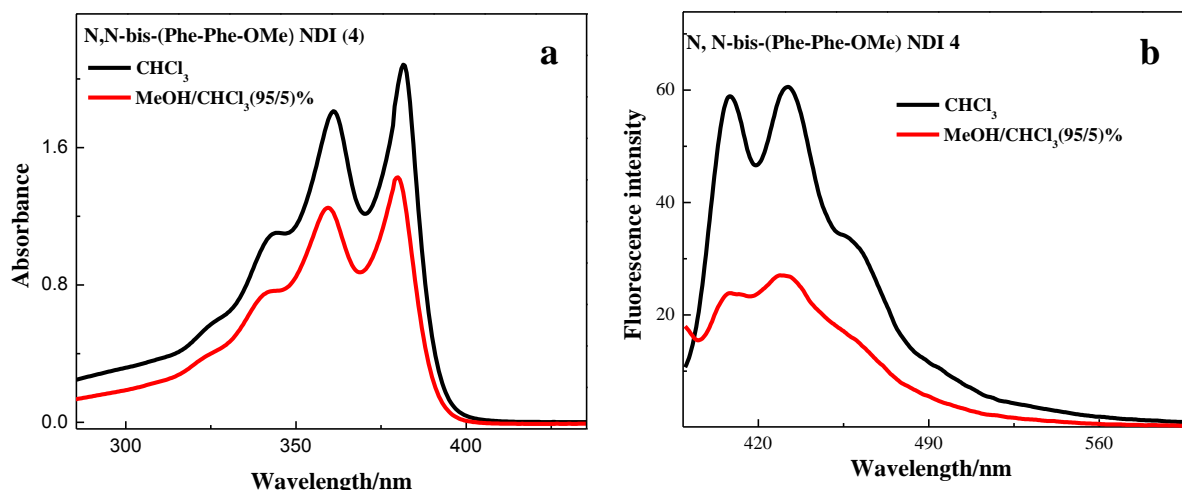


**Figure 4. 5** Photophysical studies of NDI **4** ( $5 \times 10^{-5}$  M) in  $\text{CHCl}_3$  (black curve) and in MeOH/ $\text{CHCl}_3$  (95:5) (red curve). (a) UV-vis absorption spectra, (b) photoluminescence emission spectra ( $\lambda_{\text{exi}}$  at 380 nm).

SEM micrograph showed the formation of novel architectures with vesicular in MeOH/ $\text{CHCl}_3$  (95:5,  $5 \times 10^{-5}$ ) solvent system (Figure 4.6a and b). From these observation we conclude that MeOH assist to break amide hydrogen bonding and facilitates the  $\pi$ - $\pi$

interactions between the NDI **4** molecules. The  $\pi$ - $\pi$  staking is the main driving force for the NDI **4** to form vesicular nanostructures.

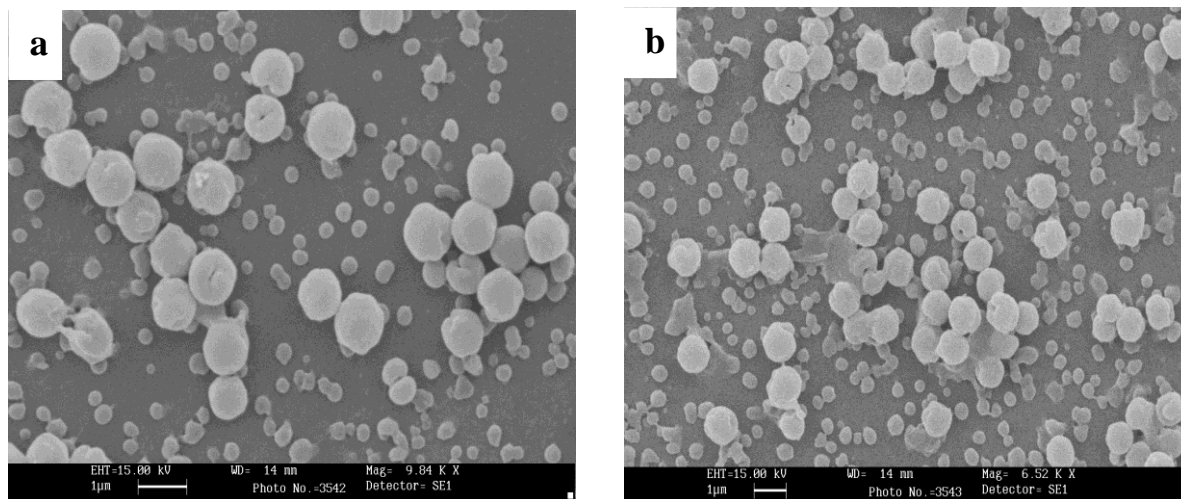


**Figure 4. 6** (a) and (b) SEM micrograph open mouth nanovesicles obtained from the solution of NDI **4** [MeOH/CHCl<sub>3</sub> (95:5)] on glass substrate.

#### 4.5.3. 4 H<sub>2</sub>O/DMSO solvent system

NDI **4** in H<sub>2</sub>O/DMSO solvent system showed slight red shift in the absorbance spectra and an interesting eximer formation at 482 nm (Figure 4.7a and b). SEM micrographs revealed that NDI **4** self-assemble into 1D nanostructure in this solvent system as shown in Figure 4.7 (c and d). Addition of water induces hydrophobic effect on planar  $\pi$ -conjugated NDI core and aromatic side chains on dipeptides and NDI **4** tries to minimise the total surface area exposed to polar medium (water). In this process NDI **4** undergo molecular  $\pi$ - $\pi$  stacking in a highly directional fashion to form one dimensional nanostructures.

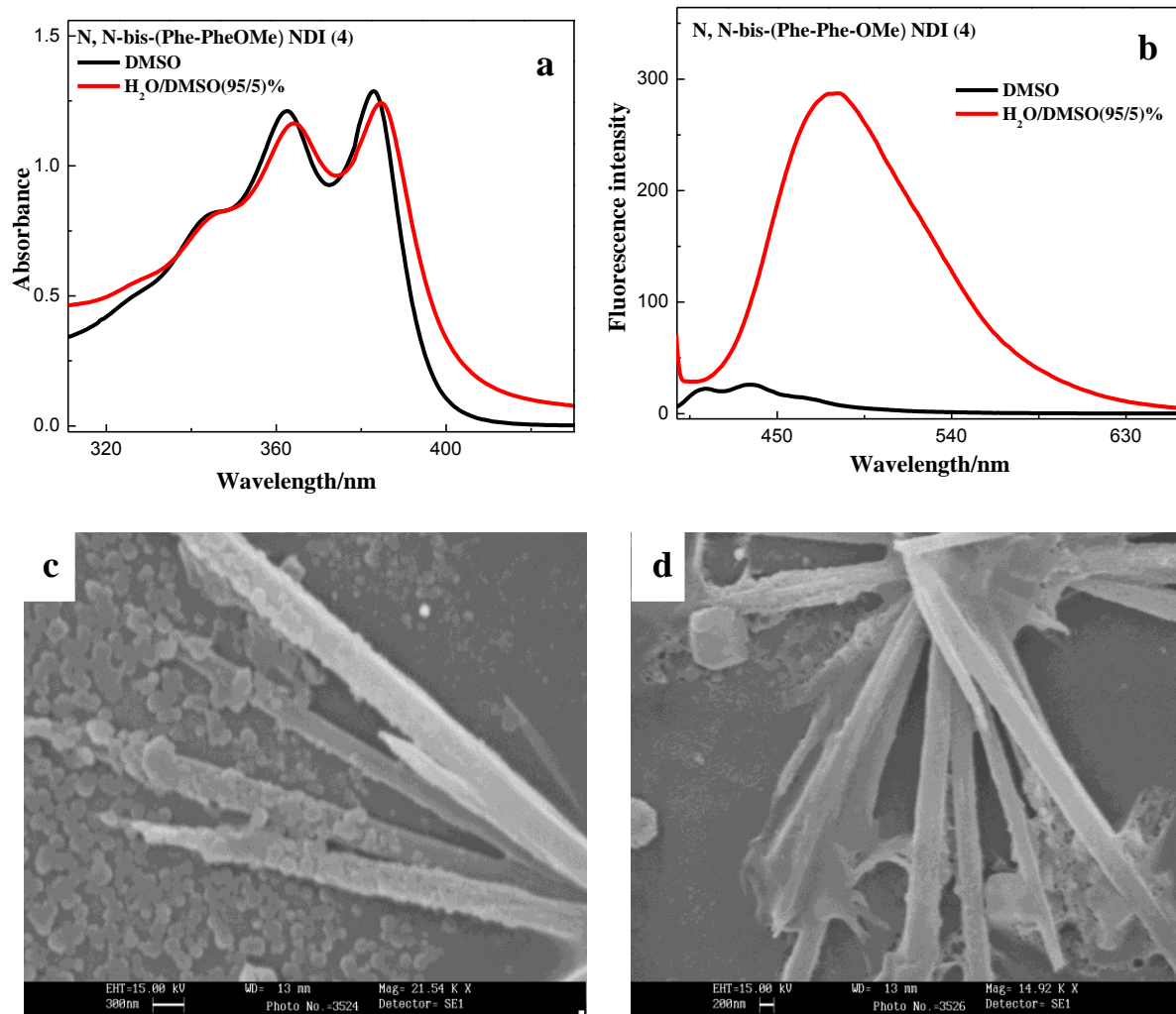


**Figure 4.7** Photophysical studies of NDI **4** ( $5 \times 10^{-5}$  M) in DMSO (black curve) and in H<sub>2</sub>O/DMSO (95:5) (red curve). (a) UV-vis absorption spectra, (b) photoluminescence emission spectra ( $\lambda_{\text{exi}}$  at 380 nm), (c) and (d) SEM micrograph of NDI **4** nanotapes obtained from H<sub>2</sub>O/DMSO (95:5) solvent system on glass substrate.

Thus we were able to induce well defined molecular organisation and morphology control mediated by molecular recognition. We were able to successfully tune the morphology of NDI **4** in to well-defined architectures including nanospheres, open mouth nanovesicles and 1-D nanotapes through solvation processing by cleverly choosing solvent system.

## 4.5. 2 NDI 5 [N, N-bis-(Phe-trp-OMe) appended NDI]

### 4.5.4. 1 MCH/CHCl<sub>3</sub> and H<sub>2</sub>O/DMSO solvent system

UV-vis absorption and photoluminescence studies have been performed for NDI 5 in the same solvent systems (MCH/CHCl<sub>3</sub>, H<sub>2</sub>O/DMSO and MeOH/CHCl<sub>3</sub>) that were used in the case of NDI 4. With the addition of MCH to CHCl<sub>3</sub> solution of NDI 5 the UV-vis absorption spectra showed slight red shift along with decrease in absorbance (Figure 4.8a). However increase in the photoluminescence intensity was observed (Figure 4.8b).

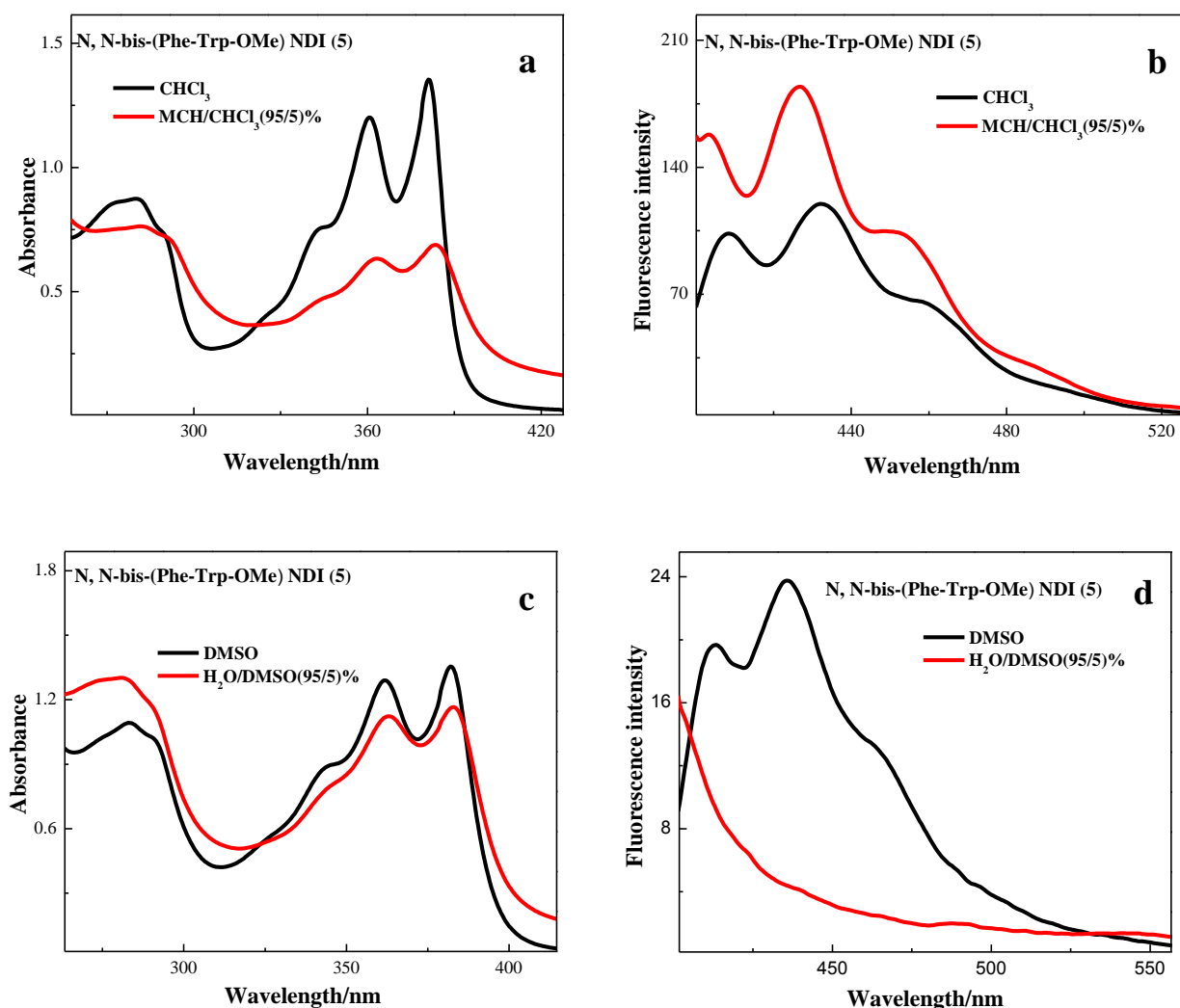


**Figure 4. 8** Photophysical studies of NDI 5 ( $5 \times 10^{-5}$  M), UV-vis absorption spectra (a and c), Photoluminescence emission spectra ( $\lambda_{\text{exi}}$  at 380 nm) (b and d).

Photophysical studies suggest the self-assembly of NDI **5** in this solvent system. However with the addition of H<sub>2</sub>O to the solution of NDI **5** in DMSO there was no excimer like emission ( Figure 4.8d).

#### 4.5.4. 2 MeOH/CHCl<sub>3</sub> solvent system

The photophysical and SEM studies of NDI **5** in (95:5) MeOH/CHCl<sub>3</sub> solvent system are shown in Figure 4. NDI **5** exhibited similar spectral (absorbance and emission) and morphological features to that of NDI **4** (Figure 4.9a and b). SEM micrograph showed the formation of open mouth nanovesicles (Figure 4.10a and b)

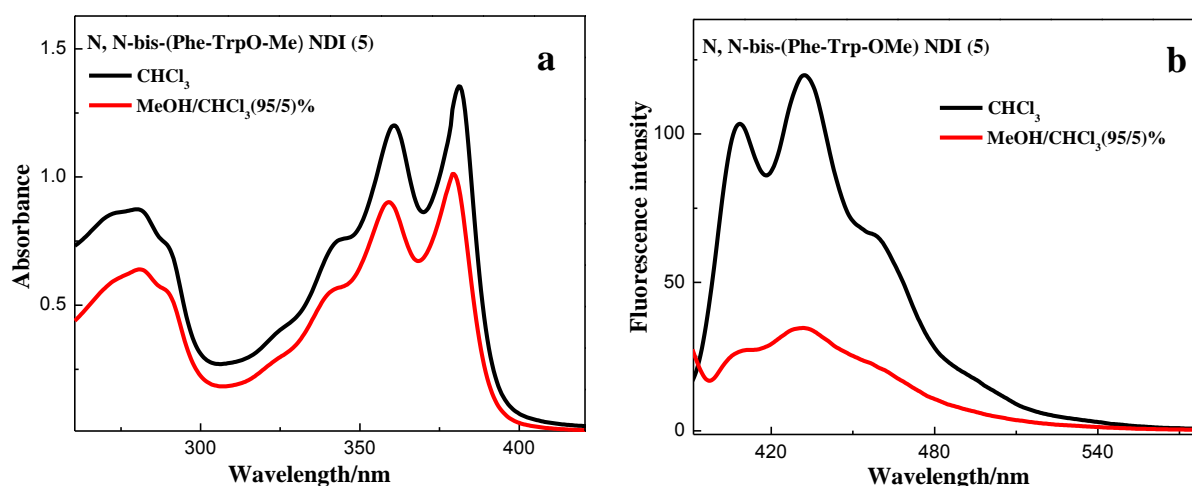


**Figure 4. 9** Photophysical studies of NDI **5** ( $5 \times 10^{-5}$  M) in CHCl<sub>3</sub> (black curve) and in MeOH/CHCl<sub>3</sub> (95:5) (red curve). (a) UV-vis absorption spectra, (b) photoluminescence emission spectra ( $\lambda_{\text{exi}}$  at 380 nm).

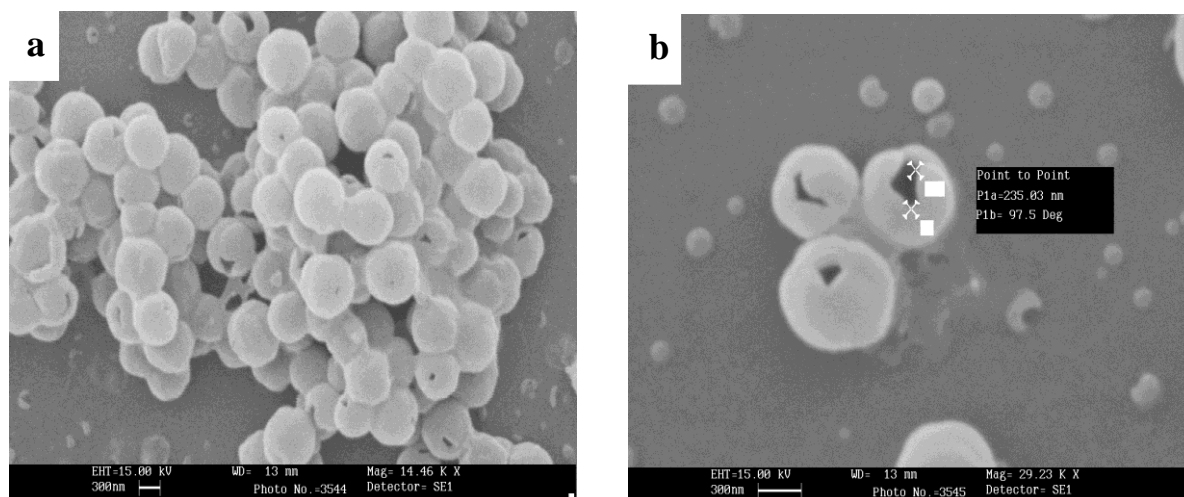


**Figure 4. 10** Microscopic studies of NDI **5**. (a) and (b) SEM micrograph of open mouth nanovesicles obtained from the solution of NDI **5** in MeOH/CHCl<sub>3</sub> (95:5) solvent system on glass substrate.

### 4.5. 3 NDI **6** [N, N-bis-(Trp-Trp-OMe) appended NDI]

#### 4.5.5. 1 MCH/CHCl<sub>3</sub> solvent system

UV-vis absorption and photoluminescence studies have been done for the NDI **6** in MCH/CHCl<sub>3</sub> solvent system. With the addition of MCH to solution of NDI **6** in CHCl<sub>3</sub> the intensity of absorbance significantly decreased and increase in fluorescence intensity was observed as shown in the Figure 4.11a and b. SEM micrograph revealed the presence of three dimensional aggregates (nanocubes) of NDI **6** in this solvent system (Figure 4.11c and d).



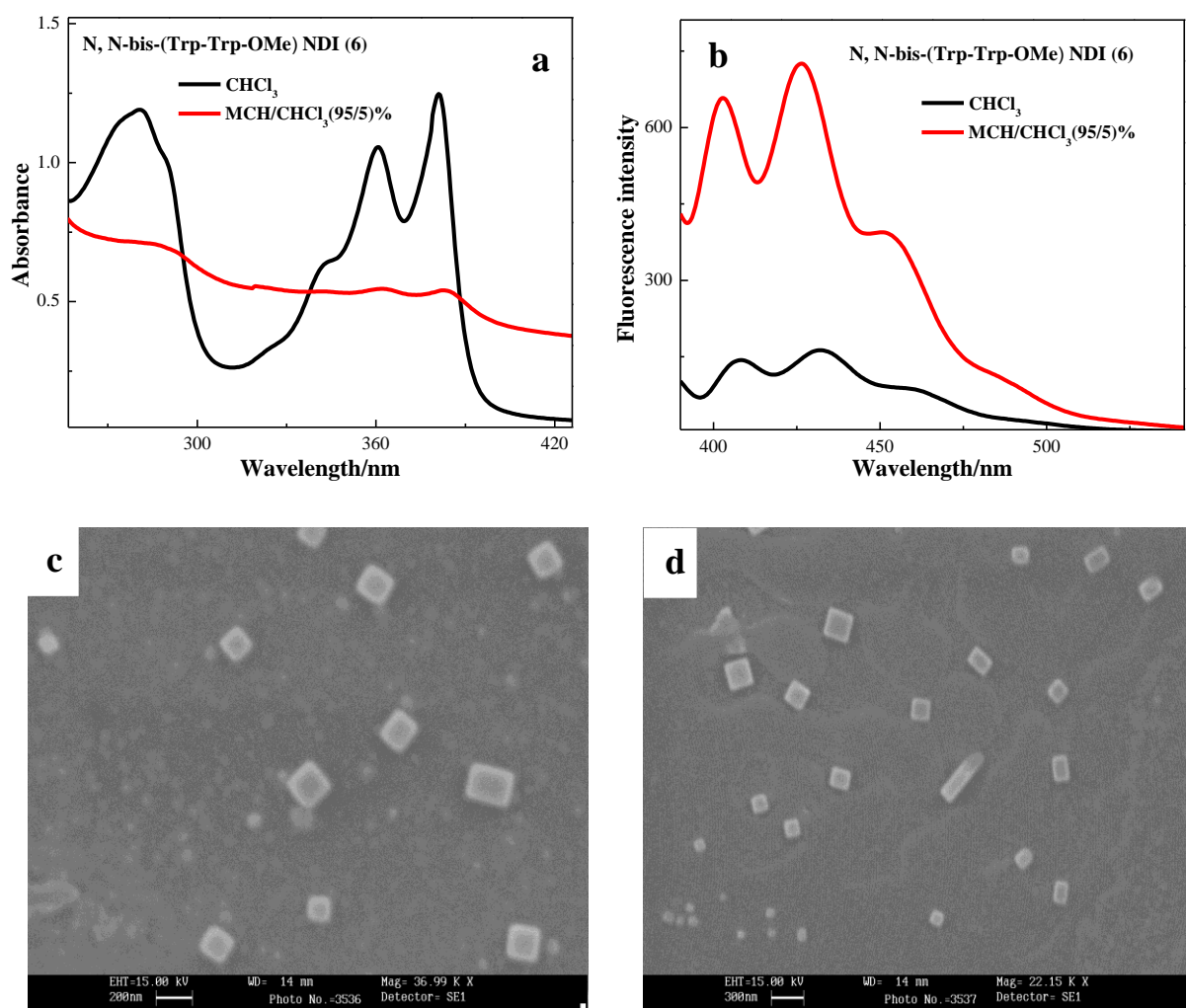


**Figure 4. 11** Photophysical studies of NDI **6** ( $5 \times 10^{-5}$  M) in CHCl<sub>3</sub> (black curve) and in MCH/CHCl<sub>3</sub> (95:5) (red curve). (a) UV-vis absorption spectra, (b) photoluminescence emission spectra ( $\lambda_{\text{exi}}$  at 380 nm), (c) and (d) SEM micrograph of NDI **6** nanocubes obtained from the MCH/CHCl<sub>3</sub> (95:5) solution on glass substrate.

#### 4.5.5. 2 MeOH/CHCl<sub>3</sub> and H<sub>2</sub>O/DMSO solvent system

In H<sub>2</sub>O/DMSO NDI **6** formed three dimensionally organized self-assembled nanocubes as shown in Figure 4.12 e. This suggest that the  $\pi$ - $\pi$  stacking is the main driving force for the self-assembly of NDI **6** to form nanocubes in polar as well as non-polar solvents.

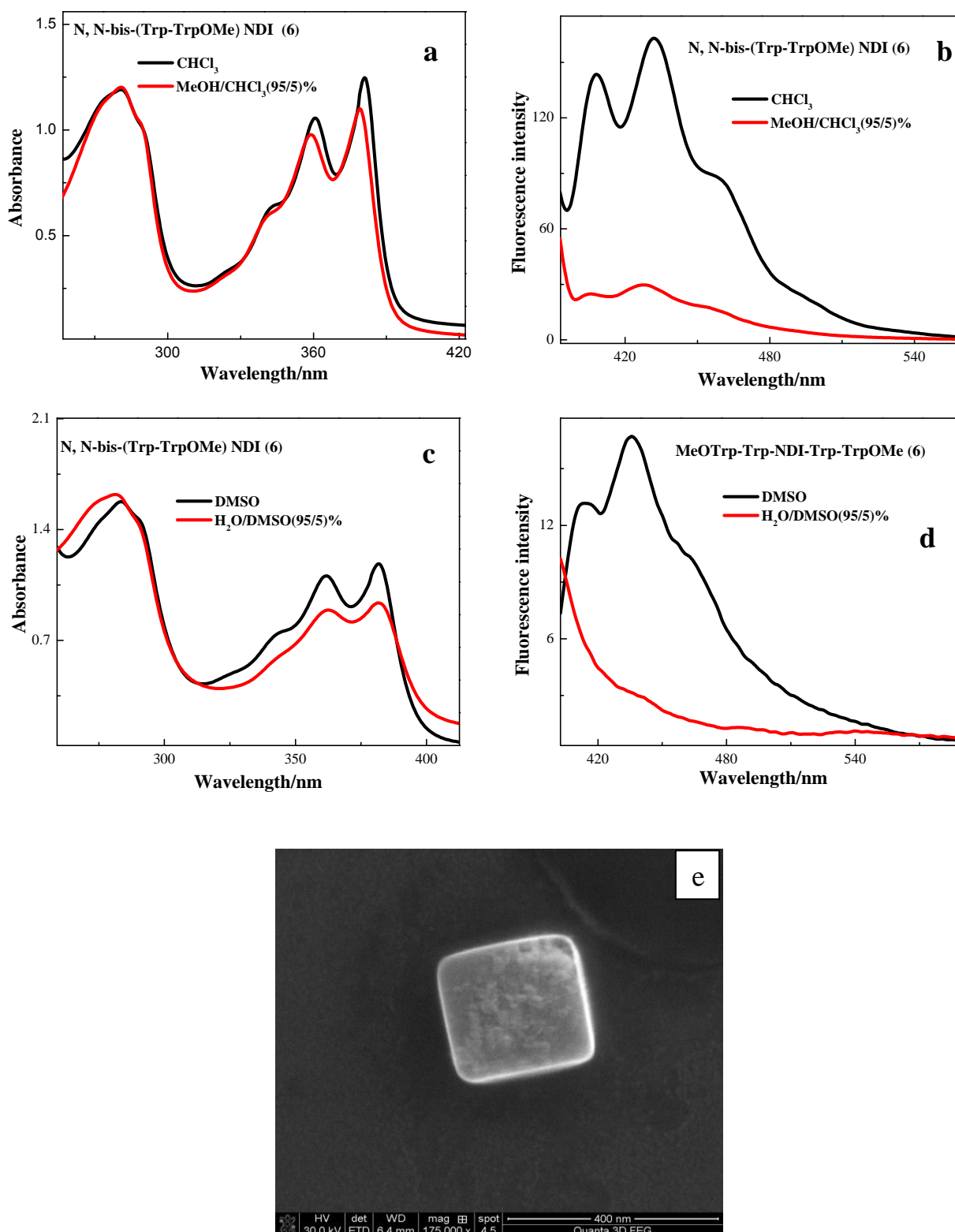


**Figure 4. 12** Photophysical studies of NDI 6 ( $5 \times 10^{-5}$  M), (a) and (c) UV-vis absorption spectra, (b) and (d) Photoluminescence emission spectra ( $\lambda_{\text{exi}}$  at 380 nm), (e)FESEM micrograph of NDI 6 nanocubes obtained from the  $\text{H}_2\text{O}/\text{DMSO}$  (95:5) solvent system.

#### 4. 5 Proposed mechanism

Based on the photophysical and morphological data of NDIs **4**, **5** and **6** we proposed the schematic model to explain the various nanostructures formed by N, N-bis-(dipeptide) appended NDI systems as illustrated in Figure 4.13. SEM images revealed the existence of self-assembled nanodimensional structures with well defined morphologies. In a single solvent system (acts as a good solvent) like  $\text{CHCl}_3$  and DMSO molecules of NDIs **4**, **5** and **6** are fully solvated hence the molecules are randomly oriented in all possible directions. By the addition of a poor solvent, it will induce the solvophobic effect on the NDIs **4**, **5** and **6** molecules. To overcome solvophobic effect molecules of NDIs **4**, **5** and **6** tries to come closer and closer in order to minimise the total surface area exposed to solvent molecules. At certain distance, the  $\pi$ - $\pi$  interactions and hydrogen bonding between the molecules will starts forming which will arrange the molecules into the proper direction as shown in Figure 4.13. Stacked molecules of NDIs **4**, **5** and **6** further organised to form a self-assembled two dimensional nanostructures of different dimenssions. The geometrically-restricted interactions of the aromatic moieties and their complex hydrophobic and electrostatic nature, various changes in the electronic environment of the aromatic system in the context of very small peptide, can significantly affect the organization of the assembled NDIs.<sup>21</sup> The final morphology of NDIs **4**, **5** and **6** depends on direction of folding or organisation of initially self-assembled NDI structure. For example three dimensional arrangements of initial self-assembly structure will leads to the formation of 3D nanocubes. If the arrangements in one dimensional way then we see one dimensional nanotape formation. Figure 4.13 showing schematic model for various possible ways of organization of NDIs **4**, **5** and **6** to form nanostrucres of zero-, one-, two- and three-dimensional with well defined morphology.

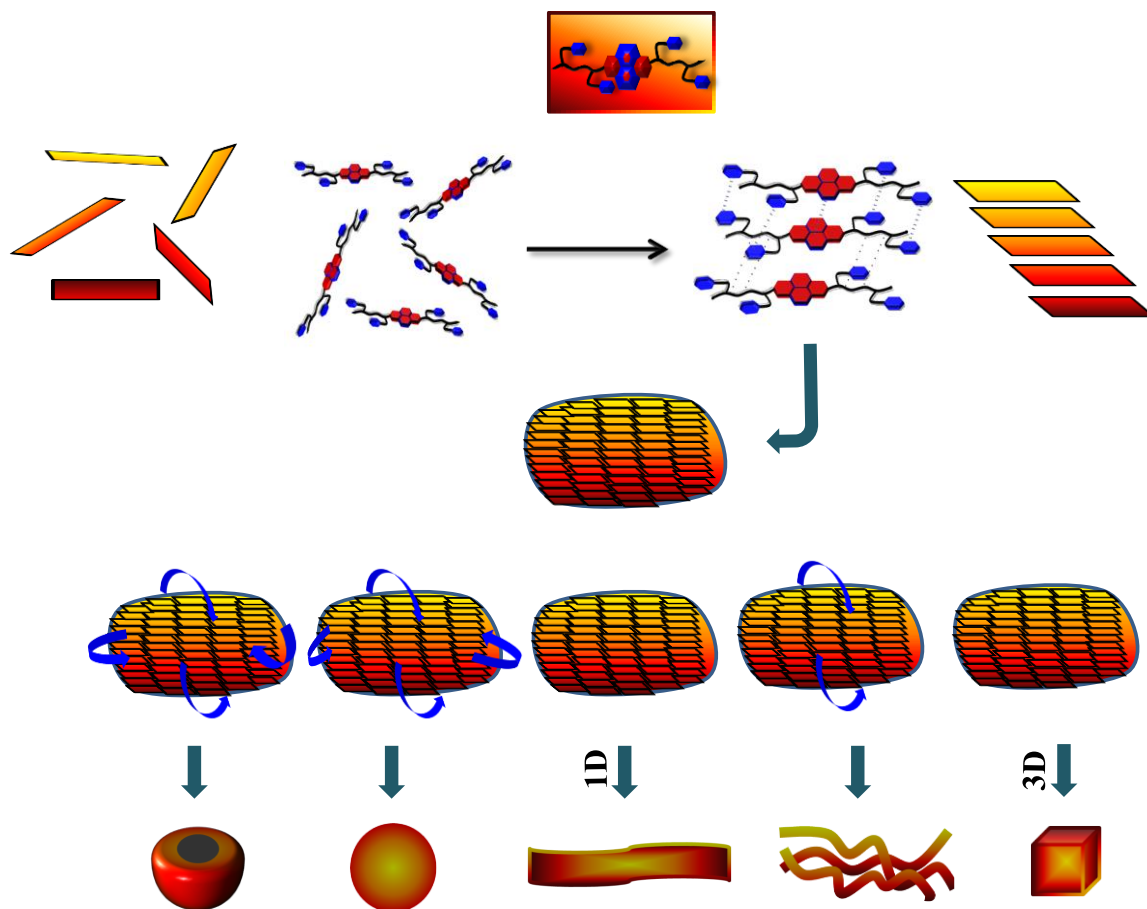


**Figure 4. 13** Proposed schematic model to explain the self-assembly process of N, N-bis-(dipeptide) appended NDI systems **4**, **5** and **6** into zero-, one-, two- and three-dimensional nanostructures (nanosphere, nanotape, open mouth nanovesicle and nanocube)

#### 4. 6 Conclusion

We have designed and synthesized N, N-bis-(dipeptide) appended naphthalenediimides NDIs **4**, **5** and **6**. NDIs **4**, **5** and **6** undergo self-assembly to form interesting new novel nanostructures with well defined architectures. Morphology of NDIs nanostructure were tuned by utilising solvophobic effect. We were successful in tuning the morphology into distinct structures such as nanospheres, nanotapes, open mouth nanovesicles and nanocubes. These NDI-dipeptide conjugate based nanostructures may find potential applications as biomaterials and in organic electronics.

## 4.7 Experimental

### (a) General Experimental Procedure

All the solvents and reagents were obtained from Sigma-Aldrich and used as received unless otherwise mentioned.  $^1\text{H}$  and  $^{13}\text{C}$  NMR spectra were measured on a Bruker AV-400 spectrometer with chemical shifts reported as ppm.

### (b) Synthesis of *L*-phenylalanine-appended naphthalenediimide (1)

*L*-phenylalanine (610 mg, 3 mmol) and NDA-dianhydride (500 mg, 1.8 mmol) was dissolved in dry DMF (30 ml). After 15 min triethyl amine was added to reaction mixture and allowed to reflux at 110 $^{\circ}\text{C}$  for 12 h. after cooling to room temperature, the solvent was removed under reduced pressure and washed with water. The organic layer was separated out and purified by column chromatography ( $\text{CH}_2\text{Cl}_2$ : MeOH 10:2) to afford product as brown solid (68%); *Characterization data*:  $^1\text{H}$  NMR ( $\text{CHCl}_3$ -*d*, 400 MHz)  $\delta_{\text{H}}$  3.30-3.55 (m, 4H,  $\text{CH}_2$ ), 5.69-5.73 (m, 2H, CH), 6.86-7.05 (m, 10H, Ar H), 8.49 (m, 4H, Ar H).

### 4.4.4 Synthesis of *L*-tryptophan-appended naphthalenediimide (2)<sup>19</sup>

*L*-Tryptophan (760 mg, 3.7 mmol) and NDA-dianhydride (500 mg, 1.8 mmol) was added to dry DMF (30 ml) in a 250 ml conical flask. Triethyl amine (0.5 ml) was added to suspension and sonicated until the reaction mixture become homogeneous. The reaction mixture was heated under microwave irradiation at full power for 3 min. in steps of 30 sec and with 30 sec interval. The resulting dark brown oil was taken into methanol (400 mL). The solution was added under stirring to 600 ml of 1N HCl. The resulting suspension was allowed to coagulate overnight and then filtered through a sintered glass funnel. The solid was then washed with 200 mL deionised water and dried in vacuo to obtain a brown solid of (2). Yield 90%.

#### 4.4.5 General procedure for the Synthesis of N, N-bis-(dipeptide) appended NDIs (4, 5 and 6)

Amino acid appended naphthalenediimide (300 mg, 0.5 mmol), 1-ethyl-3-(3-dimethylaminopropyl) carbodiimide hydrochloride (220 mg, 1.1 mmol) and 1-hydroxybenzotriazole (230 mg, 1.1 mmol) were dissolved in DMF (4 ml). After 15 min amino acid methylester (230 mg, 1 mmol) and N, N-diisopropylethylamine (440 mg, 3.4 mmol) were added to reaction mixture and allowed to stir at room temperature for 12 h. Reaction progress was monitored by TLC. The solvent was removed under reduced pressure and washed with water. The organic layer was separated out and purified by column chromatography (CH<sub>2</sub>Cl<sub>2</sub>: MeOH, 10:2).

**Characterization data: NDI 4.** Yield 50 %, <sup>1</sup>H NMR (CDCl<sub>3</sub>, 400 MHz) δ<sub>H</sub> 3.00-3.51 (m, 8H, CH<sub>2</sub>), 3.74 (m, 6H, CH<sub>3</sub>), 4.89-4.94 (m, 2H, NH), 5.96-6.20 (m, 4H, CH), 6.90-7.26 (m, 20H, ArH), 8.63 (s, 4H, ArH); <sup>13</sup>C NMR (CDCl<sub>3</sub>, 400 MHz) δ<sub>C</sub> 34.6, 37.7, 52.3, 53.3, 55.9, 126.6, 128.3, 128.9, 131.1, 136.3, 136.6, 162.4, 171.6. MW. 884.93[M+H<sup>+</sup>] calcd for C<sub>52</sub>H<sub>44</sub>N<sub>4</sub>O<sub>10</sub>.

**NDI 5.** Yield 40 %, <sup>1</sup>H NMR (CDCl<sub>3</sub>, 400 MHz) δ<sub>H</sub> 3.13-3.60 (m, 8H, CH<sub>2</sub>), 3.72 (m, 6H, CH<sub>3</sub>), 4.87-5.01 (m, 2H, NH), 5.96-6.46 (m, 4H, CH), 6.65-7.55 (m, 19H, ArH), 8.34-8.40 (m, 2H, NH), 8.43-8.47 (m, 4H, ArH). MW. 962.09 [M+H<sup>+</sup>] calcd for C<sub>56</sub>H<sub>46</sub>N<sub>6</sub>O<sub>10</sub>.

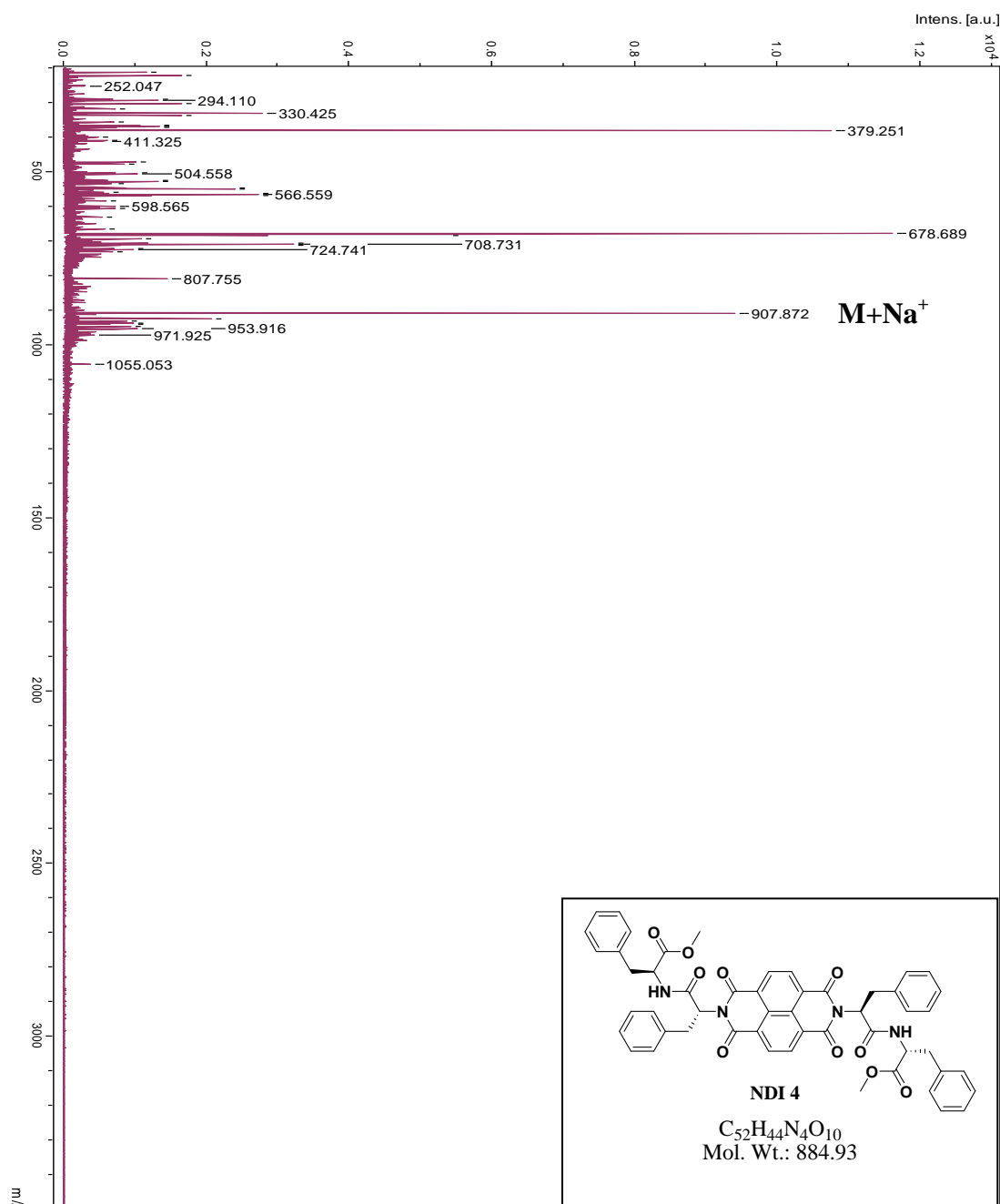
**NDI 6.** Yield 40 %, <sup>1</sup>H NMR (CDCl<sub>3</sub>, 400 MHz) δ<sub>H</sub> 2.87-3.40 (m, 8H, CH<sub>2</sub>), 3.59 (m, 6H, CH<sub>3</sub>), 4.59 (s, 2H, NH), 5.74 (s, 2H, CH), 6.78-7.42 (m, 20H, ArH), 8.38-8.54 (m, 4H, ArH), 10.59-10.86 (m, 4H, NH); <sup>13</sup>C NMR (CDCl<sub>3</sub>, 400 MHz) δ<sub>C</sub> 23.6, 26.5, 109.5, 110.2, 111.1, 111.3, 117.6, 117.9, 118.1, 118.3, 120.6, 120.8, 123.3, 123.6, 125.9, 126.3, 126.9, 127.1, 130.3, 135.8, 136.0, 168.6, 172.5. MW. 1,041 [M+H<sup>+</sup>] calcd for C<sub>60</sub>H<sub>48</sub>N<sub>8</sub>O<sub>10</sub>.

#### **4. 8 Appendix**

- MALDI-TOF
- $^1\text{H}$  NMR
- $^{13}\text{C}$  NMR

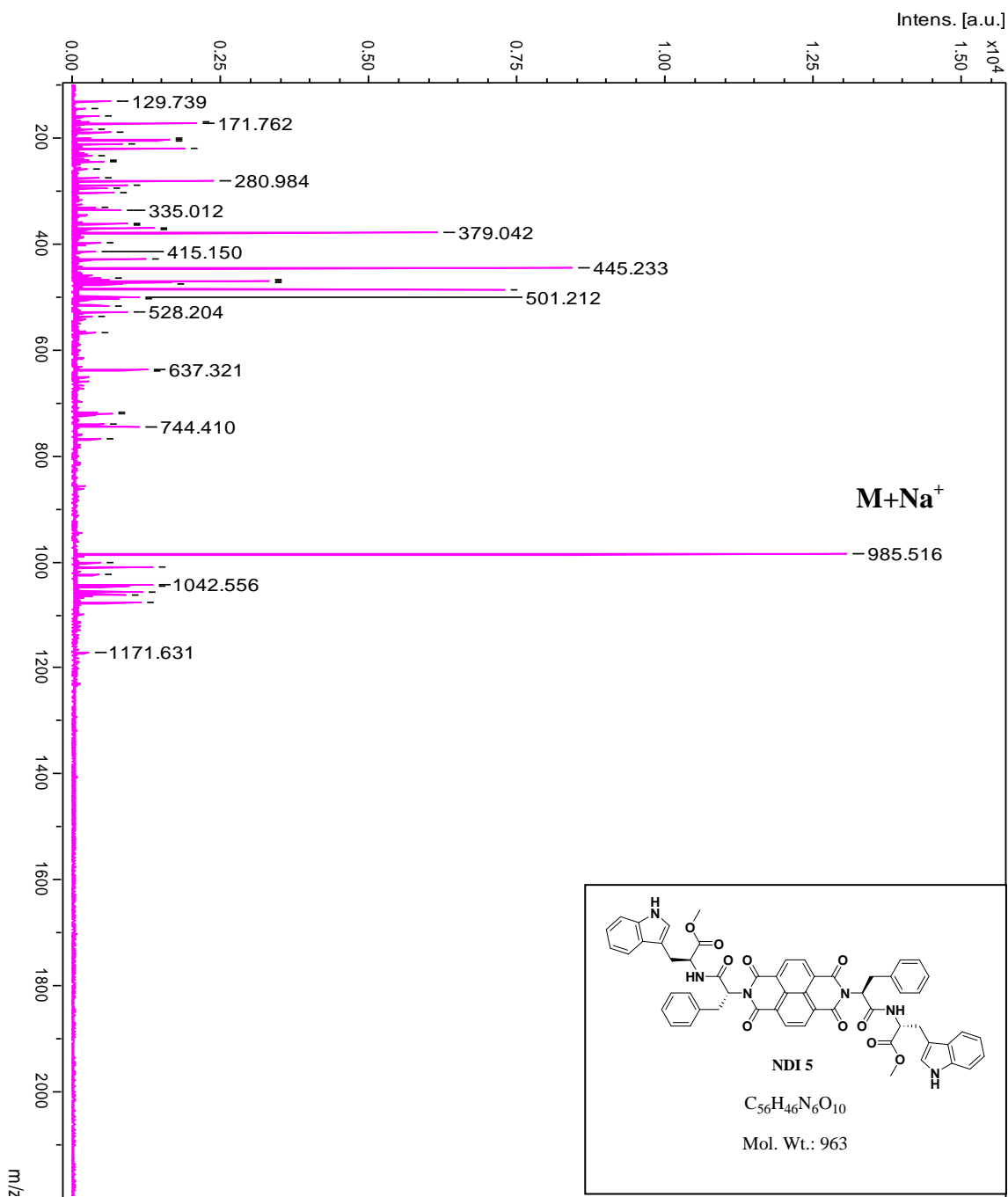
**Matrix-assisted laser desorption ionization time-of-flight (MALDI-TOF).** MALDI-TOF spectra were obtained on a Bruker ultraflex 2 MALDI-TOF mass spectrometer with  $\alpha$ -cyano-4-hydroxycinnamic acid matrix.

### MALDI-TOF of NDI 4

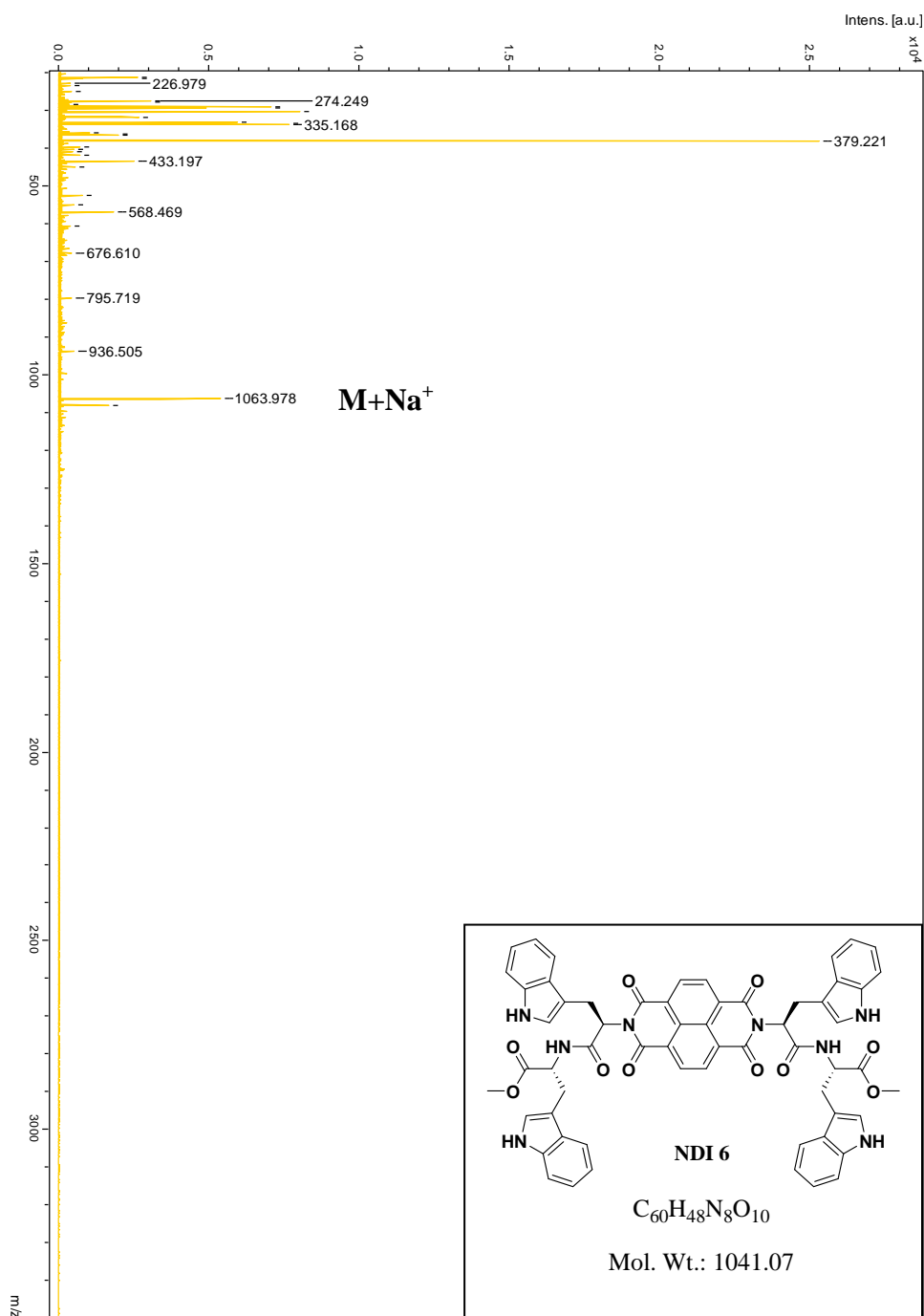




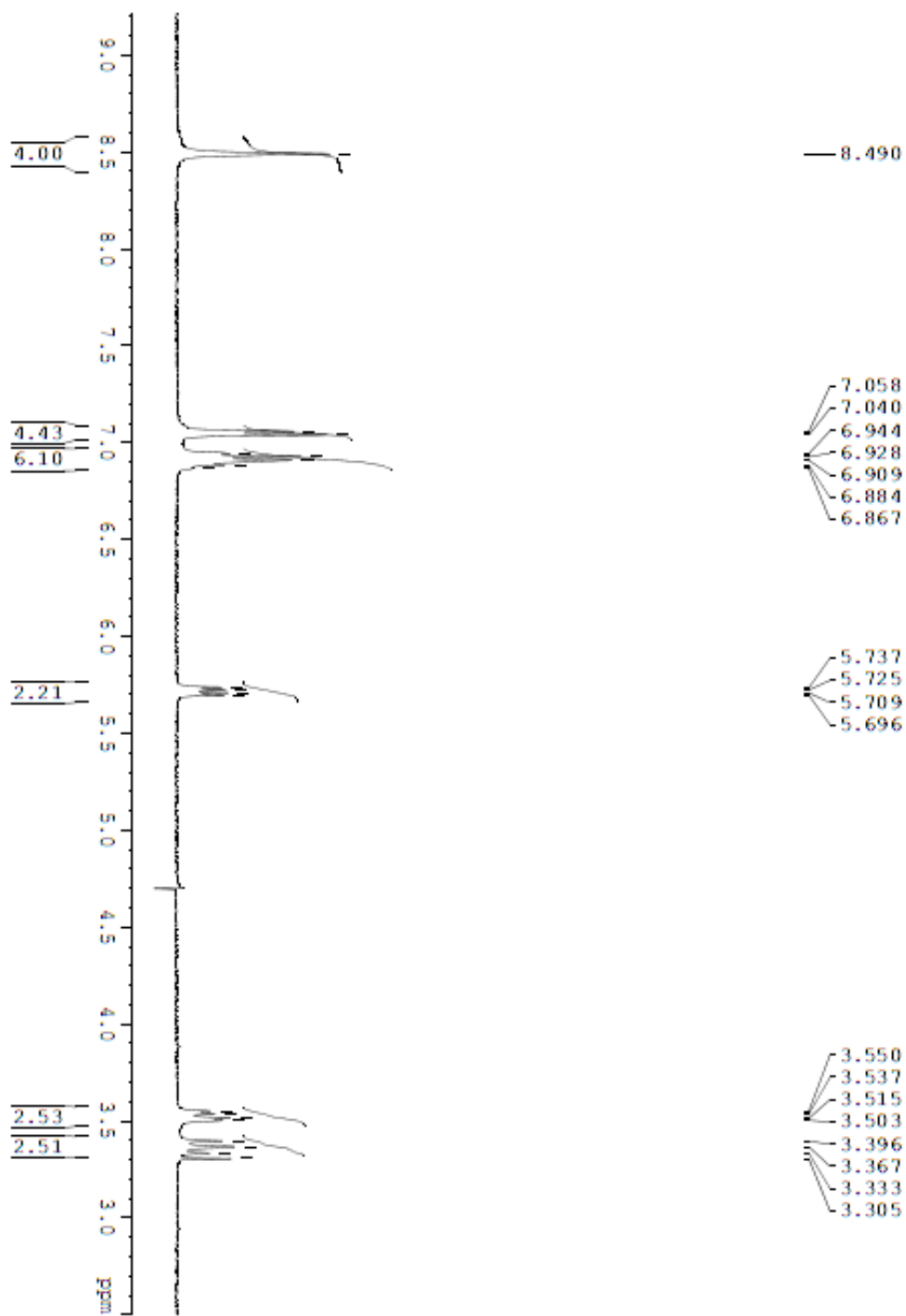
# MALDI-TOF of NDI 5



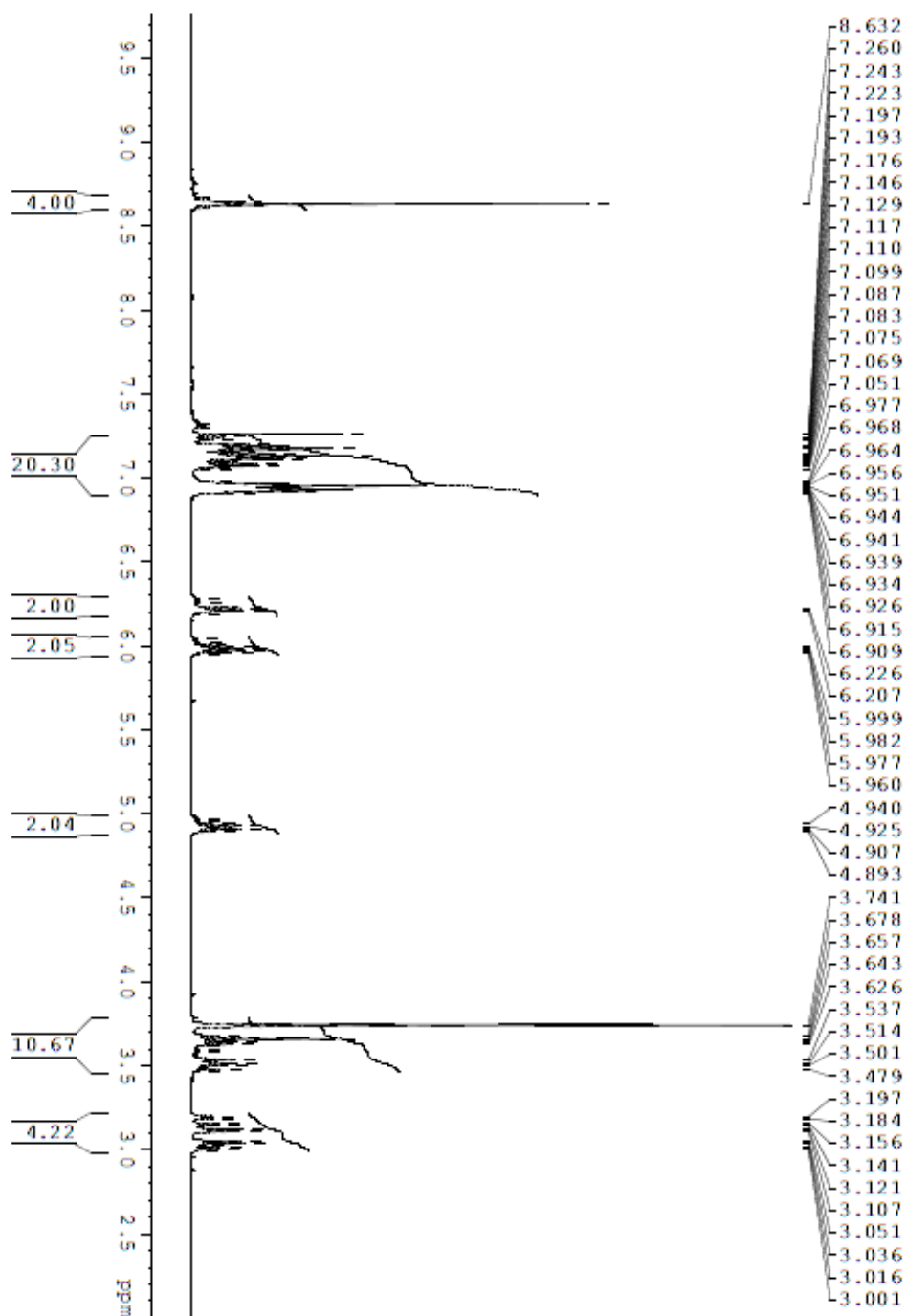
# MALDI-TOF of NDI 6



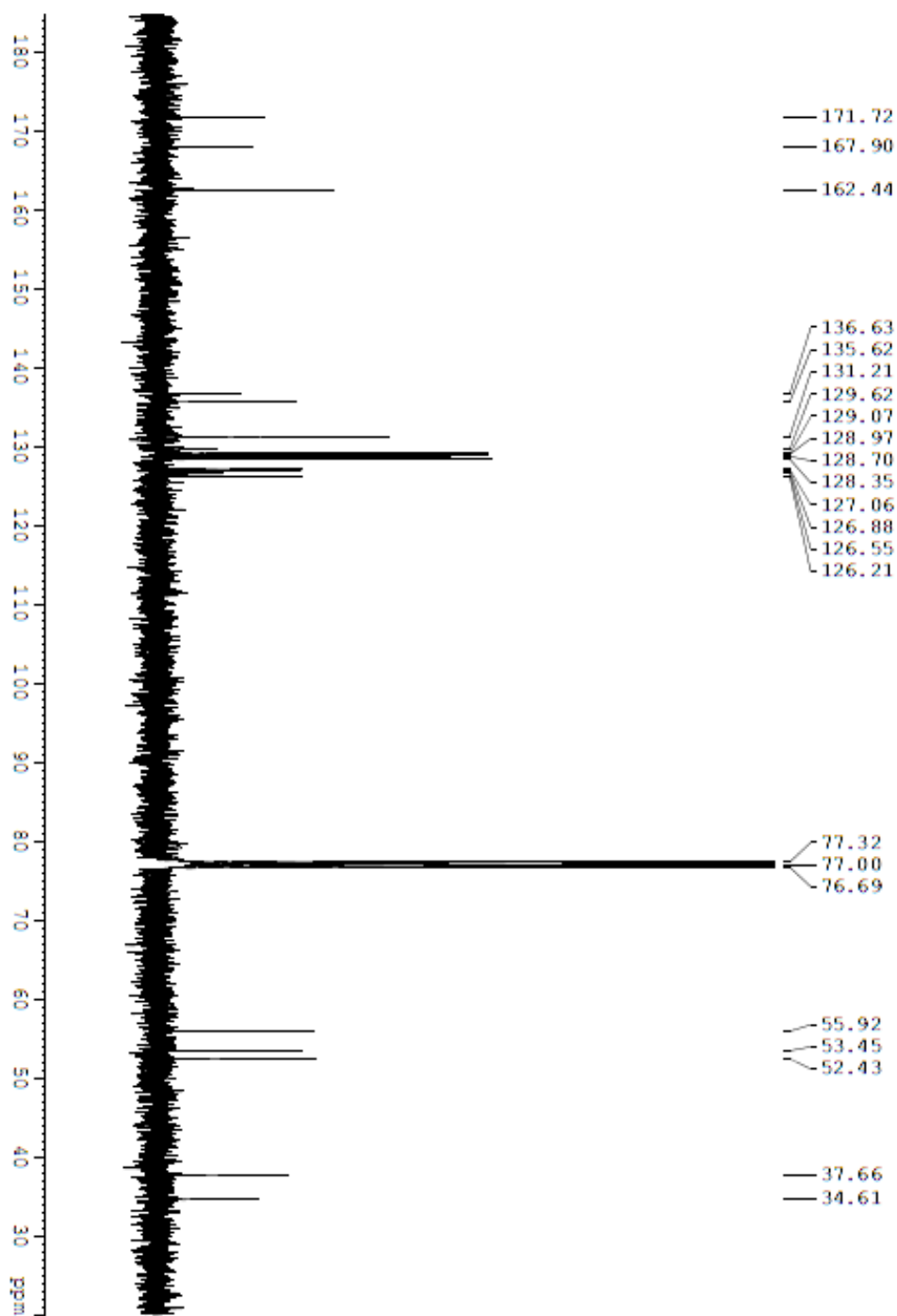
$^1\text{H}$  NMR ( $\text{CDCl}_3$ , 400 MHz) of NDI 1



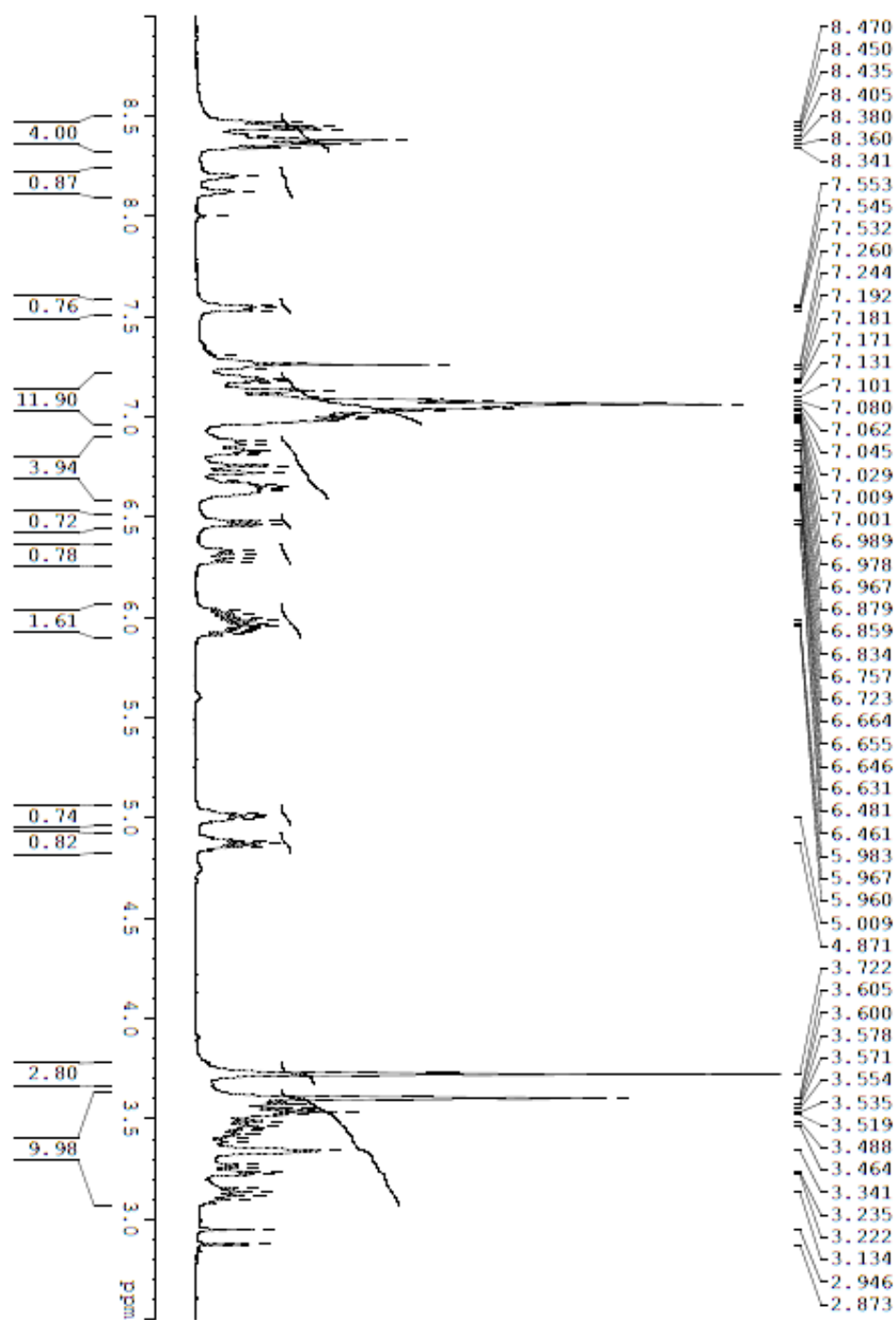
<sup>1</sup>H NMR (CDCl<sub>3</sub>, 400 MHz) of NDI 4



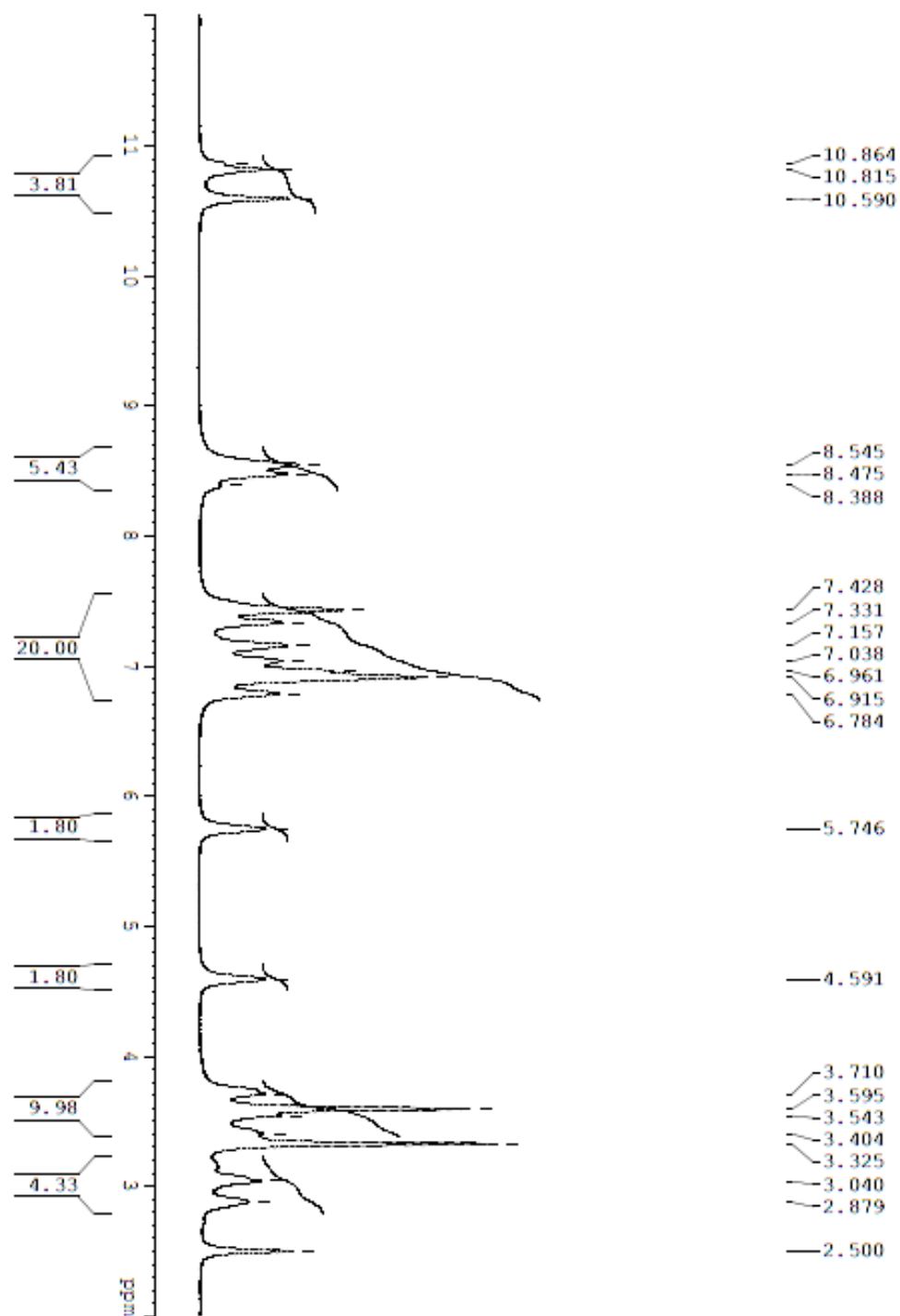
$^{13}\text{C}$  NMR ( $\text{CDCl}_3$ , 400 MHz) of NDI 4



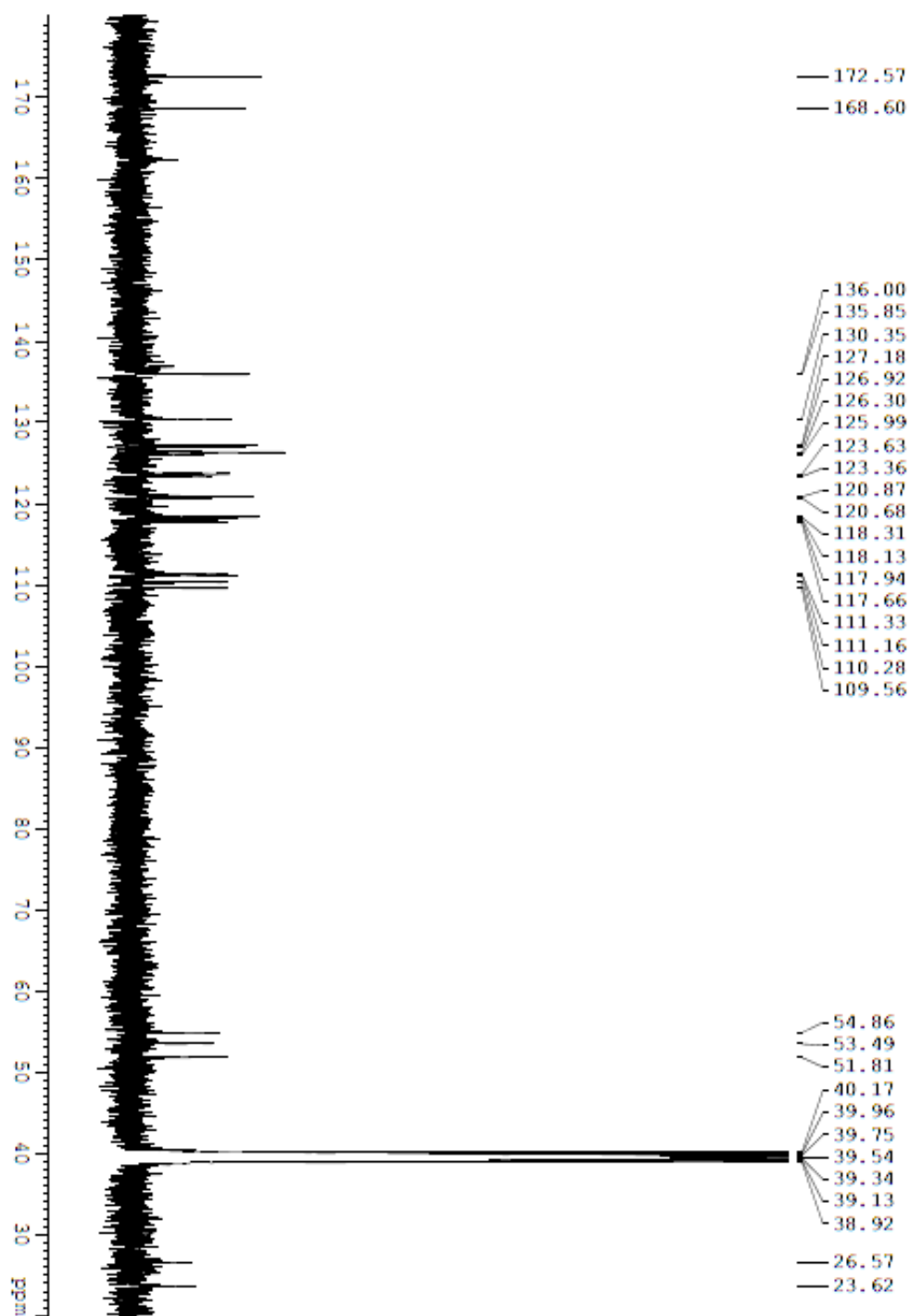
<sup>1</sup>H NMR (CDCl<sub>3</sub>, 400 MHz) of NDI 5



<sup>1</sup>H NMR (DMSO, 400 MHz) of NDI 6



$^{13}\text{C}$  NMR (DMSO, 400 MHz) of NDI 6





## 4. 9 References

1. H. E. Katz, A. J. Lovinger, C. Kloc, T. Siegrist, W. Li, Y.-Y. Lin, A. Dodabalapur, *Nature* **2000**, *404*, 478–481
2. S. J. Langford, M. J. Latter and C. P. Woodward, *Photochem. Photobiol* **2006**, *82*, 1530–1540
3. S. Takenaka, K. Yamashita, M. Takagi, Y. Uto, H. Kondo, *Anal. Chem.* **2000**, *72*, 1334–1341
4. Yen, S. F.; Gabbay, E. J.; Wilson, W. D. *Biochemistry* **1982**, *21*, 2070–2076
5. Brana, M. F.; Ramos, A. *Curr. Med. Chem. Anti-Cancer Agents* **2001**, *1*, 237–255
6. Liu, Z. R.; Hecker, K. H.; Rill, R. L. *J. Biomol. Struct. Dyn.* **1996**, *14*, 331–339
7. Ingrassia, L.; Lefranc, F.; Kiss, R.; Mijatovic, T. *Curr. Med. Chem.* **2009**, *16*, 1192–1213
8. G. D. Fallon, M. A.-P. Lee, S. J. Langford and P.J. Nichols, *Org. Lett.*, **2004**, *6*, 655–658
9. J. G. Hansen, N. Feeder, D. G. Hailton, M. J. Gunter, J. Becher, J. K. M. Sanders, *Org. Lett* **2000**, *2*, 449–452
10. T. C. Barros, Brochsztains, V. G. Toscano, Bercifp, M. J. Politi, *J Photochem Photobiol A: Chem* **1997**, *111*, 97-104
11. F. W rthner, S. Ahmed, C. Thalacker, T. Debaerdemaeker, *Chem.–Eur. J.*, **2002**, *8*, 4742 4750
12. S. V. Bhosale , C. H. Jani , S. J. Langford , *Chem. Soc. Rev.* **2008** , *37* , 331
13. C. Ego , D. Marsitzky , S. Becker , J. Zhang , A. C. Grimsdale , K. Müllen , J. D. MacKenzie , C. Silva , R. H. Friend , *J. Am. Chem. Soc.* **2003** , *125* , 437
14. M. Sadrai , L. Hadel , R. R. Sauers , S. Husain , K. Krogh-Jespersen , J. D. Westbrook , G. R. Bird , *J. Phys. Chem.* **1992** , *96* , 7988
15. M. P. O. Neil , M. P. Niemczyk , W. A. Svec , D. Gosztola , G. L. Gaines III , M. R. Wasielewski, *Science* **1992** , *257* , 63
16. K.-Y. Law, *Chem. Rev.* **1993**, *93*, 449
17. A. P. H. J. Schenning , J. v. Herrikhuyzen , P. Jonkheijm , Z. Chen , F. Würthner , E. W. Meijer , *J. Am. Chem. Soc.* **2002** , *124* , 10252
18. G. Colombo, P. Soto, E. Gazit, *Trends Biotechnol.* **2007**, *25*, 211

19. M. B. Avinash, T. Govindaraju, *Nanoscale*. **2011**, DOI: 10.1039/C0NR00766H
20. H. Shao, J. Seifert, N. C. Romano, M. Gao, J. J. Helmus, C. P. Jaroniec, D. A. Modarelli, J. R. Parquette, *Angew. Chem.* **2010**, *122*, 7854–7857
21. Reches M, Gazit E, *Phys Biol.***2006**, *3*, 10–19